

Analyzing the effectiveness of self-healing mortar using encapsulated and externally applied bacteria.

Analyzing the effectiveness of self-healing mortar using encapsulated and externally applied bacteria.

By

Ayushi Shah

To obtain the degree of Master of Science
at the Delft University of Technology, to
be defended publicly on August,29,2024

Student Number –	5711304	
Master Programme –	Civil Engineering	
Track –	Construction Material Engineering	
Thesis Committee –	Prof. Dr. H.M. Jonkers	Tu Delft, Chairman
	Dr. O. Copuroglu	Tu Delft
	Dr.ir. Y. Mosleh	Tu Delft
	Ir. B. Aytekin Turkoglu	Tu Delft

Preface

This thesis concludes my educational career at the Delft University of Technology, which I started in September 2022. During my Master I followed the newly started Construction Materials Track which was an amazing experience.

During the course of my master program, I learnt about self-healing materials which piqued my interest. Therefore, I am grateful to be given the opportunity to further my knowledge of the topic.

I am grateful to everyone who contributed to this thesis. First of all, I would like to thank Prof Henk Jonkers, the chairman of my committee for not only providing me with the opportunity to examine such an intriguing subject, but also for his supervision and support. I also want to express my gratitude to Prof. Oguzhan Copuroglu and Prof. Yasmine Mosleh for their constructive feedback and motivation.

Furthermore, I would like to thank Burcu Aytekin Turkoglu for her help and support during this thesis.

Special thanks also to Maiko van Leeuwen and Ton Blom without whom preparation and testing of the mortar mixtures would not have been possible. I really appreciated working together. Also, I would like to express my gratitude for Arjan Thijssen for his advice and help in the laboratory.

This preface would not be complete before I express my gratitude to my friends and family, particularly my parents. I will always be thankful for their support during my time at TU Delft to become an engineer.

Ayushi Shah
August, 2024

Abstract

Since more than a decade, TU Delft has been working on the development of bacteria based self-healing concrete. The self-healing ability of the material is based on a biological mechanism in which a limestone producing bacteria is added to the material to repair cracks.

The purpose of this study was to understand and compare the efficiency of different methods and materials used for incorporating bacteria into mortar. The aim of the study was to create a self-healing mortar mix for practical applications.

Concrete is a widely used construction material. Most structural elements are made using concrete and covered by a protective layer of mortar, called plaster. Cracks usually propagate from the surface to the inside, which means that the plaster is the first to crack. If the mortar is made self-healing, then the concrete underneath can be better protected from the elements, and this could effectively increase the lifespan of the structure.

For this project, fibre reinforced mortar is healed using bacteria (*Bacillus Cohnii*) which is applied to the concrete using internal (different types of embedded capsules) and external methods (paste applied to the cracks).

This is done to check the effectiveness of the bacteria in repairing damaged concrete and to observe which method of application works best. The effectiveness is analysed using optical and electron (BSE) microscopy and a permeability test to observe the water tightness of the sample after cracking.

Additionally, characterization tests are performed on the capsules and performance tests are carried on the mortar samples, to better understand their behaviour.

This study would help in making concrete structures more durable which would make them more sustainable and cheaper in the long term.

This study found that crack healing is dependent on the crack width and the number of capsules present in the material near the crack. The compressive and flexural strength at 28 and 84 days was found to be higher in samples embedded with alginate capsules and PLA capsules. External healing was found to be a good method for healing existing materials but the healing was found to be dependent on the amount of paste that adhered to the crack wall.

CONTENTS

RESEARCH INTRODUCTION	16
1.1 RESEARCH CONTEXT –	16
1.2 RESEARCH PROBLEM –	17
1.3 RESEARCH OBJECTIVES –	17
1.4 RESEARCH SCOPE –	17
1.5 RESEARCH LIMITATIONS –	18
1.6 RESEARCH QUESTIONS –	18
1.7 RESEARCH THEORY AND METHODS –	18
1.8 OUTLINE –	19
LITERATURE STUDY	21
2.1 OVERVIEW –	21
2.2 MIX DESIGNS AND MATERIALS USED FOR HEALING –	23
2.3 MECHANISM OF HEALING –	25
2.3.1 <i>Biological Healing Agents</i> –	25
2.3.2 <i>Hydration of Cement</i> –	27
2.3.2.1 Types and Classification –	27
2.3.2.2 Chemical Composition –	29
2.3.2.3 Hydration Process –	30
2.4 CAPSULE RESEARCH –	33
2.4.1 <i>Expanded Clay Capsules</i> –	33
2.4.2 <i>Alginate Capsules</i> –	34
2.4.3 <i>PLA Capsules</i> –	35
2.5 POLYETHYLENE FIBERS –	36
2.6 DURABILITY AND PERMEABILITY –	38
2.7 EFFECT OF SELF-HEALING COMPONENTS ON MORTAR MIXES –	41
DESIGN OF THE EXPERIMENT	43
3.1 EXPERIMENT PROCESS –	43
3.2 HYPOTHESES –	45
MATERIALS AND METHODS	46
4.1 HEALING AGENT –	46
4.1.1 <i>Bacteria</i> –	46
4.1.2 <i>Calcium Lactate</i> –	46
4.1.3 <i>Yeast Extract</i> –	46
4.2 CAPSULES –	47
4.2.1 <i>Introduction</i> –	47
4.2.2 <i>Capsule Materials</i> –	47
4.2.3 <i>Method for Preparing Capsules</i> –	48
4.2.3.1 Expanded Clay Capsules –	48
4.2.3.2 Alginate Capsules –	49
4.2.4 <i>Tests on Capsules</i> –	49
4.2.4.1 Particle Size Distribution –	49
4.2.4.1.1 PLA Capsules –	49
4.2.4.1.2 Expanded Clay –	50
4.2.4.1.3 Alginate Capsules –	51
4.2.4.2 Specific Gravity and Water Absorption –	52

4.2.4.2.1 Expanded Clay –	52
4.2.4.2.2 PLA Capsules –	53
4.2.4.2.3 Alginate Based Capsules –	53
4.2.4.3 Surface Texture of Capsules –	53
4.2.4.3.2 Expanded Clay Capsules –	54
4.2.4.3.2 PLA Capsules –	54
4.2.4.3.3 Alginate Capsules –	55
4.3 MIX DESIGN –	55
4.3.1 Design Criteria –	56
4.3.1.1 Compatibility –	56
4.3.1.2 Ease and Practicality –	56
4.3.1.3 Strength –	56
4.3.1.4 Comparability –	56
4.3.2 Material Selection –	57
4.3.2.1 Cement –	57
4.3.2.2 Sand –	57
4.3.2.3 Fibers –	57
4.3.2.4 Capsules	57
4.3.3 MIXTURE DESIGNS –	58
MORTAR MIXTURE TESTING	59
5.1 TEST OBJECTIVES –	59
5.2 PERFORMANCE TESTS –	59
5.2.1 Slump and Consistency test –	60
5.2.2 Flexural Test –	60
5.2.3 Compressive test –	62
5.2.4 4 Point Bending – (Induction of Cracks)	62
5.2.5 Optical Microscopy –	63
5.2.6 Permeability Test –	63
5.2.7 Microscopy –	64
5.2.8 Porosity –	64
5.3 TEST RESULTS –	64
5.3.1 Slump and Consistency Test –	64
5.3.2 Flexural Strength –	65
5.3.3 Compressive Strength –	66
5.3.4 4-Point Bending –	67
5.3.5 Permeability Test Results –	70
.....	73
5.3.6 Surface Crack Width Progression –	73
5.3.7 Microscopy –	76
5.3.8 Void Analysis –	80
DISCUSSION	81
6.1 FRESH PROPERTIES –	81
6.2 COMPACTION –	82
6.3 FLEXURAL STRENGTH –	82
6.4 COMPRESSIVE STRENGTH –	83
6.5 4-POINT BENDING TEST –	84
6.6 PERMEABILITY –	85
6.7 HEALING EFFICIENCY –	87
6.8 VOID ANALYSIS –	88

6.9 CRACK SURFACE CLOSURE –	88
6.9.1 <i>The relation between visually observed surface healing and permeability</i> –	89
6.10 PROBABILITY OF CRACK HEALING –	89
CONCLUSIONS AND RECOMMENDATIONS	91
7.1 CONCLUSIONS –	91
7.1.1 <i>Mechanical Properties</i> -	91
7.1.2 <i>Quantification of Healing</i> –	92
7.2 EXPERIMENTAL LIMITATIONS –	93
7.3 FUTURE RECOMMENDATIONS –	93
REFERENCES	95
APPENDIX A –	98
A.1 PARTICLE SIZE DISTRIBUTION –	98
A.1.1 <i>Sand</i> –	98
A.1.2 <i>Expanded Clay</i> –	99
APPENDIX B –	100
B.1 SPECIFIC GRAVITY AND WATER ABSORPTION TEST –	100
APPENDIX C –	101
C.1 DETAIL OF MIX DESIGNS –	101
C.1.1 <i>Type 1 Mix (Plain Reference Mix)</i> –	101
C.1.2 <i>Type 2 (PLA Mix)</i> –	101
C.1.3 <i>Type 3 (Expanded Clay Mix)</i> –	102
C.1.4 <i>Type 4 (Alginate Mix)</i> –	103
C.1.5 <i>Type 5 (Externally Applied Paste)</i> –	104
APPENDIX D –	105
APPENDIX E –	135
E.1 FLEXURAL STRENGTH –	135
E.2 COMPRESSIVE STRENGTH –	135
E.3 PERMEABILITY TEST –	137
E.4 SURFACE CRACK WIDTH PROGRESSION –	139
E.5 OPTICAL MICROSCOPY –	139
E.6 POROSITY –	141
E.6 HEALING EFFICIENCY –	145
E.7 HEALING EFFICIENCY –	146
APPENDIX F –	147
<i>Preparation of Polished Samples</i> –	147

TABLE OF FIGURES –

Figure 1 - Possible autogenous-healing mechanisms for crack closure: (a) Calcium carbonate formation; (b) hydration of anhydrous cement particles; (c) swelling of hydration products; (d) closure due to spalled edges and impurities.[14].....	25
Figure 2 – Mortar sample embedded with self-healing capsules (yellow).....	27
Figure 3 - Crack initiation in sample and capsule rupture due to crack.....	27
Figure 4 -Crack opening and Oxygen and water ingress in the sample. Fibers holding the sample together (crack bridging).....	27
Figure 5 - Healing product precipitated on fibers and crack wall	27
Figure 6 – Crack healing in progress	27
Figure 7 -Schematic illustration of formation of reaction products over time in Portland cement paste [30]	33
Figure 8 - Expanded Clay Particles with different impregnation types [10]	34
Figure 9 - Sodium Alginate conversion to Calcium Alginate	34
Figure 10 - Alginate beads showing the "egg-box" structure.....	35
Figure 11 - Relationship between permeability and w/c ratio	40
Figure 12 - Relationship between water flow rate and initial crack width for 160 plain mortar samples [22].....	41
Figure 13 - Sample types and their contents	43
Figure 14- Flowchart of Internal application samples.	44
Figure 15 - Flowchart of External Application Samples.....	44
Figure 16- Measurements of PLA capsules. Scale- 1000 μ m	50
Figure 17 - Sieving of expanded clay particles in a sieve shaker.....	50
Figure 18-Alginate capsule. Scale :1000 μ m	52
Figure 19 - Pycnometer after 24 hours	53
Figure 20 - Optical Microscope	54
Figure 21- Roughness measurement of the expanded clay particles. Scale:1mm	54
Figure 22 -Roughness measurement of the expanded clay particles. Scale:1mm.....	54
Figure 23- Surface of a PLA capsule. Scale: 100 μ m.....	55
Figure 24 - Alginate capsule with a broken tail. Scale: 1000 μ m	55
Figure 25 - Undulation on the surface of the alginate capsule. Scale: 1000 μ m	55
Figure 26 - Slump Cone	60
Figure 27 -Sketch of 3-point bending set-up.....	61
Figure 28 -Saw for cutting the prism samples	62
Figure 29 -Type 2 specimen undergoing flexure strength test	62
Figure 30 -Testing sample in 4-point bending	63
Figure 31 - Setup for permeability test.....	64
Figure 32 -Consistency of Type 2 mix.....	65
Figure 33 - Consistency of Type 3 Mix showing segregation.....	65
Figure 34-Crack in Type 2 sample with some visible crack bridging.....	67
Figure 35 -Photomicrographs of sample PLA5 (Type 2) at cracking (left), 1 month healing (middle), 2 months healing (right). Healing can be seen in the crack. Scale: 1000 μ m.....	75
Figure 36- Photomicrographs of sample EC1 (Type 3) at cracking (left), 1 month healing (middle), 2 months healing (right). Healing can be seen in the crack at 1 month. Scale: 1000 μ m	76

<i>Figure 37-Photomicrographs of sample A1(Type 4) at cracking (left), 1 month healing (middle), 2 months healing (right). Healing can be seen in the crack. Scale: 1000 μm.....</i>	76
<i>Figure 38-Photomicrographs of sample E1 (Type 5) at cracking (left), 1 month healing (middle), 2 months healing (right). Healing can be seen in the crack. Scale: 1000 μm.....</i>	76
Figure 39 -Electron micrograph of PLA1 polished section showing irregular shaped PLA capsules (black spots). Scale: 500μm	77
Figure 40 – Electron micrograph of PLA1 polished section showing an imprint of PE fiber near the crack. Scale: 300μm	77
Figure 41 – Electron micrograph of PLA1 polished section showing CaCO ₃ precipitate on the crack walls. Scale: 1mm.....	77
Figure 42 – Electron micrograph of PLA1 polished section Scale: 500μm	78
Figure 43- Elemental mapping of PLA1 polished section Scale: 500μm.....	78
Figure 44 - Elemental mapping of PLA1 polished section Scale: 500μm.....	78
Figure 45- Electron micrograph of EC3 polished section showing an expanded clay capsule. Scale: 1mm	79
Figure 46 - Electron micrograph of EC3 polished section showing the inside of an expanded clay capsule. The crack walls show healing. Scale: 100μm	79
Figure 47 -Electron micrograph of EC3 polished section showing a crack going through a capsule. Scale: 500μm.....	79
Figure 48 -Elemental mapping of EC3 polished section. Showing CaCO ₃ deposition along the crack wall Scale: 500μm.....	79
Figure 49 -Elemental mapping of EC3 polished section Scale: 500μm	79
<i>Figure 50 - Photomicrograph of polished sample A1 showing crack. Scale: 1000μm.....</i>	80
Figure 51- C/S of Type 3 sample.	82
Figure 52 -Photomicrograph of fiber pullout across the crack. Scale: 1000μm.....	84
Figure 53 - Photomicrograph of elongation of fibers across the crack. Scale: 1000μm	84
Figure 54 -Photomicrograph of precipitate along the fiber across the crack. Scale: 1000μm	92
Figure 55 - Photomicrograph of mortar sample P1 showing crack. Scale: 1000μm	105
Figure 56 - Photomicrograph of mortar sample P2 showing crack. Scale: 1000μm	105
Figure 57 - Photomicrograph of mortar sample P3 showing crack. Scale: 1000μm	105
Figure 58 -Photomicrograph of mortar sample P4 showing crack. Scale: 1000μm	105
Figure 59 - Photomicrograph of mortar sample PLA1 showing crack. Scale: 1000μm	106
Figure 60 -Photomicrograph of mortar sample PLA2 showing crack. Scale: 1000μm	106
Figure 61 - Photomicrograph of mortar sample PLA3 showing crack. Scale: 1000μm	106
Figure 62 - Photomicrograph of mortar sample PLA4 showing crack. Scale: 1000μm	106
Figure 63 -Photomicrograph of mortar sample PLA5 showing crack. Scale: 1000μm	107
Figure 64 -Photomicrograph of mortar sample EC1 showing crack. Scale: 1000μm.....	108
Figure 65 - Photomicrograph of mortar sample EC2 showing crack. Scale: 1000μm	108
Figure 66- Photomicrograph of mortar sample EC3 showing crack. Scale: 1000μm.....	108
Figure 67 -Photomicrograph of mortar sample EC4 showing crack. Scale: 1000μm.....	108
<i>Figure 68- Photomicrograph of left side of mortar sample EC4 showing crack. Scale: 1000μm</i>	109
Figure 69 -Photomicrograph of mortar sample A1 showing crack. Scale: 1000μm	110
Figure 70 -Photomicrograph of mortar sample A2 showing crack. Scale: 1000μm	110
Figure 71-Photomicrograph of mortar sample A3 showing crack. Scale: 1000μm.....	110
Figure 72-Photomicrograph of mortar sample A4 showing crack. Scale: 1000μm.....	110

Figure 73 -Photomicrograph of mortar sample E1 showing crack. Scale: 1000µm	111
Figure 74-Photomicrograph of mortar sample E2 showing crack. Scale: 1000µm	111
Figure 75-Photomicrograph of mortar sample E3 showing crack. Scale: 1000µm	111
Figure 76 -Photomicrograph of mortar sample E4 showing crack. Scale: 1000µm	111
Figure 77 - Photomicrograph of mortar sample P1 showing crack. Scale: 1000µm	112
Figure 78 - Photomicrograph of mortar sample P2 showing crack. Scale: 1000µm	112
Figure 79 - Photomicrograph of mortar sample P3 showing crack. Scale: 1000µm	112
Figure 80 -Photomicrograph of mortar sample P4 showing crack. Scale: 1000µm	112
Figure 81 - Photomicrograph of mortar sample PLA1 showing crack. Scale: 1000µm	113
Figure 82 -Photomicrograph of mortar sample PLA2 showing crack. Scale: 1000µm	113
Figure 83 - Photomicrograph of mortar sample PLA3 showing crack. Scale: 1000µm	113
Figure 84 - Photomicrograph of mortar sample PLA4 showing crack. Scale: 1000µm	113
Figure 85 -Photomicrograph of mortar sample PLA5 showing crack. Scale: 1000µm	114
Figure 86 -Photomicrograph of mortar sample EC1 showing crack. Scale: 1000µm	115
Figure 87 - Photomicrograph of mortar sample EC2 showing crack. Scale: 1000µm	115
Figure 88- Photomicrograph of mortar sample EC3 showing crack. Scale: 1000µm	115
Figure 89 -Photomicrograph of mortar sample EC4 showing crack. Scale: 1000µm	115
<i>Figure 90- Photomicrograph of left side of mortar sample EC4 showing crack. Scale: 1000µm</i>	116
Figure 91 -Photomicrograph of mortar sample A1 showing crack. Scale: 1000µm	117
Figure 92 -Photomicrograph of mortar sample A2 showing crack. Scale: 1000µm	117
Figure 93-Photomicrograph of mortar sample A3 showing crack. Scale: 1000µm	117
Figure 94-Photomicrograph of mortar sample A4 showing crack. Scale: 1000µm	117
Figure 95 -Photomicrograph of mortar sample E1 showing crack. Scale: 1000µm	118
Figure 96-Photomicrograph of mortar sample E2 showing crack. Scale: 1000µm	118
Figure 97-Photomicrograph of mortar sample E3 showing crack. Scale: 1000µm	118
Figure 98 -Photomicrograph of mortar sample E4 showing crack. Scale: 1000µm	118
Figure 99 - Photomicrograph of mortar sample P1 showing crack. Scale: 1000µm	119
Figure 100 - Photomicrograph of mortar sample P2 showing crack. Scale: 1000µm	119
Figure 101 - Photomicrograph of mortar sample P3 showing crack. Scale: 1000µm	119
Figure 102 -Photomicrograph of mortar sample P4 showing crack. Scale: 1000µm	119
Figure 103 - Photomicrograph of mortar sample PLA1 showing crack. Scale: 1000µm	120
Figure 104 -Photomicrograph of mortar sample PLA2 showing crack. Scale: 1000µm	120
Figure 105 - Photomicrograph of mortar sample PLA3 showing crack. Scale: 1000µm	120
Figure 106 - Photomicrograph of mortar sample PLA4 showing crack. Scale: 1000µm	120
Figure 107 – PLA 4 sample showing precipitate along the crack Scale: 1000µm	121
Figure 108 -Photomicrograph of mortar sample PLA5 showing crack. Scale: 1000µm	121
Figure 109 -Photomicrograph of mortar sample EC1 showing crack. Scale: 1000µm	122
Figure 110 - Photomicrograph of mortar sample EC2 showing crack. Scale: 1000µm	122
Figure 111- Photomicrograph of mortar sample EC3 showing crack. Scale: 1000µm	122
Figure 112 -Photomicrograph of mortar sample EC4 showing crack. Scale: 1000µm	122
<i>Figure 113- Photomicrograph of left side of mortar sample EC4 showing crack. Scale: 1000µm</i>	123
Figure 114 -Photomicrograph of mortar sample A1 showing crack. Scale: 1000µm	124
Figure 115 -Photomicrograph of mortar sample A2 showing crack. Scale: 1000µm	124
Figure 116-Photomicrograph of mortar sample A3 showing crack. Scale: 1000µm	124

Figure 117-Photomicrograph of mortar sample A4 showing crack. Scale: 1000µm	124
Figure 118 -Photomicrograph of mortar sample E1 showing crack. Scale: 1000µm	125
Figure 119 - Photomicrograph of mortar sample E1 precipitate along the crack wall. Scale: 1000µm	125
Figure 120- Photomicrograph of mortar sample E2 showing crack. Scale: 1000µm	125
Figure 121-Photomicrograph of mortar sample E3 showing crack. Scale: 1000µm	125
Figure 122-Photomicrograph of mortar sample E4 showing crack. Scale: 1000µm	126
Figure 123 - Photomicrograph of mortar sample P1 showing crack. Scale: 1000µm.....	128
Figure 124 - Photomicrograph of mortar sample P2 showing crack. Scale: 1000µm.....	128
Figure 125 - Photomicrograph of mortar sample P3 showing crack. Scale: 1000µm.....	128
Figure 126 -Photomicrograph of mortar sample P4 showing crack. Scale: 1000µm	128
Figure 127 - Photomicrograph of mortar sample PLA1 showing crack. Scale: 1000µm.....	130
Figure 128 -Photomicrograph of mortar sample PLA2 showing crack. Scale: 1000µm	130
Figure 129 - Photomicrograph of mortar sample PLA3 showing crack. Scale: 1000µm.....	130
Figure 130 - Photomicrograph of mortar sample PLA4 showing crack. Scale: 1000µm.....	130
Figure 131 -Photomicrograph of mortar sample PLA5 showing crack. Scale: 1000µm	131
Figure 132 -Photomicrograph of mortar sample EC1 showing crack. Scale: 1000µm	132
Figure 133 - Photomicrograph of mortar sample EC2 showing crack. Scale: 1000µm	132
Figure 134- Photomicrograph of mortar sample EC3 showing crack. Scale: 1000µm.....	132
Figure 135 -Photomicrograph of mortar sample EC4 showing crack. Scale: 1000µm	132
Figure 136 -Photomicrograph of mortar sample A1 showing crack. Scale: 1000µm	133
Figure 137 -Photomicrograph of mortar sample A2 showing crack. Scale: 1000µm	133
Figure 138-Photomicrograph of mortar sample A3 showing crack. Scale: 1000µm	133
Figure 139-Photomicrograph of mortar sample A4 showing crack. Scale: 1000µm	133
Figure 140 -Photomicrograph of mortar sample E1 showing crack. Scale: 1000µm	134
Figure 141 - Photomicrograph of mortar sample E2 precipitate along the crack wall. Scale: 1000µm	134
Figure 142- Photomicrograph of mortar sample E3 showing crack. Scale: 1000µm	134
Figure 143-Photomicrograph of mortar sample E4 showing crack. Scale: 1000µm	134
Figure 144 -Photomicrograph of polished sample P3 showing crack. Scale: 1000µm	139
Figure 145-Photomicrograph of polished sample P3 showing crack. Scale: 1000µm	139
Figure 146 -Photomicrograph of polished sample PLA1 showing crack. Scale: 1000µm.....	140
Figure 147- Photomicrograph of polished sample PLA1 showing crack. Scale: 1000µm.....	140
Figure 148 - Photomicrograph of polished sample EC3 showing crack. Scale: 1000µm	140
Figure 149 -Photomicrograph of polished sample EC3 showing crack. Scale: 1000µm	140
Figure 150 - Photomicrograph of polished sample A1 showing crack. Scale: 1000µm.....	141
Figure 151- Photomicrograph of polished sample A1 showing crack. Scale: 1000µm	141
Figure 152 -Photomicrograph of polished sample E1 showing crack. Scale: 1000µm	141
Figure 153 -Photomicrograph of polished sample E1 showing crack. Scale: 1000µm	141
Figure 154 - Prepared surface of sample P3	142
Figure 155 – Processed image of left side of the sample	142
Figure 156 - Processed image of right side of the sample	142
Figure 157- Threshold value	142
Figure 158-Threshold value	142
Figure 159 - Prepared surface of sample PLA1	143

Figure 160- Processed image of left side of the sample	143
Figure 161- Processed image of right side of the sample	143
Figure 162 -Threshold value	143
Figure 163- Threshold value	143
Figure 164 -Prepared surface of sample A1.....	144
Figure 165 - Processed image of full sample minus crack.....	144
Figure 166 -Threshold value of the full sample without crack.....	144
Figure 167 -Prepared surface of sample E1.....	144
Figure 168 -Processed image of left side of the sample	144
Figure 169-Threshold value.....	144
Figure 170 - Part of polished section of sample EC3.....	145
Figure 171 - WEKA segmentation result [Green: Binder, Red: Clay particles, Black: Voids]	145
Figure 172 - Threshold value of Expanded Clay	145
Figure 173 -Threshold value of Binder.....	145
Figure 174 -Threshold value of voids.....	145
Figure 175 -Sketch for cutting the prism. Not to scale.	147
Figure 176 - Oven dried sawed samples	147
Figure 177- Oven for drying samples	147
Figure 178 - Epoxy Impregnation Setup	148
Figure 179 - Epoxy Impregnated Samples	148
Figure 180 - Polishing Machine.....	148
Figure 181- Ultrasonic Cleaner.....	149

TABLE OF GRAPHS –

Graph 1- Expanded Clay Gradation Curve	51
Graph 2 - Percentage of Aggregates Retained on different sieves.....	51
Graph 3- Normsand Particle Size Distribution Curve	57
Graph 4 -Comparison of Flexural Strength of Uncracked Specimens	66
Graph 5 -Comparison of Compressive Strength of Specimens	66
Graph 6 – Compressive Strength of 56 days healed samples compared to the surface crack width	67
Graph 7-Graph of 4-point bending test for Type 1 samples	68
Graph 8 -Graph of 4-point bending test for Type 2 samples	69
Graph 9 - Graph of 4-point bending test for Type 3 samples.....	69
Graph 10-Graph of 4-point bending test for Type 4 samples	70
Graph 11 – Permeability of Plain (Reference) Sample	71
Graph 12 -Permeability of PLA sample	71
Graph 13 – Permeability of Expanded Clay Sample	71
Graph 14 – Permeability of Alginate Sample	71
Graph 15.....	72
Graph 16 - Graph showing the comparison of permeability of different samples having a crack width of under 500µm	72
Graph 17-Graph showing the comparison of permeability of different samples having a crack width of higher than 500µm	73
Graph 18 - Surface Crack Width Progression for Type 1 (plain) Samples.....	74
Graph 19- Surface Crack Width Progression for Type 2 (PLA) Samples	74
Graph 20 - Surface Crack Width Progression for Type 3 (Expanded Clay) Samples.....	75
Graph 21 - Surface Crack Width Progression for Type 4 (Alginate) Samples	75
<i>Graph 22- Surface Crack Width Progression for Type 5 (External Healing) Samples</i>	<i>75</i>
Graph 23- Permeability efficiency vs change in surface crack width.....	86
Graph 24 – Healing efficiency vs Average current surface crack width.....	87

TABLE OF TABLES –

Table 1- Mix Designs and Materials used in literature	23
Table 2 - Mechanism of self-healing material.....	27
Table 3 – Classification of cements adapted from NEN EN 197-1.[28].....	28
Table 4 - Strength Classes according to NEN EN 197-1	29
Table 5 - Phase composition of Portland Cement [29]	29
Table 6 -Composition of various cements [29]	30
Table 7 -Percentage of sodium alginate used for making capsules and their corresponding hardness. [33].....	35
Table 8 -Physical properties of PE fibers	37
Table 9 - Overview of Mix Designs.....	58
Table 10-Parameters of the test – (Load controlled)	61
Table 11 -Parameters of the test – (Load controlled).....	62
Table 12 - Slump values of the mixes.....	65
Table 13 - Flow rate corresponding to the crack width and healing period. Crack width 500µm	72
Table 14- Flow rate corresponding to the crack width and healing period. Crack width higher than 500µm	73
Table 15 - Porosity of samples.....	80
Table 16- Particle Size distribution of Normsand	98
Table 17- Particle Size Distribution of Expanded Clay Aggregates	99
Table 18 - Specific Gravity, Apparent Specific Gravity and Water Absorption of Expanded Clay Aggregates.....	100
Table 19 - Reference Mix Design.....	101
Table 20 - List of ingredients in 1Kg of PLA capsules	101
Table 21 - Calculation for determining the quantities of the healing agent mix.....	101
Table 22 - Mix Design with PLA Capsules	102
Table 23 - Mix design for Expanded Clay Based Mix	103
Table 24 - Ingredients and their quantities for making Expanded Clay Capsules	103
Table 25- Ingredient list for making alginate-based capsules.....	104
Table 26 - Mix design for alginate-based capsules.....	104
Table 27 - Paste for External Healing	104
Table 28 - Photomicrographs of samples 1 week after cracking	105
Table 29- Photomicrograph of the samples after 1st permeability test (1 month healing duration)	119
Table 30 - Photomicrograph of the samples after 2nd permeability test (2 month healing duration).....	127
Table 31-Flexural Strengths of 7 days specimens	135
Table 32 -Flexural Strengths of 28 days specimens	135
Table 33 - Flexural Strength of 84 days uncracked samples	135
Table 34 – 7 days compressive strengths of specimens.....	136
Table 35- 28 days compressive strengths of specimens	136
Table 36 - 84 days compressive strengths of specimens	136
Table 37 -Compressive Strength of 56 days healed samples (Sample age :84 days).....	136
Table 38 - 1st permeability test	137

Table 39 - 2nd Permeability Test	138
Table 40 – Surface Crack width progression.....	139
Table 41 -Permeability Efficiency	145
Table 42 - Healing Efficiency	146

TABLE OF EQUATIONS –

Equation 1	26
Equation 2	30
Equation 6	31
Equation 7	31
Equation 3	32
Equation 5	32
Equation 4	32
Equation 8	102
Equation 9	102
Equation 10	85
Equation 11	87

Nomenclature

Abbreviations –

EC	Expanded Clay
HA	Healing Agent
PE	Polyethylene
PLA	Poly-Lactic Acid
CEM I	Portland Cement
ITZ	Interfacial Transition Zone
N	Normal Hardening Class of Cement
R	Rapid Hardening Class of Cement (Rapid early strength development)
L	Low Early Strength
AAS	Alkali-activated slag
ECC	Engineered Cementitious Composites
ASR	Alkali Silica Reaction
P / Type 1	Plain Mix
PLA / Type 2	PLA Mix
EC / Type 3	Expanded Clay Mix
A / Type 4	Alginate Mix
E / Type 5	Externally applied mix

1

Research Introduction

In this chapter, a general introduction to the background and state of the art of the current investigation into bacterial self-healing mortar is provided. This includes the problem statement and objective of this thesis, which can be derived from the research motivation. Finally, both the scope and outline of this thesis are presented.

1.1 Research context –

Mortar is a widely used building material. It is made of the same materials as concrete but does not contain coarse aggregates. Mortar is used as a protective cover on the structural concrete and is a durable and robust material, but it has a few drawbacks. When mortar sets, it undergoes shrinkage which causes microcracks. These microcracks become a weak link in the structure, as they tend to propagate over time which allows detrimental elements to weaken the structural concrete, and the structure as a whole loses its strength and durability.

Once concrete is damaged enough so as to affect the reinforcement, the structure as a whole is deemed unfit for service and needs to be demolished. Globally, most of the demolished concrete does not go into recycling and instead gets dumped into landfills. The environmental cost of producing new concrete is very high. So, if microcracks are repaired in time, then the concrete would not lose its structural integrity and would remain in service for a long time, which would be cost effective as well as sustainable. Therefore, there is a need to develop self-healing technology.

Self-healing of concrete refers to a matrix that can sense damages to itself and repair them on its own. Cement paste has an inherent capacity to heal cracks by processes, such as secondary hydration and swelling of unreacted particles. [1] This process of autogenous healing is slow and only a narrow crack can be healed i.e. width up to 0.2mm at 28 days [2]. While autonomic healing, heals concrete by incorporating microorganisms, fibers, capsules or glass tubes containing a repair agent [3-5]. Compared to autogenous healing, this method is more effective, and the healing effect is more controllable.

1.2 Research Problem –

The topic chosen in this study is “Self-healing, fibre reinforced mortar using bacteria”. There are many different types of bacteria, but the one chosen for this study are picked from literature. [3, 6-9]

There are several points that make this research new –

- Incorporating reinforcing fibres (6mm PE) with encapsulated bacteria, where the capsules are made of different materials.
- Comparing the efficiency of different types of capsules in self-healing.
- Comparing the effectiveness of internal and external application methods of healing.
- In all the sets of samples, the amount of bacteria i.e. number of bacterial spores and nutrient (healing agent) was kept equal.

1.3 Research objectives –

The objective of this research project was to study the self-healing of cracks in mortar matrix using bacteria and to find the most suitable encapsulation method for it. External application of the bacteria and nutrients was also investigated.

This research also observes the water tightness regain of the matrix, along with the flexural, compressive strength and compressive strength regain of samples depending on their crack width.

1.4 Research Scope –

There are many different types of cements and bacteria but in this study, the focus is on the bacteria *Bacillus cohnii* which is encapsulated and embedded in a fibre reinforced mortar sample made of CEM I cement.

The materials used for encapsulation are –

- PLA Capsules.
- Expanded clay particles
- Alginate based capsules

All of the above materials are impregnated with the healing agent which includes bacteria along with calcium lactate which provides the nutrients and yeast extract which provides the vitamin to the bacteria. [10]

The material used for external application is a paste of calcium lactate and yeast extract mixed with the bacteria.

1.5 Research Limitations –

This research only focuses on –

- Bacillus cohnii bacteria.
- One type of cement (CEM I) is used in the sample.
- The samples are made of mortar and have no coarse aggregate.
- The sample size is 40mm x 40mm x 160mm.
- 0.5 w/c ratio is considered
- One type of fiber is used as core reinforcement (6-mm-long polyethylene (PE) fiber.
- The percentage of fibers used in the matrix is 3.2% by volume of cement i.e. 0.5% by volume of mortar.
- The number of spores used in the samples is **7.5x10⁶spores/L of mortar**.
- Flexural and compressive strength of uncracked samples is checked at 7, 28 and 84 days after casting.
- At 8 weeks after induced cracking, compressive strength of healed samples is checked, and the percentage strength regain is found.

1.6 Research questions –

One main question that the research aims to address is that whether bacteria healing helps in water tightness regain i.e. healing of cracks in mortar. There are several research sub-questions that this study aims to answer, namely –

- How much would the compressive and flexural strength differ for different samples? And why?
- How much limestone (CaCO₃) is precipitated by each method?
- What is the maximum crack width that can be healed?
- How much would the compressive strength regain be at the end of the healing period?
- Which method of healing works the best, External or Internal? Why?

1.7 Research Theory and Methods –

The research proposed for this project is to create self-healing mortar using bacteria. The bacteria used in this study is readily available.

The bacteria in the study are encapsulated in different sets of capsules made of Polylactic Acid (PLA), expanded clay and calcium alginate.

These capsules are prepared and embedded in the matrix during casting of prism shaped mortar samples.

External application of the bacteria to a cracked sample is also carried out. The number of bacteria spores are kept equal in all the samples, in order to compare the efficiency

of the capsules that are used. PE fibers (6mm) are used to hold the sample together while cracks are induced.

There are several experimental methods used in this study to answer the research questions –

- Flexural strength (3-point bending) and compressive strength tests will be performed to understand the mechanical performance of the mortar samples.
- Optical microscopy will be used to observe the crack closure on the surface of the samples at monthly intervals.
- Permeability test will be performed to determine the crack healing in the samples, as the depth of the crack will not be visible during the healing process.
- At the end of the healing process, the samples will be cut, epoxy impregnated and polished to create polished sections. These sections will help in observing the limestone that is precipitated in the crack depth.
- Smooth slices of the samples can be used to find the porosity of the mixes using image processing software like ImageJ.

The minimum time required for the study is 3 months as the 1st month is required for sample preparation and 2 months for the healing process assuming the materials are readily available.

1.8 Outline –

This thesis can be divided into two parts. The first part is related to design and production of capsules while the second part is related to design and testing of mortar samples made with the capsules. Healing efficiency of different methods of application of healing agent is tested in this study so five different types of mortar mixes are investigated varying in the type of capsule used.

To investigate the effect of these capsules, as well as to verify the designs and quantify the relevant physical and mechanical properties of the mortar mixtures, several tests were conducted. These tests consisted of determining the mechanical properties and the efficiency of healing of cracks in the samples.

A literature study has been performed to support the design of the mortar mixture and to find a method and mix design for producing the capsules which help heal the cracks.

The first part of the thesis contains details on the production and tests conducted on the capsules. The second part of this thesis is focused on the mechanical properties of samples and understanding the mechanism behind it as well as conducting tests that relate the crack width to the efficiency of crack heal. This part also consists of calculations on healing efficiency and a discussion on the reliability of surface crack for understanding the healing inside the crack. The second part requires a considerable of input from the first part.

Details on the design of the thesis are provided under Design of the Experiment.

2

Literature Study

The first step of the research was to get a better understanding of the properties and behaviour of capsules, mortar and fiber used in the thesis. Hence, a literature study has been done

2.1 Overview -

A concrete structure is usually protected by a layer of mortar i.e. the cover. This is done to protect the underlying reinforced concrete, as most degradation occurs from the outside, which means that the cover layer is the layer that is damaged first [11]. Therefore, in order to protect the inside, the surface layer is made self-healing.

When cement sets, it undergoes shrinkage which causes microcracks. The combined effect of both the microcracks and the cracks induced by external factors lead to the degradation of the structure [12, 13] as these cracks tend to propagate further into the structure due to the effect of stresses and the influence of the natural elements, and eventually reach the reinforcement through the concrete underneath [14].

Cracks allow easy penetration of liquid and gas containing harmful substances into the concrete matrix. If microcracks grow and reach the reinforcement, moisture and other elements like sulphate and chloride ions would attack the reinforcement leading to its corrosion[12]. Sometimes, the corrosion products formed are expansive which leads to spalling of the structure [15-17]. So, to prevent the cracks from propagating, the concrete is made to be self-healing using healing agents.

These agents can consist of bacteria, fungi or epoxy resin and can be applied using various methods[15, 18]. They can be applied externally using sprays, can be embedded into the concrete directly while casting or can be encapsulated and embedded in concrete.

In this study, self-healing technology has been explored based on the encapsulated materials i.e., healing agents and the materials that are used to encapsulate the healing agent.

In the last decade, a lot of work has been done on self-healing concrete including the healing agent and the materials used for encapsulation. According to previous studies, PLA, light weight aggregates, alginate-based materials, glass [19] and soil based materials have been used as viable carriers for bacteria and inorganic healing agents [20]. The mechanism behind the working of the capsule is the same for all materials. The healing agent is encapsulated in the carrier and when a crack forms, the capsule breaks, releasing the bacteria which heals the concrete.

For self-healing concrete using bacteria, the most important factor is the pH tolerance of the bacteria, as the pH of concrete tends to go as high as 13. So, in this study the bacteria used are *Bacillus Cohnii* (DSM 6307, purchased from the German Collection of Microorganisms and Cell Cultures (DSMZ), Braunschweig, Germany) which according to (Jonkers, Thijssen et al. 2010) [8] and Tziviloglou, Wiktor [10] can withstand the high pH of concrete and can heal the matrix by precipitating CaCO_3 .

This section highlights the following topics –

- Mix Design for the mortar
- Materials used for Healing i.e. materials for capsules and healing agents
- Mechanisms for healing
- Permeability Test

2.2 Mix Designs and Materials used for healing –

Researchers have experimented with different mix designs and variety of healing agents and capsule types, over the years. According to existing literature there are several mix designs and materials used that have been used for self-healing.

Table 1- Mix Designs and Materials used in literature

Serial No.	Unit	Cement Type	Cement	Sand	Water	w/c ratio	Healing Agent	Healing Agent Type	Capsule Type	Additional			Ref.
1	%	CEM I 42.5N	21	52	11	0.5	16	Bacteria (Bacillus)	Expanded Clay	-			[21]
2	Ratio	CEM I	1	2	0.4	0.4	-	-	-	-			[22]
			1	1.95	0.4		0.05	Expansive admixtures and anhydrate gypsum	Urethane-based coagulant and a liquid rubber coating	-			
			1	1.92	0.4		0.08		Sodium carbonate and zeolite embedded with calcium stearate + mixing with calcium sulfoaluminate	-			
			0.65	1.80	0.4	0.35		Clinker particles replacing 15% cement and 10% sand	0.2 GGBFS				
3	kg/m ³	CEM I 42.5N	463	855 - 0.125/ 1mm	231.5	0.5	0	Bacteria (Bacillus)	Expanded Clay (1-4mm)	-			[23]
				825- 1/4mm			257			-			
				855 - 0.125/ 1mm 0- 1/4mm			280			-			
4	kg/m ³	CEM III/B	1060	-	424	0.4	0	-	-	Lime-stone Pwd.	PVA fibre	SP	[6]
			1036	-	415	0.4	26	Bacteria (Bacillus Cohnii)	PLA Capsule	530	26	2	
5	kg/m ³		1060		424	0.4	0			530	26	2	[3]

		CEM III/B	1048		419	0.4	13	Bacteria (Bacillus Cohnii)	PLA Capsule	524	26	2	
			1036		415	0.4	26			518	26	2	
			1014		406	0.4	51			507	26	2	
6	g	CEM I	130	320	65	0.5		Fusarium Oxysporum	Direct application	Water Reducer			[17]
										0.39			
7	kg/m ³	CEM I 52.5N	360	-	180	0.5	Fine LWA 405 Course LWA 525	Sodium Silicate	Expanded Clay coated with PVA		-		[24]
8	Ratio	CEM I 42.5N	C:S		-	0.45	-	Polymeric Precursor	Encapsulation with glass tubes		-		[5]
			1:3										
9	kg/m ³	CEM I 52.5	671	1342	302	0.45	0	Sodium Alginate and Calcium Sulphoaluminate cement particles	Polyethylene Glycol and epoxy Resin		-		[25]
			671	1274	287		80						
			604	1208	272		160						
10	Ratio	CEM I	1	3	-	0.5	Bacterial Sol - Nutrient Solution -	-	Dissolved in water used for casting	Zeolite	PVA fibers + HRWRA	[12]	
								-		-			
			2.836	-	-	0.25	0.25	S.pasteurii S.ureae		0.122			
11	g	CEM I 42.5N	450	1350	225	0.5	Bacterial Conc. = 8.8*10 ⁷ cfu/mL Modified Urea broth = Nutrient broth 4 g, NH4Cl 10 g, NaHCO ₃ 2.15 g, urea 20 g, Distilled water 100 mL	Sporosarcina pasteurii	External Healing				[26]

2.3 Mechanism of Healing –

From the section above Table 1, there are various methods tested by researchers for the purpose of healing cracks in cementitious materials. Each method has a different mechanism to heal cracks like limestone formation by bacteria or fungi, formation of hydration products and crack closure due to impurity ingress and spalled edges of the crack.

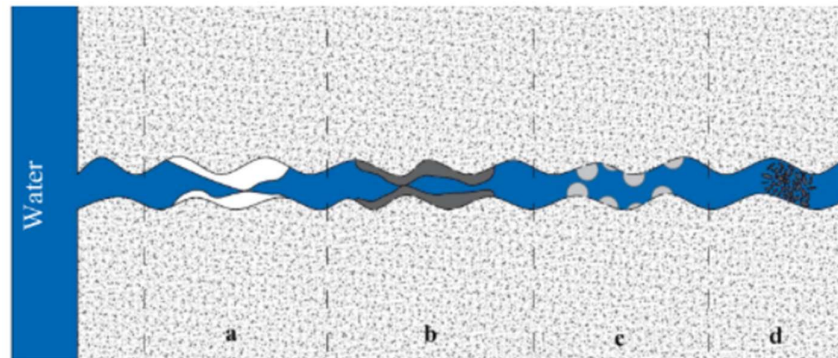


Figure 1 - Possible autogenous-healing mechanisms for crack closure: (a) Calcium carbonate formation; (b) hydration of anhydrous cement particles; (c) swelling of hydration products; (d) closure due to spalled edges and impurities.[14]

2.3.1 Biological Healing Agents –

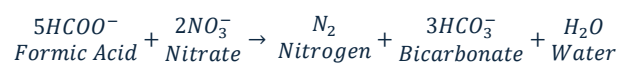
Several studies have used biological healing agents like bacteria and fungi. There is extensive research happening on both as there are multiple types of bacteria and fungi that can precipitate limestone. Calcium carbonate can be produced in cementitious materials in several ways depending on the metabolic pathways followed by bacteria or fungi [26].

The three most common bacteria for calcite precipitation are the ureolytic, denitrifying and aerobic bacteria.[14]

Bacteria like *Sporosarcina Pasteurii*, *Bacillus Sphaericus*, *Sporosarcina Ureae* and *Bacillus Megaterium* are ureolytic bacteria. These bacteria produce carbonate and ammonium ions by urea decomposition. The precipitate produced are inorganic homogeneous crystals [27].



Denitrifying bacteria, such as *Diaphorobacter Nitroreducens* and *Pseudomonas Aeruginosa* are capable of carbonate production even in the absence of oxygen by using nitrate ions.



While aerobic bacteria metabolise organic compounds under favourable conditions to form calcite.

Calcium carbonate formed as a result of bacterial activity can lead to water-tightness regain and minimization of penetration of harmful chemicals inside the concrete matrix. Additionally, calcium carbonate precipitated, is compatible with existing concrete with a good bonding capacity which can lead to the densification of the concrete matrix by filling up voids.

The cement, mortar or concrete matrix is embedded with capsules which upon matrix cracking, cracks open, which lets water and oxygen ingress into the sample. This ingress of water and oxygen activates the organic or inorganic healing agent which helps seal the crack and regain water tightness.

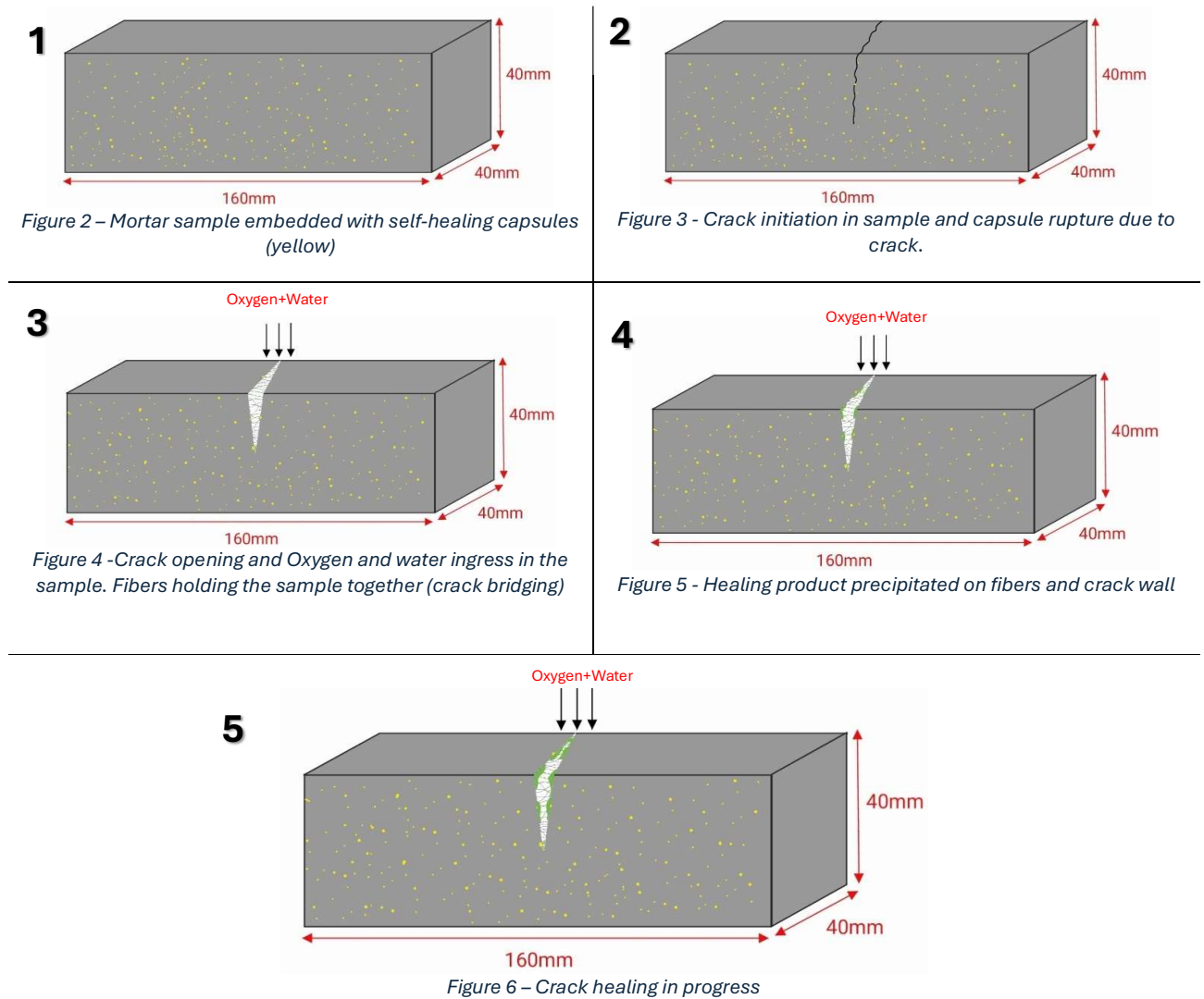
For this study the bacteria, bacillus cohnii is chosen as it can withstand the high pH of the cement matrix [10]. The healing mechanism for this bacteria is based on its capacity to precipitate CaCO_3 which is dependent on the amount of oxygen [6] and nutrition that it gets which in this case is yeast extract and Calcium Lactate [10]. The more nutrition and oxygen it gets, the faster and more amount of CaCO_3 is precipitated. The reaction is given below [8]–

Equation 1-Mechanism of the bacteria to precipitate calcium carbonate.



The figures below show the mechanism of self-healing in a mortar specimen.

Table 2 - Mechanism of self-healing material



2.3.2 Hydration of Cement –

Cement is a finely ground, inorganic material that forms a paste/slurry initially after mixing with water but over time this mixture hardens. The hardening of cement paste happens due to a chemical reaction between the components of the cement with water. This chemical reaction is responsible for autogenous healing of the microcracks i.e. 200-300 μm width. Therefore, knowledge of the ingredients present in cement is required to better understand the process of hydration of the cement.

2.3.2.1 Types and Classification –

Globally, the most used cement is Portland Cement, and its modified derivatives i.e. cements produced by replacement of Portland cement by adding other cementitious

materials like BFS, fly-ash etc. The classification of cements is mentioned in NEN-EN 197-1.

Table 3 – Classification of cements adapted from NEN EN 197-1.[28]

Main types	Notation of the 27 products (types of common cement)		Composition (percentage by mass ^a)										Minor additional constituents	
			Main constituents											
			Clinker	Blast-furnace slag	Silica fume	Pozzolana		Fly ash		Burnt shale	Limestone			
						natural	natural calcined	siliceous	calca-reous		L	LL		
K	S	D ^b	P	Q	V	W	T	L	LL					
CEM I	Portland cement	CEM I	95-100	–	–	–	–	–	–	–	–	–	–	0-5
CEM II	Portland-slag cement	CEM II/A-S	80-94	6-20	–	–	–	–	–	–	–	–	–	0-5
		CEM II/B-S	65-79	21-35	–	–	–	–	–	–	–	–	–	0-5
	Portland-silica fume cement	CEM II/A-D	90-94	–	6-10	–	–	–	–	–	–	–	–	0-5
	Portland-pozzolana cement	CEM II/A-P	80-94	–	–	6-20	–	–	–	–	–	–	–	0-5
		CEM II/B-P	65-79	–	–	21-35	–	–	–	–	–	–	–	0-5
		CEM II/A-Q	80-94	–	–	–	6-20	–	–	–	–	–	–	0-5
		CEM II/B-Q	65-79	–	–	–	21-35	–	–	–	–	–	–	0-5
	Portland-fly ash cement	CEM II/A-V	80-94	–	–	–	–	6-20	–	–	–	–	–	0-5
		CEM II/B-V	65-79	–	–	–	–	21-35	–	–	–	–	–	0-5
		CEM II/A-W	80-94	–	–	–	–	–	6-20	–	–	–	–	0-5
		CEM II/B-W	65-79	–	–	–	–	–	21-35	–	–	–	–	0-5
	Portland-burnt shale cement	CEM II/A-T	80-94	–	–	–	–	–	–	6-20	–	–	–	0-5
		CEM II/B-T	65-79	–	–	–	–	–	–	21-35	–	–	–	0-5
	Portland-limestone cement	CEM II/A-L	80-94	–	–	–	–	–	–	–	6-20	–	–	0-5
		CEM II/B-L	65-79	–	–	–	–	–	–	–	21-35	–	–	0-5
		CEM II/A-LL	80-94	–	–	–	–	–	–	–	–	6-20	–	0-5
	Portland-composite cement ^c	CEM II/B-LL	65-79	–	–	–	–	–	–	–	–	21-35	–	0-5
		CEM II/A-M	80-88	←----- 12-20 ----->										0-5
	CEM II/B-M	65-79	←----- 21-35 ----->										0-5	
CEM III	Blast furnace cement	CEM III/A	35-64	36-65	–	–	–	–	–	–	–	–	–	0-5
		CEM III/B	20-34	66-80	–	–	–	–	–	–	–	–	–	0-5
		CEM III/C	5-19	81-95	–	–	–	–	–	–	–	–	–	0-5
CEM IV	Pozzolanic cement ^c	CEM IV/A	65-89	–	←----- 11-35 ----->					–	–	–	0-5	
		CEM IV/B	45-64	–	←----- 36-55 ----->					–	–	–	0-5	
CEM V	Composite cement ^c	CEM V/A	40-64	18-30	–	←----- 18-30 ----->			–	–	–	–	0-5	
		CEM V/B	20-38	31-49	–	←----- 31-49 ----->			–	–	–	–	0-5	

^a The values in the table refer to the sum of the main and minor additional constituents.

^b The proportion of silica fume is limited to 10 %.

^c In Portland-composite cements CEM II/A-M and CEM II/B-M, in pozzolanic cements CEM IV/A and CEM IV/B and in composite cements CEM V/A and CEM V/B the main constituents other than clinker shall be declared by designation of the cement (for examples, see Clause 8).

The table above shows the type and composition of the cements. CEM followed by roman numerals denotes the type of cement and the alphabet following it denotes the clinker content in the cement where the clinker content decreases from A to C while the cementitious material increases from A to C. The next letter denotes the type of cementitious material that is added to the cement.

The standard also provides an indication of the standard strength (32.5,42.5,52.5) and early strength (N,R,L) of the cement. The class L is only applicable for CEM III cements.

Table 4 - Strength Classes according to NEN EN 197-1

Strength class	Compressive strength MPa			Initial setting time	Soundness (expansion)
	Early strength		Standard strength		
	2 days	7 days	28 days	min	mm
32,5 L ^a	-	≥ 12,0	≥ 32,5	≤ 52,5	≥ 75
32,5 N	-	≥ 16,0			
32,5 R	≥ 10,0	-			
42,5 L ^a	-	≥ 16,0	≥ 42,5	≤ 62,5	≤ 10
42,5 N	≥ 10,0	-			
42,5 R	≥ 20,0	-			
52,5 L ^a	≥ 10,0	-	≥ 52,5	-	≥ 45
52,5 N	≥ 20,0	-			
52,5 R	≥ 30,0	-			

^a Strength class only defined for CEM III cements.

The cement used in this thesis is CEM I 42.5N which consists of 95-100% clinker with a standard strength of 42.5MPa at 28 days and a normal early strength (N).

2.3.2.2 Chemical Composition –

Portland cement consists of various constituents in different percentages which make the cement unique. These percentages highly depend on the manufacturer.

Table 5 - Phase composition of Portland Cement [29]

Name of compound	Oxide designation	Abbreviation	Composition (% by mass)
Tricalcium silicate	3CaO.SiO ₂	C ₃ S	45-65
Dicalcium silicate	2CaO.SiO ₂	C ₂ S	10-30
Tricalcium aluminate	3CaO.Al ₂ O ₃	C ₃ A	5-15
Tetracalcium aliminoferrite	4CaO.Al ₂ O ₃ .FeO ₃	C ₄ AF	5-12

The table above shows the composition of clinker compounds in Portland cement.

Over the last century, researchers found that there are other materials which exhibit cement like properties which when mixed with Portland cement imparts different properties to the cement. The cements that consist of more than 5% of other cementitious materials are called blended cements.

Blended cements are now widely used, and their consumption is being promoted by government as their carbon footprint was found to be low as compared to Portland cement.

Table 6 -Composition of various cements [29]

Component	Composition (% by mass)			
	Portland cement	GGBS	Puzzolan	Fly ash
CaO	60-67	35-48	2-10	2-10
SiO ₂	17-25	28-38	48-71	45-65
Al ₂ O ₃	3-8	6-17	16-22	20-35
Fe ₂ O ₃	1-6	1-3	3-10	4-15

In the Netherlands, the most used type of cement is the GGBS (Granulated Blast Furnace Slag) cement where the blast furnace slag (BFS) comes from steel plants as it is a byproduct of steel manufacturing. GGBS has a much lower carbon footprint as compared to Portland cement as the clinker is the material that is responsible for the carbon footprint and CEM 1 cement contains 95-100% clinker while CEM III cement contains about 35-64% clinker.

2.3.2.3 Hydration Process –

Hydration is the process which hardens and strengthens cement. It is a set of complex exothermic reactions which gets triggered when water is added to cement.

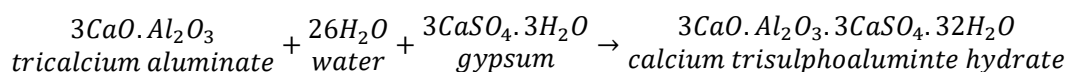
When water is added to the cement, the silicates and aluminates i.e. Tricalcium silicate (C_3S), Dicalcium silicate (C_2S), Tricalcium aluminate (C_3A), Tetracalcium aluminoferrite (C_4AF), form hydration products over time which produces a solid mass.

Initial Stage (15 minutes) –

The process starts immediately after the addition of water. Water penetrates the surface of the cement particles, dissolving some of the components into ions. C_3A dissolves in the water to create aluminate hydrate. This reaction is the fastest and can cause misunderstanding between setting and flash-setting which is the rapid hardening of the cement paste resulting in loss of workability. Flash setting can be overcome by vigorous agitation of the paste and by adding gypsum which is a retardant to the cement.

When C_3A dissolves in water and reacts with gypsum, it forms ettringite which is an aluminate hydrate called calcium tri-sulphoaluminate hydrate. The ettringite is formed on the surface of the cement particles which obstructs the interaction between the water and the cement. Hence, obstructing further hydration of cement.

Equation 2



Dormant Stage (2 hours) –

Following the first stage, the rate of reaction slows down, and the paste remains workable for a period as ettringite crystals are too small to bridge the gap between two particles, so stiffness is not developed. This induction period can last from one to three hours, during which little heat is evolved, and the paste can be manipulated. This period is crucial for the placement and compaction of the concrete.

Acceleration Period (12 hours) –

After the induction period, the main hydration reactions accelerate. This acceleration happens due to the growth of big ettringite crystals at the expense of the smaller ones. This creates space for water to get through to the cement grain and the surface layer of ettringite is broken down.

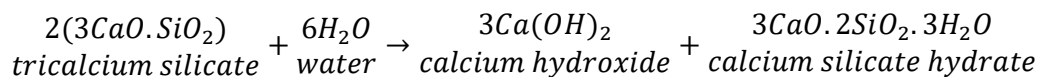
This phase is marked by the rapid formation of hydration products like CSH and CH and release of heat. Inner and outer CSH are produced during this period by dissolution of C_3S . These hydration products are formed outside and inside anhydrous cement particle.

Outer CSH is formed in the space between the cement particles. As the hydration reaction progresses, the outer CSH grows outward from the surfaces of the cement grains.

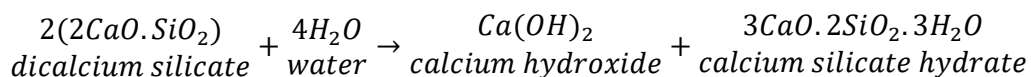
Inner CSH is formed inside the original boundary of the cement grain. As water penetrates the cement particles during the acceleration period, hydration continues inward, producing inner CSH within the grains.

The formation of both inner and outer CSH during the acceleration period significantly contributes to the development of the concrete's strength and overall microstructure.

Equation 3



Equation 4

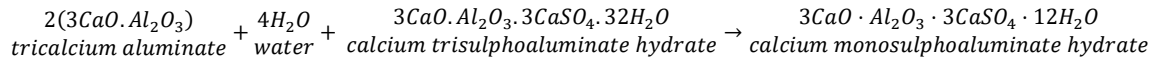


Deceleration Period (24 hours)–

Once the CSH is formed, it obstructs the interaction between the water and the cement particle. This results in slowing down of the reaction and the cement enters a deceleration period.

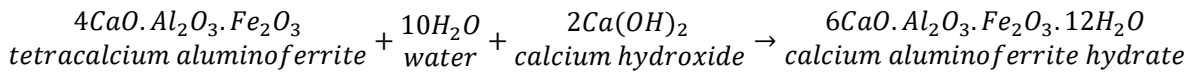
During this period, the ettringite becomes unstable and transforms into monosulfate (calcium monosulfoaluminate hydrate), by the consumption of C_3A and water.

Equation 5



Also, during this stage, hydration of C_4AF becomes noticeable. C_4AF reacts with CH produced in the previous stage to produce calcium aluminoferrite hydrate which, like the reaction products of C_3A , only regulates the hydration process and the durability of the hydrated cement paste.

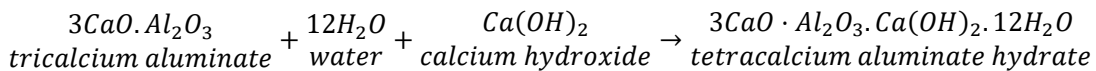
Equation 6



Steady State (infinite) –

Following the exhaustion of gypsum, the remaining C_3A reacts with water and calcium hydroxide, a product of the hydration of C_3S and C_2S , to form C_4AF .

Equation 7



During this stage, hydration proceeds very slowly, and the remaining anhydrous cement particles continue to react over time, leading to further development of the microstructure and strength of the concrete. Secondary ettringite formation is also associated with this stage.

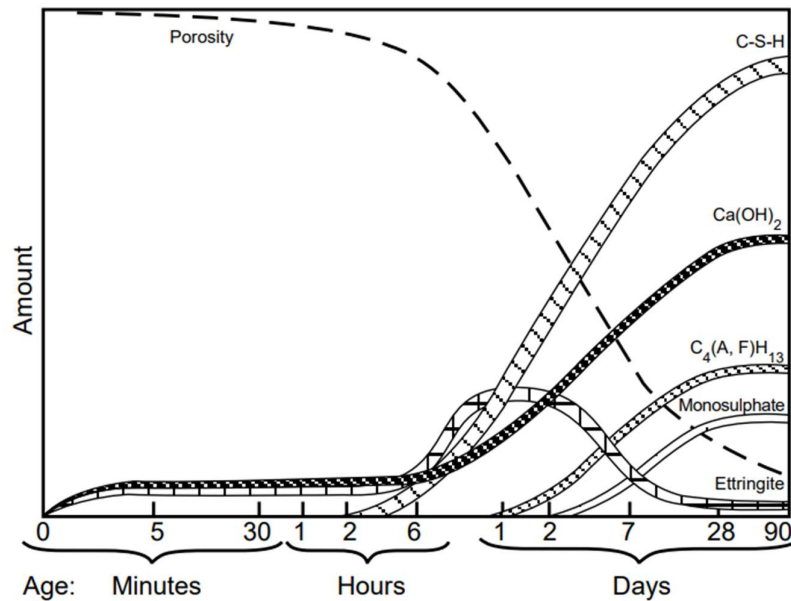


Figure 7-Schematic illustration of formation of reaction products over time in Portland cement paste [30]

As the process of hydration progresses, the porosity of the cement matrix decreases as the hydration gels fill the space between the cement particles.

2.4 Capsule Research –

Capsules are small particles containing healing agent. Research has been done on capsules for quite some time. There are various methods to make viable, healing agent filled capsules, according to the material of the capsules.

2.4.1 Expanded Clay Capsules –

Tziviloglou, Wiktor [10] checked the best way of preparation of expanded clay capsules. They checked 4 types of samples which are listed below –

- No Vacuum and low feed (calcium lactate and yeast extract) [NV-L]
- No Vacuum and high feed [NV-H]
- Vacuum and low feed [V-L]
- Vacuum and high feed [V-H]

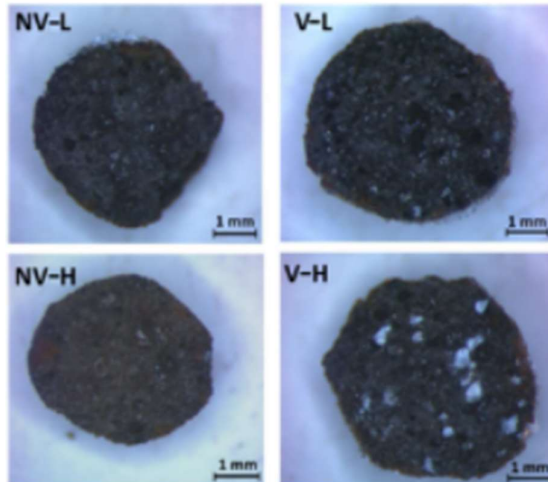


Figure 8 - Expanded Clay Particles with different impregnation types [10]

The results found that the by using the V-H method, expanded clay particle retains the most amount of healing agent within itself followed by V-L method. As for the No Vacuum methods, the healing agent only coats the surface of the particle.

They also checked for the best drying process and found that cooling the sample at 4°C for 24 hours and then at 20°C was the most effective drying process. The solubility of calcium lactate drops when the sample cools, while the water evaporates leaving behind nutrient residue inside the expanded clay particle.

2.4.2 Alginate Capsules –

Alginate capsules are made by crosslinking of sodium alginate and calcium lactate. Sodium alginate is a polysaccharide, extracted from brown seaweed and calcium lactate is a white crystalline salt consisting of two lactate anions for each calcium cation. It is commonly used as a food additive.

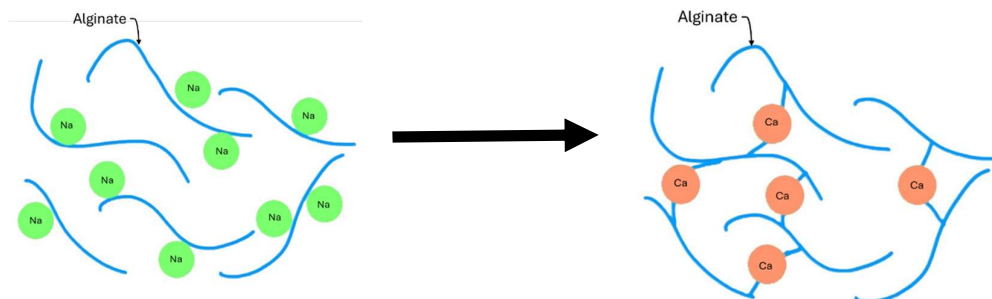


Figure 9 - Sodium Alginate conversion to Calcium Alginate

When sodium alginate reacts with calcium lactate, a three-dimensional gel network is formed, often referred to as an “egg-box” structure, due to the specific arrangement of the alginate chains around the calcium ions. [31]



Figure 10 - Alginate beads showing the "egg-box" structure

For alginate capsules, there are various methods used to prepare the capsules. Abbasiliasi, Shun [32], prepared gelatine-sodium alginate capsules and found that the thickness of the capsule shell influences the physicochemical properties of the shells, such as colour and transparency, water-holding capacity, strength and rupture time.

The hardness of capsules should be such that the capsules should break when cracks are induced while they should not be too soft that they break while mixing. So, before making the capsules, the percentage concentration of the sodium alginate was checked in this study.

Table 7 -Percentage of sodium alginate used for making capsules and their corresponding hardness. [33]

Concentration of sodium alginate	Sodium alginate solubility at 35 °C	Color of microcapsules	Shape of microcapsules	Hardness of microcapsules
0.5%	Very good	Colorless	Irregular	Soft
1%	Very good	Colorless	Irregular/ circular	Resilient
2%	Very good/ good	Slightly turbid	Circular	Resilient
3%	Good	Slightly turbid/ yellowish	Circular	Resilient/ hard
4%	Good/ poor	Turbid/ yellowish	Circular	Hard
5%	Very poor	Yellowish/ brownish	Circular	Hard

The process of making the capsules was described in Fahimizadeh, Diane Abeyratne [4]. The same process for making capsules has been used in this study which is described under section 4.2.3.2 Alginate Capsules – on page 49.

2.4.3 PLA Capsules –

Polylactic Acid (PLA) capsules are small, irregular shaped capsules which contain 2.1% by weight yeast extract, 0.1% by weight bacterial spores and 97.8% by weight PLA. The

PLA acts as the nutrient for the bacteria. When water reacts with the PLA shell of the capsule, the PLA hydrolyses to form lactic acid which becomes the food for the bacteria. The lactic acid produced, neutralises some of the alkalinity of surrounding matrix [6]. This reduces the pH of the matrix which creates a more favourable environment for the bacteria to thrive.

According to literature, [34] the addition of PLA capsules can alter the fracture properties of the material by introducing new ITZ and by deviating crack path, possibly even increasing the crack widths and therefore having contradictory effects on self-healing ability.

Also, studies found that PLA capsules which were activated by cracks had the outer layer converted into calcium carbonate which restricted further hydrolysis of the PLA and thus limited the discharge of bacterial spores. This behaviour of the capsule is beneficial as preservation of certain portion of the capsule can produce a repeated healing effect, when the material is damaged again while on the other hand the self-limiting behaviour of the PLA capsule is detrimental as it impedes the pace of crack-healing by limiting the number of spores and nutrients released by each particle.[3]

2.5 Polyethylene Fibers –

Fibers have been extensively studied and used in cementitious materials. The idea behind using fibers is to create a network inside the material which in case of material damage holds the piece together. Fibers also help in increase the strength of the cementitious material in tension as concrete structures are strong in compression but not tension. These fibers act as small reinforcement providing tensile support.

Fibers have been roughly divided into natural and polymer fibers depending on their origin.

Polyethylene (PE) fibers are thermoplastic polymeric fibers. It is made from the polymerization of ethylene and is a member of the family of polyolefin resins. In recent times PE fibers have been used in cementitious materials to create Engineered Cementitious Composites (ECC) [35]. These fibers are lightweight, low cost and have good physical and mechanical properties. They have the following characteristics –

- High tensile strength
- Low density
- Good resistance to chemicals
- Low moisture absorption
- Impact resistance

Concrete structures are exposed to a variety of environments. It is inevitable for them to experience damage and fracture. PE fibers when used in cement paste imparts a

resistance to sulphate attack, chloride ingress and helps control the mechanical damage caused. [36]

Table 8 -Physical properties of PE fibers

Length (mm)	Diameter (μm)	Density (kg/m^3)	Nominal Tensile Strength (MPa)	Young's Modulus (GPa)	Elongation at Break
6	20	980	3000	110	3%

The table above shows the physical properties of the PE fibers that are used in this study.

The behaviour of PE fibres in cementitious materials was found from previous literature.

Tensile Behaviour –

When PE fiber reinforced cementitious materials were subjected to tensile tests good stain hardening behaviour was observed along with multiple fine cracks which was a significantly different behaviour from normal concrete. The observed tensile strength was highest when the fiber content was 2.5%.

Flexural Behaviour –

According to Said, Razak [37] , two types of ECC were tested in flexural, one with PE fibers and the other with PP Fibers. The results showed that the PE fibers raised the ultimate load and deflection of the PE-ECC slab as compared to the PP fibers. Multiple cracks were observed in the mid-section of the PE-ECC slab.

It was also observed that PE-ECC had a better flexural performance than PP-ECC.

Ahmed, Maalej [38] also observed the influence of different ratios between PE fibers and steel fibers in cementitious composites. The samples were subjected to four-point bending test were evaluated. The composite with 1% steel fibers and 1.5% PE fibers had the highest flexural strength. The composite with 0.5% steel fibers and 2% PE fibers presented the highest deflection and flexural toughness.

Compressive Behaviour –

With the addition of any material into a continuous solid, there is a decrease in strength due to the induced discontinuity of the solid material. With the addition of PE fibres, it was observed that the compressive strength decreased. This could also be due to the increase in porosity.

Young's modulus and strain capability increased with compressive strength, while toughness decreased. The Poisson ratio had almost no relationship with the compressive strength. The compressive strength increased with the reduction of water/cement (w/c) ratio since a lowered w/c ratio decreased porosity and led to a more compacted structure.[39]

Bond Behaviour –

According to Said, Razak, the interface between PP fibers and the matrix was weak and the tensile strength and stiffness of PP fibers were low. While the bonding between the PE fibers and the matrix was comparatively better and hence the PE-ECC slab showed a higher flexural strength due to the PE fiber's high tensile strength and elastic modulus. Hence, PE-ECC was preferred in the concrete slab.

According to another study, Xu, Wan [40], where they compared the influence of PE, PVA and steel fibers, it was found that PE fibers and steel fibers had fewer reaction products adhered to them as compared to PVA fibers. It indicated that the reinforcement effects of PVA fibers on the AAS matrix included both friction bonding and chemical bonding, whereas PE and steel fibers had only friction bonding to the matrix.

2.6 Durability and Permeability –

Durability and Permeability are important properties of a material which influence the performance and lifespan of a structure.

Durability refers to the ability of a material to withstand environmental conditions and processes while maintaining its desired engineering properties over its service life. The processes that affect the material depends on the type of environment it is used in.

There are different types of degradation mechanisms that affect the durability of cementitious materials like –

- Chemical Attacks: Attacks from chemicals like sulphates, chlorides, and acids, which can cause deterioration of the structural reinforcement.
- Freeze-Thaw Cycles: Freezing and thawing cycles can cause cementitious materials to crack or spall over time. Water enters cracks in the mortar/concrete and freezes. Water when freezes, expands which causes the crack to expand and when the ice thaws, more space is created for new water to enter. This cycle continues and hence facilitates the propagation of the crack.
- Abrasion: Surface wear due to mechanical action.
- Alkali-Aggregate Reactions (ASR): Expansive reactions between alkali hydroxides (Na, K) in the cement and reactive aggregates which forms alkali silica gel. This gel when comes in contact with water, absorbs water and swells which creates an internal pressure in the surrounding matrix, creating cracks.
- Exposure to high temperatures: Exposure to high temperatures can reduce the durability of concrete/mortar to fall due to various reasons.
 - At temperatures above 100°C, free water evaporates which leads to drying shrinkage and microcracking. This also creates additional voids in the material structure.
 - Chemically bound water in the hydrated products like CSH, evaporates leading to reduction of strength.

- At temperatures above 400°C phase change occurs such as decomposition of CH which decomposes to calcium oxide and water.
- At temperatures above 700°C CSH decomposes
- Differential thermal expansion of aggregates and the matrix

All these factors lead to decrease in durability and strength of the structure and an increase in permeability and porosity.

Concrete structures are classified according to their level of exposure based on the environment to which they are exposed. These are called exposure classes and are provided in standards (NEN-EN 206).

Since degradation of concrete is linked to the infiltration of harmful substances into the material through cracks, the durability of the concrete is connected to permeability which is defined as the ease of flow of fluid through a porous medium. The permeability of a cementitious material is influenced by the properties of the hardened cement paste.

There are several factors on which permeability of cementitious materials depend on –

- Total volume of pores – A higher total pore volume leads to higher permeability because there are more voids through which fluids can travel and the chance of them being connected is more.
- The relative size of pores – Larger pores facilitate easier fluid flow which increases permeability. Conversely, smaller pores restrict fluid movement, reducing permeability. However, even a few large pores can significantly increase permeability if they are well connected.
- Degree of hydration - Higher degree of hydration results in a denser concrete matrix with fewer and smaller pores as the hydration products fill up voids, reducing permeability.
- W/C ratio of the mix – A higher w/c ratio leads to more porosity in the mix which results in a higher number of pores.

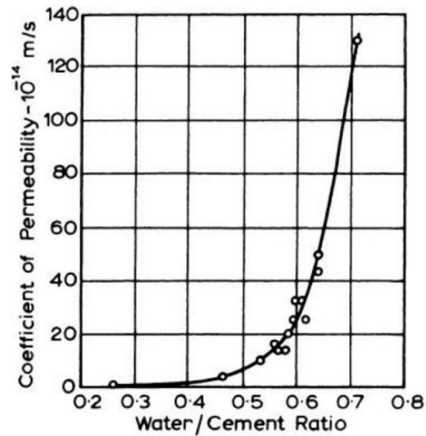


Figure 11 - Relationship between permeability and w/c ratio

- The connectivity of pores – Interconnectivity of pores creates pathways for fluid flow which increases permeability.
- Cracks - Cracks provide a path for water, ions, carbon dioxide and oxygen to penetrate the concrete. Microcracks if connected to voids of other cracks or microcracks can increase permeability. While large cracks restrict the local water tightness of the material.

Entrapped air and pores within the aggregates can also influence the permeability, but as the volume of entrapped air is generally much less than that of the capillary pores while aggregate pores are usually discontinuous, their contributions to permeability are insignificant.

Permeability is an important parameter while studying self-healing materials. This parameter has been used as an evaluative tool and there no standardized method for quantifying self-healing in a material. The method for performing this test is different for different researchers. As no standardized method is available, there are variations observed in the results for cracks of the same width. It has been theoretically proven that some parameters related to the test setup influence the results.[41]

The relation between the water flow rate and the initial crack width is (third power of the crack width). An example of which is shown in the figure below.

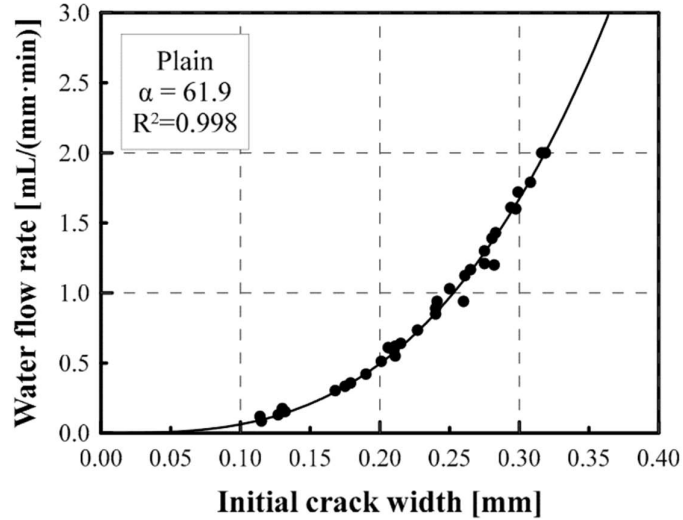


Figure 12 - Relationship between water flow rate and initial crack width for 160 plain mortar samples [22]

The higher the crack width, higher is the permeability of the material. This indicates that the material is more prone to deterioration and is less durable. In the context of self-healing, permeability serves as an indicator of healing. As the material heals, the crack seals itself and the permeability (water flow rate) decreases.

2.7 Effect of self-healing components on mortar mixes –

The table below has been constructed from the results found from previous studies. The table shows the influence of different microorganisms and encapsulation methods on compressive and flexural strength and durability of mortar.

Microorganism	Encapsulation	Effect on compressive strength		Effect on flexural strength		Effect on Durability			Ref.
		Effect	Days	Effect	Days	Permeability	Water Absorption	Days	
Bacillus subtilis	Direct	P	3	-	-	P	P	7	[13]
		P	7	-	-				
		P(31M Pa)	28	-	-				
S.Pasteurii	Direct	N	7	-	-	-	P	121	[12]
		N	14	-	-	-	P	182	
		P	28	-	-	-	P	243	
		P	60	-	-				
		P	90	-	-				
		P	180	-	-				
		P	270	-	-				
S.ureae	Direct	N	7	-	-	-	P	121	
		N	14	-	-	-	P	182	
		P	28	-	-	-	P	243	
		N	60	-	-				
		P	90	-	-				
		P	180	-	-				
	P	270	-	-					

Bacillus pseudofirmus	Alginate			N	7 days				[4]
				P	7+28 days				
				P	7+56 days				
Inorganic material	Sodium alginate and calcium sulphoaluminate	N – 5% capsules	28 days	N- 5% capsules	28 days	P	-	1	[25]
								3	
		N – 10% capsules	28 days	N– 10% capsules	28 days	P	-	1	
								3	
Bacillus Cohnii	Expanded Perlite	N	28 days	-	-	N		28	[42]

P: Positive effect i.e. better than the control specimen

N: Negative effect i.e. worse than the control specimen

3

Design of the Experiment

Before diving into the experiment phase, planning is required. This chapter focuses on the design of the study while creating some hypothesis for the study.

3.1 Experiment Process –

The study starts with determining the size of samples that can be used. So, the shape of samples chosen was prism samples according to NEN-EN 196-1[43], with dimensions 160mm x 40mm x 40mm as shown in Figure 2.

Then the method for making capsules was studied and finalised from literature. The PLA capsules were readily available while the expanded clay capsules [Page 48] and alginate capsules [Page 49] were prepared. After making the capsules, the properties of the capsules was studied which provided information that was needed to design a mix for the samples. More details regarding the capsules and mixes are given in the following chapters.

A w/c ratio was 0.5 was considered for this study. Then mixes for each type of capsule was volumetrically designed so in total 4 mixes were made for 5 different types of specimens. The different types of samples and their ingredients are shown below.



Figure 13 - Sample types and their contents

Samples needed to be allocated to different tests. So, a well-made sample allocation plan was required. For this purpose, a chart was drawn get a better understanding of the number of samples required for the experiments.

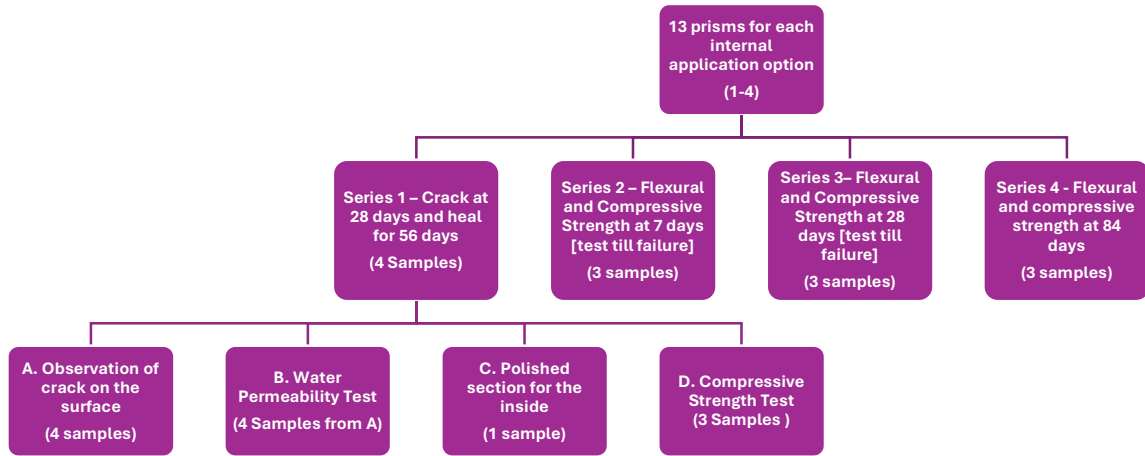


Figure 14- Flowchart of Internal application samples.

The flowchart above shows the number of samples required for specimen types 1 to 4 (Internal Application). While the chart below shows the number of samples required for Type 5 specimen (External Application).

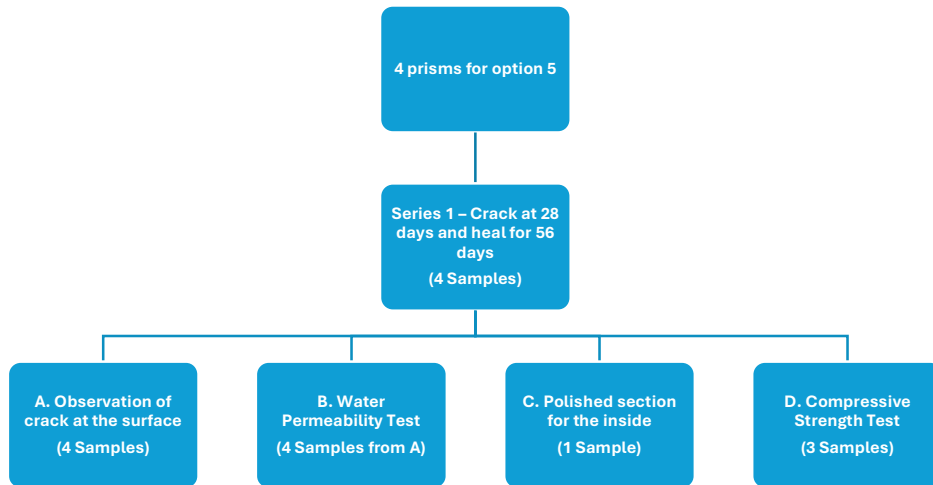


Figure 15 - Flowchart of External Application Samples

The samples at 7,28 and 84 days after casting underwent flexural and compressive strength testing while some samples were subjected to 4-point bending at 28 days. This test was done to better understand the material behaviour in flexural mode and also to induce cracks in the sample as fiber-reinforced samples usually form V-shaped multiple cracks next to each other. These samples are then observed using optical microscopy at monthly intervals for crack mouth healing and permeability. At the end of the healing period i.e. 2 months, these samples went through a compressive strength test to check

the strength regain. While one sample of each type was selected for electron microscopy (element mapping) and to check the depth of crack heal.

3.2 Hypotheses –

There are a few theories that can be hypothesised prior to the experiment –

- The healed samples would give a higher compressive strength than the samples that are healed with autogenous healing i.e. reference samples.
- The compressive strength of the healed samples would be less than the strength of the pristine samples.
- Type 2 sample (PLA Capsules) –
 - PLA capsules are the smallest in size, hence their incorporation in the matrix would cause less discontinuity which implies that they would give a higher strength in flexural.
 - As the number of spores in each capsule is less, to achieve an equal number of spores in each litre of mortar, the number of capsules required is high. So, their distribution in the matrix is dense, which increases the chance of the capsules rupturing because of a crack. This means that the healing for Type 2 samples should be higher than the rest of the samples and the permeability of these samples would be lower than the other samples.
- Type 3 sample (Expanded Clay Capsules) –
 - Low flexural strength due to bigger and overlapping ITZ.
 - Good Compressive strength due to the spherical shape of the capsules which could distribute the load well.
 - Good healing as the quantity of capsules is high.
- Type 4 sample (Alginate Based Capsules) –
 - Healing rate and strength regain is expected to be the lowest as the capsules are sparsely distributed which makes their chance of cracking lower.
- Type 5 –
 - Healing rate and strength regain is expected to depend on the amount of paste that adheres on the sample. If the paste is washed off by the water used in curing the sample, then the rate of healing and strengthening will be lower.
- In case of a deep crack, the expected outcome is the fibres would hold the sample together while the bacteria would heal the crack. Also, it is expected that the smaller capsules would work better than the larger expansive clay capsules as the ITZ would be less in case of the smaller capsules

4

Materials and Methods

Before a material can be tested for mechanical properties, the material must be designed and the constituents of the material need to be prepared and tested. This section describes the materials used, their method of preparation and the tests that have been conducted on them. The first part of this chapter has been dedicated to preparation and testing of capsules while the second part is focused on mortar specimens.

4.1 Healing Agent –

As the name suggests, healing agent is the component of the capsule that is responsible for healing the material. In this study the healing agent is a three-part substance which contains a mixture of bacteria, calcium lactate and yeast extract.

4.1.1 Bacteria –

The bacteria used in this study is *Bacillus Cohnii*. It is a specie of bacteria belonging to the genus *Bacillus*. The alkaline bacterial species *Bacillus cohnii* DSM 6307 was obtained from the German Collection of Microorganisms and Cell Culture (DSMZ), Braunschweig, Germany.

4.1.2 Calcium Lactate –

Calcium lactate is a white crystalline salt which is used as a nutrient for the bacteria. The bacteria converts the calcium lactate into lactic acid which it then uses as nutrient for growth.

4.1.3 Yeast Extract –

Yeast extract is used as vitamin for the bacteria. The yeast extract used in this study is BBL Yeast Extract which is the extract of autolysed yeast cells.

4.2 Capsules –

4.2.1 Introduction –

Capsules small, enclosed containers, usually made from gelatine or a polymer but in some cases clay. These capsules are designed to hold substances within them. In case of self-healing, capsules are designed to be containers which carry the healing agents.

This experiment studies the efficiency of different types of capsules in healing the cracks in a mortar sample. The materials for capsules chosen in this study were required to satisfy some criteria. The requirements are listed below–

- The capsules should be less stiff than the matrix. This is to ensure that the capsule breaks when the sample is cracked.
- The capsule size should be comparable to that of sand.
- The capsules should be made of either readily available materials or should be easy to make.

The capsules compared in this study are of three types –

1. Expanded Clay Capsules
2. PLA Capsules
3. Alginate Capsules

The capsules contain the same amount of healing agent so that the amount of healing efficiency can be compared.

Capsules were prepared using readily available materials.

4.2.2 Capsule Materials –

4.2.2.1 Expanded Clay Capsules –

Expanded clay is a lightweight aggregate which is made by heating clay in a kiln at 1200°C. Expanded Clay used in this study is Liapor 1-4mm which are round, porous aggregates. These aggregates act as a carrier due to their porosity which allows the healing agent to be absorbed within themselves. The method for making the capsule is provided under capsule preparation.

4.2.2.2 PLA Capsules –

These capsules are made of polylactic acid (97.8% by weight) and are filled with yeast extract (2.1% by weight) and bacteria (*Bacillus Cohnii*) (0.1% by weight). These bacteria based polylactic acid capsules are produced by Green-Basilisk B.V., The Netherlands.

4.2.2.3 Alginate Capsules –

Alginate capsules are made by the crosslinking of a mixture of sodium alginate, bacteria and yeast extract with a calcium lactate solution. These capsules are manually prepared, and the method of preparation is provided in the following section.

4.2.3 Method for Preparing Capsules –

The following part describes the method of preparation of capsules.

4.2.3.1 Expanded Clay Capsules –

According to (Tziviloglou et al. 2015) [10], the best way to impregnate expanded clay particles is by vacuuming the healing agent using an epoxy impregnation machine and then freezing the particles for 24 hours at 4°C then store them at room temperature.

Although this method is the best, it is not easy to replicate in practice and it is not feasible for large volumes, as it requires specialised equipment. So, in this study the expanded clay particles have been impregnated using only their own absorption capacity.

Ingredients and Equipment Required –

- Hot Water
- Calcium Lactate
- Bacteria
- Yeast Extract
- Expanded Clay
- Bucket
- Weighing Scale
- Stirrer

Method -

To prepare expanded clay capsules, water was taken in a bucket, the mass of which was equal to 15% of the volume of expanded clay required in the mix design [Table 23, Table 24] as the mean absorption capacity of the expanded clay aggregates was found to be 15%. Then water was heated to 60°C, as it leads to an increase of solubility of calcium lactate, then calcium lactate powder was added to it. Once dissolved, bacteria were added to the solution followed by yeast extract. Care was taken to ensure that the water was not too hot for the yeast extract to be added to it. Yeast extract has a shorter temperature tolerance range as compared to the bacteria. At the end, the expanded clay particles were added to the solution and was left untouched for the HA solution to get absorbed until there was no solution left in the bucket to be absorbed.

4.2.3.2 Alginate Capsules –

These capsules were made using the spherification method as specified in previous literature [4]

Ingredients and Equipment Required –

- Water
- Sodium Alginate
- Calcium Lactate
- Bacteria
- Yeast Extract
- Weighing Scale
- Beakers
- Magnetic Stirrer with heater
- Syringe
- Sieve

The method of making alginate-based capsules is given below and the quantities of ingredients are mentioned in Table 25.

All ingredients were weighed using a weighing scale according to the quantities required. A lump-free mixture of sodium alginate and water was prepared. Bacteria and yeast extract were added to this solution once the solution cooled down and mixed until the solution had a uniform yellow tint to it. On the other hand, a mixture of calcium lactate and water was prepared. Then using a syringe (without needle) sodium alginate solution was manually dropped into the calcium lactate bath, such that small uniform beads were formed. The syringe was kept at a height of 2cm above the bath. The capsules were transferred to an oven at 40°C for 24 hours for dehydration.

4.2.4 Tests on Capsules –

Several tests were conducted on capsules to better understand their behaviour. These tests are detailed below.

4.2.4.1 Particle Size Distribution –

Particle size distribution is a test performed to determine the size of particle in the aggregate mix. There are different types of materials used in this study, some of whose particle size distributions are predetermined. [44]

4.2.4.1.1 PLA Capsules –

For PLA capsules a sieving test was not performed as according to previous literature[3], the PLA capsules have a particle size distribution between 0.1 and 1.0 mm with a density of 1200Kg/m³.



Figure 16- Measurements of PLA capsules. Scale- 1000µm

4.2.4.1.2 Expanded Clay –

The expanded clay of size 1-4mm was taken for this study. The particle size distribution of the expanded clay was seen by sieving using a sieve shaker.

Method –

Sieves of different aperture sizes, ranging from 4mm to 53µm were taken [Table 17]. 1Kg of the sample was fed into the sieves and the sieves were shaken for 20 minutes for all the particles to be well sieved. After the sieving process was complete, the weights of all particles retained on each sieve was measured. From the test it was found that the expanded clay was in the range of 1-4mm but most of the aggregates were retained on the 2mm sieve which indicated that most of the aggregates were between 4 and 2mm. So, aggregates >2mm and < 4mm were not discarded.

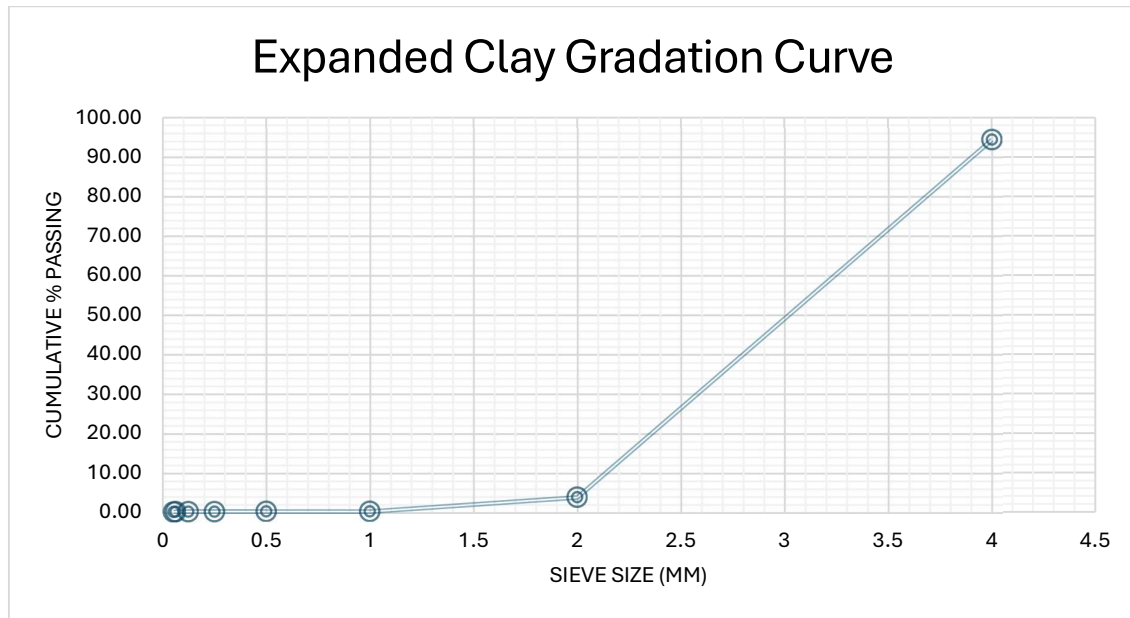
The results of the particle size distribution are tabulated in Table 17 (appendix).

A gradation curve was made based on the data obtained from the test. [Graph 1]



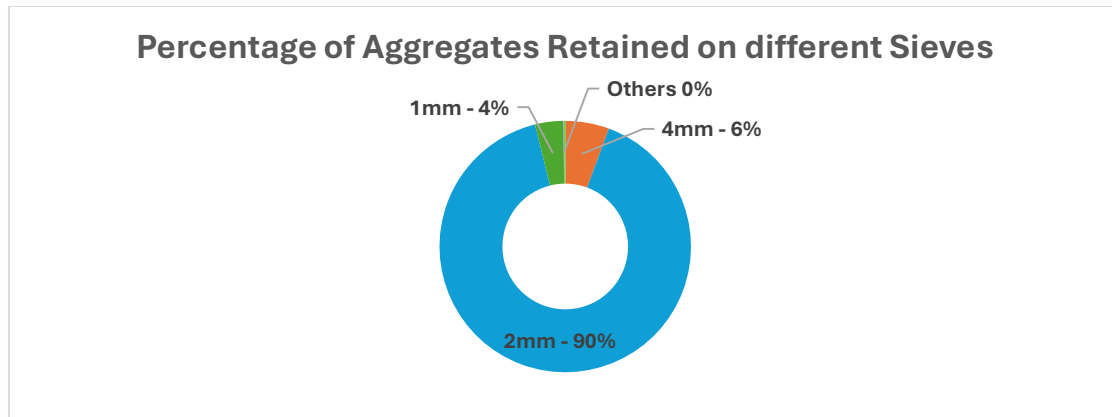
Figure 17 - Sieving of expanded clay particles in a sieve shaker.

Graph 1- Expanded Clay Gradation Curve



From the graph above, the aggregates could be seen as open graded.

Graph 2 - Percentage of Aggregates Retained on different sieves.



4.2.4.1.3 Alginate Capsules –

The capsules after being prepared, as mentioned later under method for making capsules, were observed under an optical microscope. The size of particles were observed to be in the range of 2.5-3mm.



Figure 18-Alginate capsule. Scale :1000μm

4.2.4.2 Specific Gravity and Water Absorption –

Water absorption test is used to evaluate the water absorption capacity, specific gravity and apparent specific gravity of aggregates. It requires sieves, pycnometers, water, weighing scale, oven and towels/tissues.

The specific gravity and water absorption of the capsules was found in order to determine the mix designs later. These tests were performed according to NEN-EN 1097-6.[45]

4.2.4.2.1 Expanded Clay –

These particles have a porous microstructure which would absorb water from the mortar mix, making the mix less workable. Thus, determining their water absorption is very crucial for designing a workable mix design. The water absorption was determined by using the pycnometer test. The specific gravity was found to be 0.7, apparent specific gravity was 0.76 and the water absorption was found to be 15%. (Appendix)

During the water absorption test, it was observed that most of the expanded clay particles were less dense than water as they floated upwards. After 24 hours of being submerged, the portion of floating particles did not significantly change which indicated that the particles had entrapped air them and the voids were not connected.



Figure 19 - Pycnometer after 24 hours

4.2.4.2.2 PLA Capsules –

The PLA capsules were not tested for water absorption as they work on the principle of hydrolysis. If they are kept in water, then the shell will breakdown and the bacteria will be released. These capsules functions through alkaline hydrolysis of the PLA shell to release bacteria when water enters a crack.[6] So, the water used while mixing is a concern as it could trigger the hydrolysis process, which may potentially alter the properties of mortar.

4.2.4.2.3 Alginate Based Capsules –

A modified water absorption test was performed on these capsules as quantity of capsules were not sufficient to perform a regular test using a pycnometer. 2 sets of samples were submerged in a water filled container for 24 hours.

After 24 hours, there was no weight changed observed in the samples. So, the mix design for this capsule was prepared with the assumption that there was no absorption of water by the capsules.

4.2.4.3 Surface Texture of Capsules –

Texture of capsules is an important feature of the capsule. It is the same idea as with aggregates, a smooth particle has less bonding with the cement paste as compared to an angular or rough particle. But on the other hand, a smooth particle provides better workability than a rough particle. In order to better understand the interaction of the capsules with the fibers and the matrix it is important to know the texture of these capsules.

The capsules after preparation were observed under an optical microscope (Keyence VHX) to better under their behaviour in the mortar.



Figure 20 - Optical Microscope

4.2.4.3.2 Expanded Clay Capsules –

These capsules had a spherical shape with dents on the surface. On closer observation more surface undulations were observed.

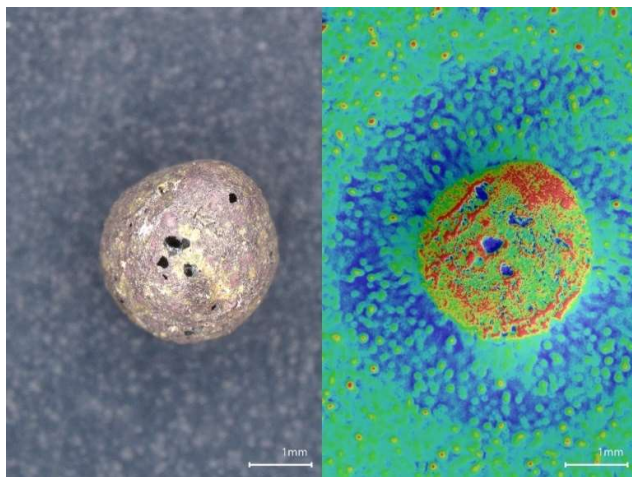


Figure 21- Roughness measurement of the expanded clay particles. Scale:1mm

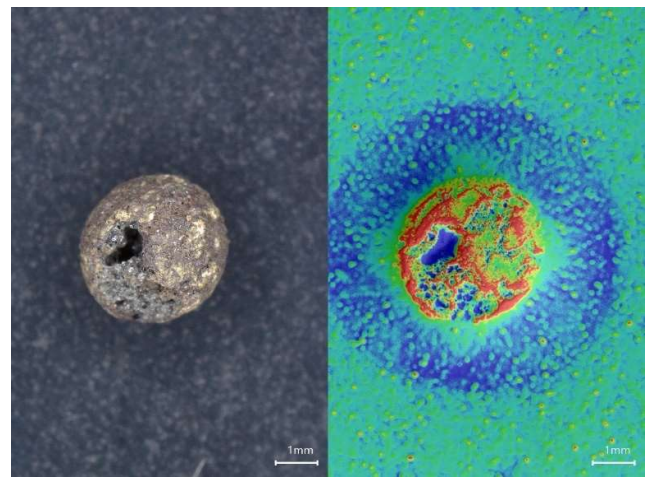


Figure 22 -Roughness measurement of the expanded clay particles. Scale:1mm

In the figures above, red denotes the peaks while blue denotes the dents on the surface which infers that the capsules had a rough surface texture which could influence the behaviour of the mortar.

4.2.4.3.2 PLA Capsules –

The capsules had an irregular shape and according to literature, had a particle size of range 0.1 to 1mm. The texture of the capsules appeared smooth and brittle.



Figure 23- Surface of a PLA capsule. Scale: 100 μ m

4.2.4.3.3 Alginate Capsules –

These capsules had a drop-like shape which gave an uneven wall thickness. This happened due to the viscosity of the alginate solution and distance at which the alginate solution was dropped into the calcium lactate solution while preparing the capsules.

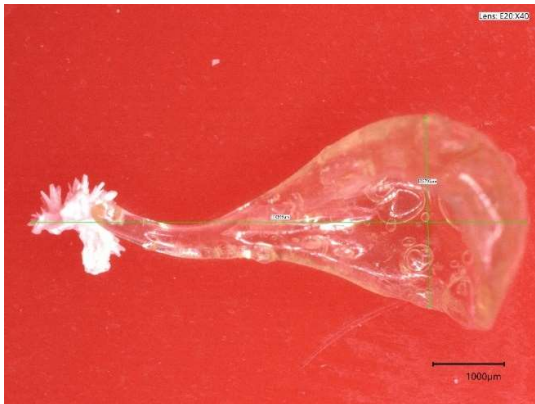


Figure 24 - Alginate capsule with a broken tail. Scale: 1000 μ m

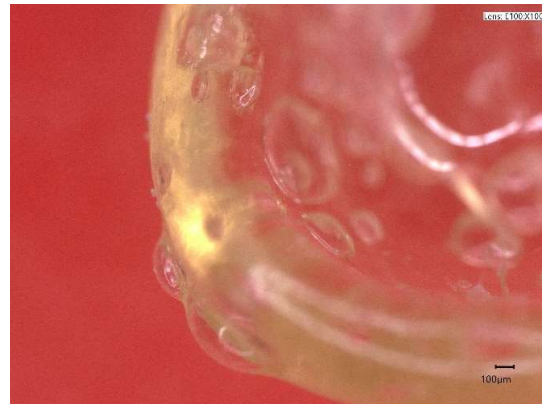


Figure 25 - Undulation on the surface of the alginate capsule. Scale: 1000 μ m

The shell of the alginate capsules had uneven brittleness. The tail of the drop was more brittle than the base of the drop. So, there was a possibility of the tail breaking during mixing. The shell of the capsules had a smooth appearance overall but had a few bubble-like undulations on the surface. This could have been because of air pockets that may have formed while preparing the capsule. These undulations imparted a little roughness to the capsules.

4.3 Mix Design –

Before any mortar specimen is subjected to tests it first needs to be designed. This part of the chapter dives into the preparation of the mixes using the prepared capsules. This

part includes the procedure, selection of ingredients and proportions, and an overview of the compositions of the various mortar mixtures that were eventually investigated.

4.3.1 Design Criteria –

The mortar mixture intended as a cover for underlying concrete structures needs to be watertight. The mortar mixes prepared are intended to demonstrate the crack-healing capacity of bacteria based self-healing technology. The mortar mix forms the basis of the study on which experiments are conducted. The mixes also influence the strength development of the cover. Therefore, several considerations were taken into account in the design of the mixtures.

4.3.1.1 Compatibility –

Bacteria in the healing agent needs an optimal pH of 10 while the pH in the cement matrix is 13. So, the compatibility of the bacteria with the matrix is important. The pH of the matrix depends on the type of cement used as it is related to the composition of the hydrated cement and the alkalinity of the pore water solution. So, previous literature was studied to check if OPC was compatible with the bacteria. It was observed that cements with high levels of clinker was compatible with the bacteria.

4.3.1.2 Ease and Practicality –

There are various materials which have the ability to encapsulate the healing agent, materials chosen in this study were either easily available or were easy to prepare. This was done to ensure that these types of self-healing mortars could be easily made on site. This made the mixes more realistic and practical to prepare.

4.3.1.3 Strength –

During the designing phase, there was no requirement for strength as the idea of the study was to compare the healing capacity of the different mortar mixes. A medium strength of mortar mixture was used.

4.3.1.4 Comparability –

In this study there are 4 types of mixtures and 5 types samples. The variations are due to the addition of different types of capsules and the method of application.

- Type 1 – Plain Mortar
- Type 2 – Mortar + PLA capsules
- Type 3 – Mortar + Expanded Clay Capsules
- Type 4 – Mortar + Alginate Capsules
- Type 5 – Plain Mortar + Externally applied HA

All mixtures are similar which makes them easy to compare and understand the variation in their behaviour as the variation would be purely due to the differences in additional materials.

The samples of Type 5 were prepared after the induction of cracks at 28 days.

4.3.2 Material Selection –

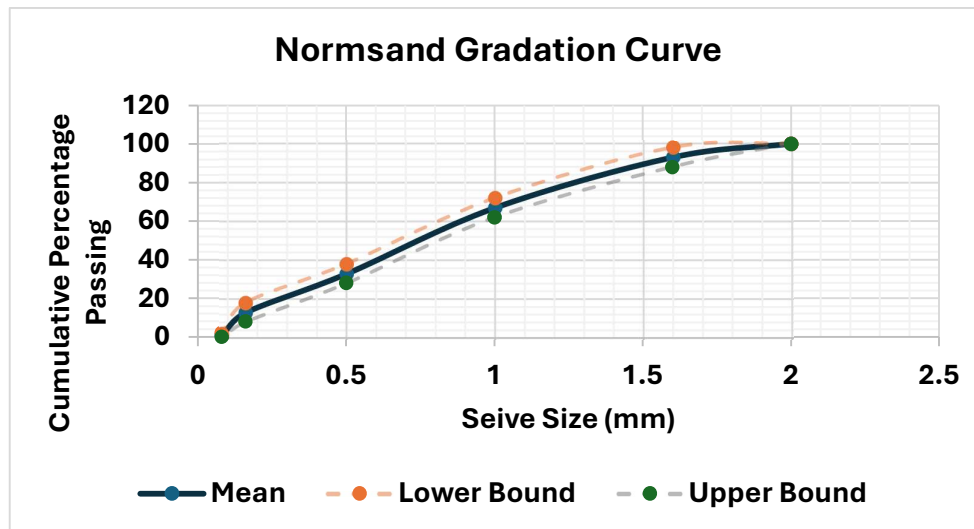
The water cement ratio for all mixes was chosen to be 0.5.

4.3.2.1 Cement –

For the binder Portland Cement CEMI 42.5N was used. The choice for this cement stems from it being the most used cement in literature for this type of bacteria. As mentioned previously, the bacteria require a suitable environment to grow which a cement with clinker content above 50% can provide.

4.3.2.2 Sand –

The sand used is 0-2mm CEN Standard Sand EN 196-1. The choice for this type was due to the easy availability of artificial sand in the market. Sieve analysis and water absorption tests were performed on this sand. There was negligible water absorption while the gradation curve for the sand has been shown below.



Graph 3- Normsand Particle Size Distribution Curve

4.3.2.3 Fibers –

To increase the number of cracks per sample during testing, fibers were used in the mortar. These fibers also help in keeping the specimen bound together which aids in creating cracks of multiple widths. The fibers used in this study were 6mm long polyethylene (PE) fibers.

4.3.2.4 Capsules –

As mentioned previously, there are multiple healing agent carriers used in this study. The expanded clay used in this study are produced by Liapor, Germany. The bacteria based polylactic acid capsules are produced by Green-Basilisk B.V., The Netherlands.

4.3.3 Mixture Designs –

Volumetric mix designs were made for 4 types of mixes. These mix designs were focused on keeping the amount of healing agent equal in all mixes. The detail of the designs is provided in the Appendix C.

The overview of the mixes for 1L mortar is given below –

Table 9 - Overview of Mix Designs

	Type 1	Type 2	Type 3	Type 4	Type 5
Cement (g)	480.77	480.77	480.77	480.77	480.77
Sand (g)	1442.31	1415.88	-	1433.43	1442.31
Water (g)	240.38	240.38	240.38	240.38	240.38
Fiber (g)	4.81	4.81	4.81	4.81	4.81
Capsule Type	-	PLA	Expanded Clay	Alginate	Externally Applied Paste
Capsule (g)	-	12.29	480.77	2.99	-

5

Mortar Mixture Testing

In this chapter the mortar mixtures have been subjected to several tests for different purposes, quantification of relevant physical and mechanical properties and investigation into the effect of the capsules on these properties. The test objectives are discussed in detail at the beginning of this chapter followed by the test procedure. The results of the tests are presented at the end of this chapter.

5.1 Test Objectives –

The test objectives are kept in line with the aim of the study. The most important objectives are the following:

- Quantification of the mechanical properties of the concrete mixtures relevant to their compressive and flexural behaviour
- Investigation of the effect of addition of healing agent filled capsules and healing agent paste on the mechanical properties of the mortar mixtures.
- Quantification of the efficiency of healing i.e. water tightness regain of different specimens relative to their crack width.

5.2 Performance Tests –

The mortar mixtures were prepared in batches of 1L. The batches were prepared with utmost precision so that all batches of the mix were identical. Mixing, pouring and compaction of each batch was done identically. Also, the ingredients of the mortar mixes came from the same batch. This ensured that all samples of the study were comparable. The testing of fresh properties, casting mortar samples and compaction by means of a vibrating table all happened while the mix was workable.

The shape of samples used was a 160mm x 40mm x 40mm prism. After casting, the specimens were covered with a sheet of polyethylene and kept at room temperature to prevent early loss of water to the environment. The specimens were demoulded 24 hours after casting and kept in a mist room (20°C, 95% humidity) for curing.

5.2.1 Slump and Consistency test –

A slump test was performed to evaluate the consistency of the mix and assess its workability. For this test a small slump cone was used as the mix prepared was not sufficient to fill up a larger slump cone.

After preparing the mixes, the mortar mix was put into the small slump cone, filling a third of the cone at a time and tamping with a rod to make sure the mortar mix was fully compacted. Then the cone was carefully removed, and the slump of the mix was measured and recorded.

The slump size is the difference between the height of the cone and the highest point of the slumped sample. The height of the slump cone was measured to be 75mm.



Figure 26 - Slump Cone

Cohesiveness of mortar is the measure of how well the components of the mortar bind together to form a homogeneous mix. This property is difficult to measure quantitatively so it was observed visually. The segregation is seen as a spread of binder, aggregate or a ring of water around the slump.

5.2.2 Flexural Test –

A 3-point bending test was performed on the samples at 7,28 and 56 days for uncracked samples. This test was not performed on healed samples. The test was performed according to NEN-EN 1015-11 (2019) [46].

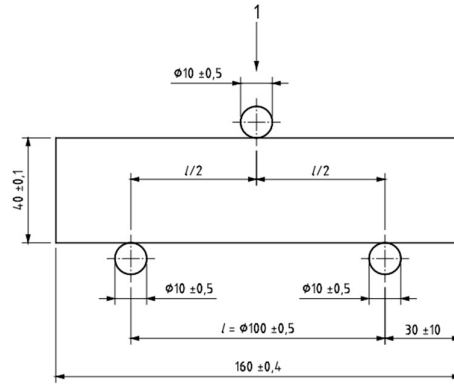


Figure 27 - Sketch of 3-point bending set-up.

A standard compressive test machine with a modified part for 3 point bending was used for this test. The input parameters used in the test are tabulated below.

Table 10-Parameters of the test – (Load controlled)

Rate	0.1kN/s
Start Load	0.1kN
Stop Load	20%
Area	266.667mm ²

The samples were tested until failure but as there were fibers in the matrix, they held the sample together and pulled the crack to close. So, the cracks were not visible, and the sample did not break into 2 pieces.

In order to proceed to the compressive strength test, the samples were cut into halves using a saw. To ensure that the flexural strength that was gotten in the first run was accurate and that a crack was indeed formed, a second flexural test was run on some samples. This run created a visible crack and showed that the flexural strength gotten in run 1 was the highest that could be got. So, it was okay to cut the sample using a saw.



Figure 28 -Saw for cutting the prism samples



Figure 29 -Type 2 specimen undergoing flexure strength test

5.2.3 Compressive test –

A compressive strength test was performed on the samples at 7 and 28 days (prior to healing) and at 56 days (post-healing). The test was performed according to NEN-EN 1015-11 (2019) [46]. The test was performed in a load control setting, at a rate of 2.4kN/s.

Table 11 -Parameters of the test – (Load controlled)

Rate	2.4kN/s
Start Load	1.0kN
Stop Load	20%
Area	1600mm ²

The specimens used for this test were the two halves that were obtained from the flexural strength test.

5.2.4 4 Point Bending – (Induction of Cracks)

To crack the samples for healing, a 4-point bending test was conducted on the 28 days samples. The test was performed using an INSTRON 8872. The test was displacement controlled with a rate of 0.005mm/s.

For this test, air dried prism samples were used. Metal holders for LVDT were glued to 2 sides of the samples, 6cm apart, using a two-part resin glue (Each side takes 10 minutes to dry). Once the glue was dry, the samples were tested in 4-point bending.



Figure 30 -Testing sample in 4-point bending

5.2.5 Optical Microscopy –

The cracks in the samples, induced by 4-point bending, were measured using an optical microscope. This was done at the time of crack induction, at 1 month of healing and at 2 months of healing. The table of measurements is given in Appendix D.

5.2.6 Permeability Test –

The samples were subjected to a permeability test after 1 and 2 months of healing. The result from this test shows the water tightness regain of the samples over time. The test was based on RILEM method No. II.4. [47]

A PVC pipe with diameter 30mm and length 30cm was used for this test. The prism specimens were dried using pressurised air such that direct air did not fall on the crack as it could damage samples with a higher crack width. Then a pipe was carefully glued to the cracked prism sample using a two-part resin glue (Permacol 3720B and a hardener). The glue was not let into the crack as much as possible. The specimens were kept for drying for 10 minutes before performing the test. Once, the glue dried, the prisms were placed on an empty container which was used for collecting the water from the test. 500ml of water was poured into the pipe, as all the water couldn't be poured into the pipe at the same time, the water was poured such that the pipe remained full of water. This was done to keep a constant pressure head. A stopwatch was used to keep track of the time from the moment water was poured into the pipe to the time when no drops of water dropped from the sample.



Figure 31 - Setup for permeability test

5.2.7 Microscopy –

To closely observe the healing around capsules and cracks, electron microscopy was done. For this purpose polished sections were prepared (Appendix F) and the specimens were observed under an electron microscope for element mapping and an optical microscope was used for observing particles that were not visible under the electron microscope due to the epoxy layer. (Appendix)

5.2.8 Porosity –

To find the porosity of the samples, sawed slices of each type of sample was taken. The surface was blackened using a permanent marker. Then white cream was spread on the blackened surface and scraped using a sharp steel ruler, making the surface of the samples even. The white cream filled up holes on the surface of the sample, indicating the surface pores which can be seen below.

The raw images were processed using ImageJ software. For samples of type 1-5 except type 3 were processed using thresholding while for type 3 samples that wasn't possible as the cream wasn't able to make all pores visible due the smoothness of the sample and the size of the pores. So, for this sample WEKA segmentation was used on an optical micrograph of the polished section.

For void analysis, the crack in the sample was not considered.

5.3 Test Results –

This part of the chapter shows the results of the tests performed on the mortar samples earlier.

5.3.1 Slump and Consistency Test –

The measured and observed fresh properties of the mortar mix are presented in the table below. The table show that the slump of all mixes is comparable. Although, the

consistency of mixes was different. All mixes except Type 3 had a good consistency. Type 3 mix showed segregation of binder, but the aggregates remained in place hence the slump value did not change.

Table 12 - Slump values of the mixes

Mix Name	Slump Value (mm)
Type 1 (Ref. Mix)	0
Type 2	0
Type 3	0
Type 4	0



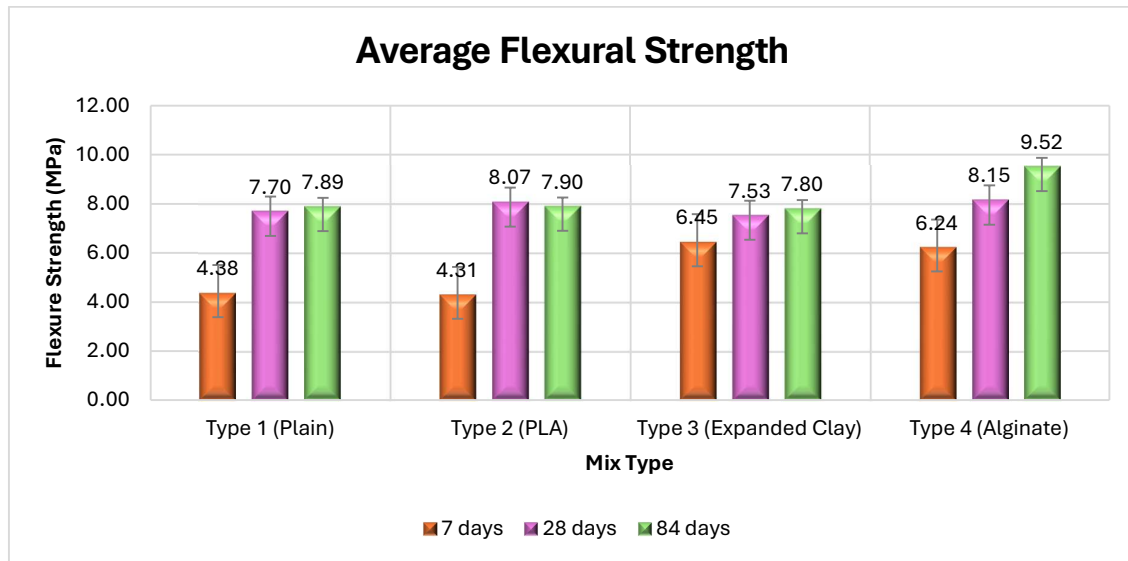
Figure 32 - Consistency of Type 2 mix



Figure 33 - Consistency of Type 3 Mix showing segregation

5.3.2 Flexural Strength –

The flexural strength of the prism samples was measured using a flexural strength test for all mix types at 7, 28 and 84 days. The results of the flexural strength tests are shown below –



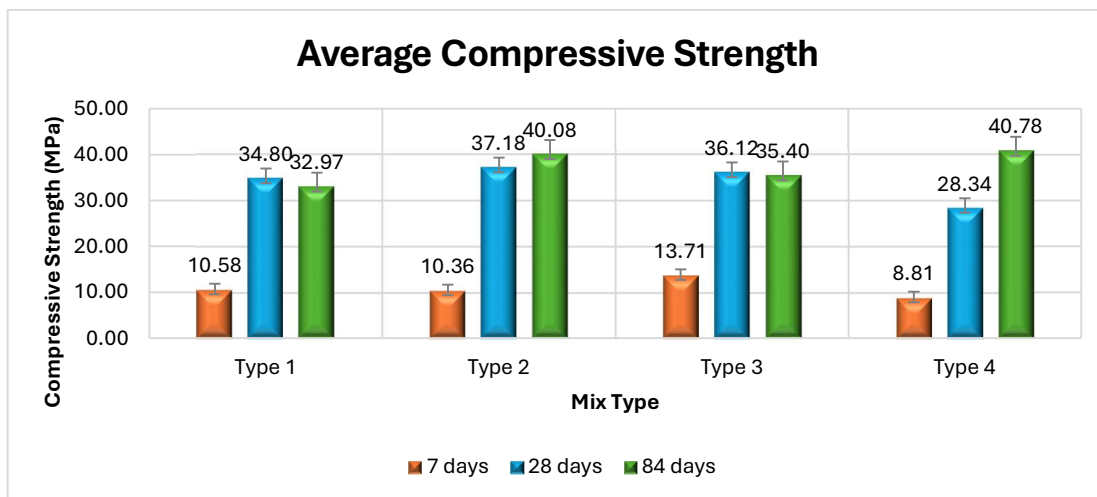
Graph 4 - Comparison of Flexural Strength of Uncracked Specimens

The observations made are listed below –

- At 7 days, Type 1 and 2 samples showed a lower strength as compared to Types 3 and 4.
- At 28 days, all types except expanded clay had a flexural strength higher than the type 1 samples (Plain sample).
- At 84 days, type 1,2 and 3 samples had a similar value for flexural strength, but alginate samples (type 4) had a higher value.

5.3.3 Compressive Strength –

The compressive strengths of all types of mixes for 7,28 and 84 days are shown below–

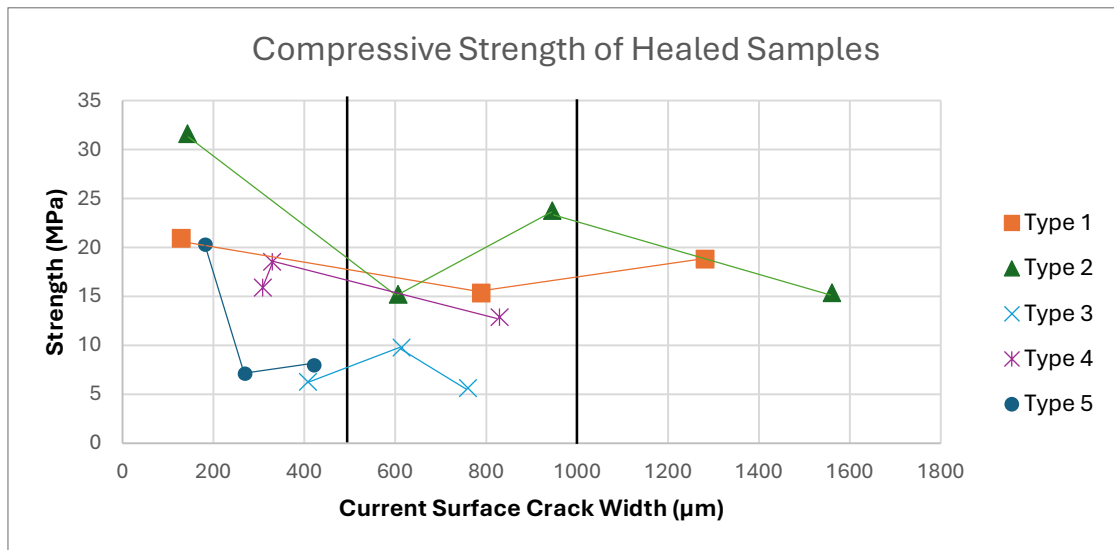


Graph 5 - Comparison of Compressive Strength of Specimens

The observations from the graph are listed below –

- At 7 days, Type 3(Expanded Clay) has a higher compressive strength than all the other types while type 2 (PLA) and 4 (Alginate) have a lower strength than type 1 (plain) which is used as a control.
- At 28 days, types 2 and 3 had a slightly higher strength than the reference (type 1) while type 4 had a lower strength than the reference.
- At 84 days, type 4 had the highest strength followed by type 2, 3 and reference.

The compressive strength of healed samples was checked at 56 days of healing. The results are shown in the graph below.



Graph 6 – Compressive Strength of 56 days healed samples compared to the surface crack width

The compressive strength of the sample depends on the width of the crack in the sample. So, in the graph above, the compressive strengths have been compared to the crack width of the specimen. It can be observed that in general, higher the crack width lesser is the compressive strength of the sample. But in some cases, even with a higher crack width, the sample shows a higher compressive strength.

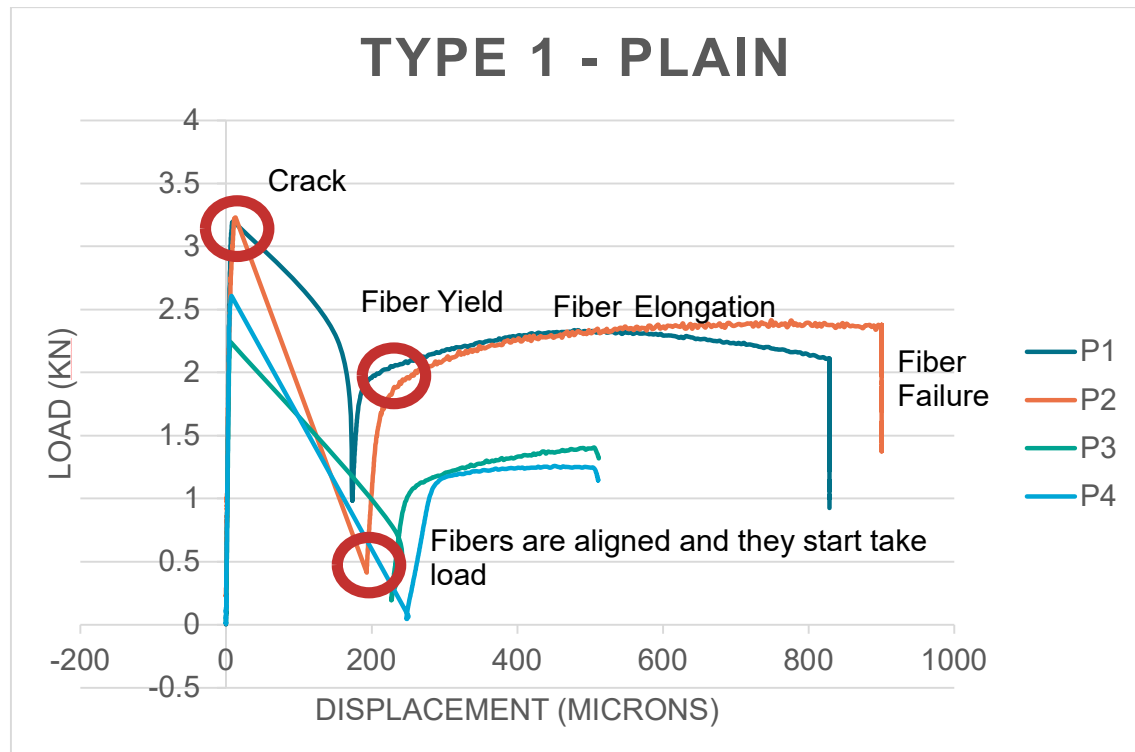
5.3.4 4-Point Bending –

After the test, it was observed that in all samples only one crack was formed instead of multiple cracks as expected in case of fiber reinforced samples. The possible causes of this are discussed in the discussion chapter.



Figure 34-Crack in Type 2 sample with some visible crack bridging

Given below are the graphs obtained from 4-point bending test.

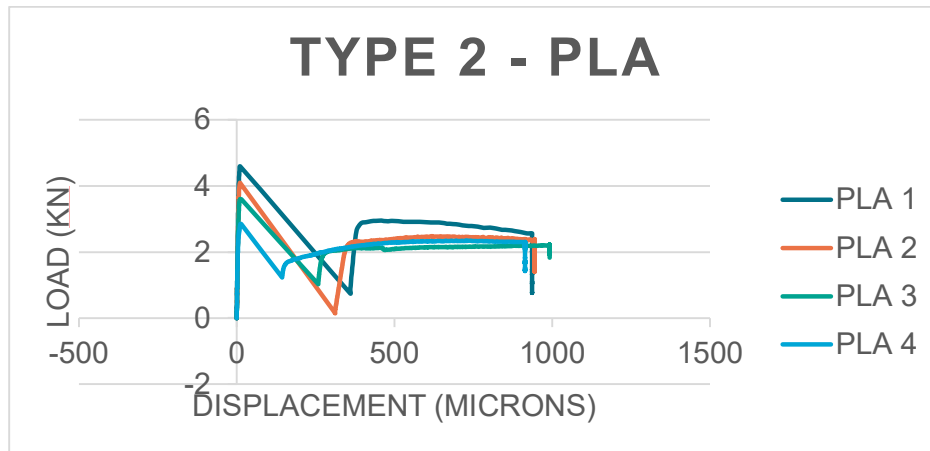


Graph 7-Graph of 4-point bending test for Type 1 samples

Young's Modulus (E)= 0.363

The observation made from the graph above are –

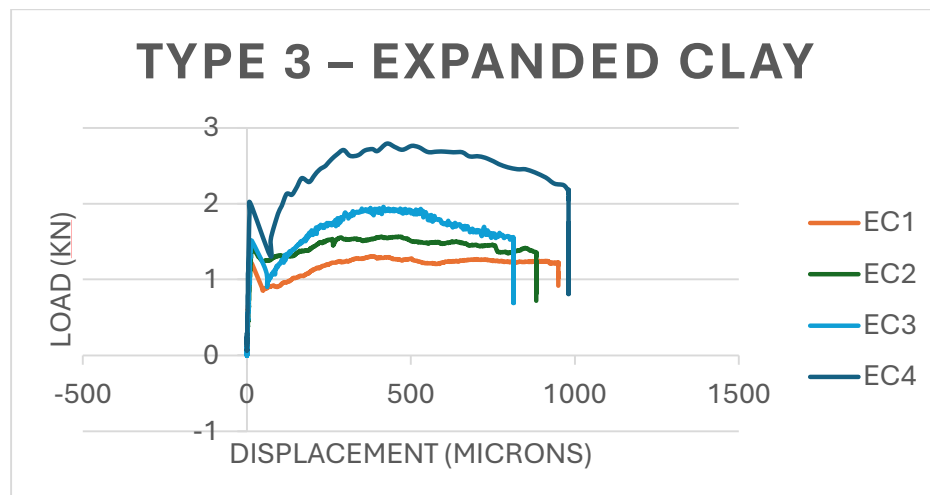
- At first the load increases with almost no displacement.
- Then there is a crack initiated after which there is a displacement without further increase in load.
- The load decreases (decrease in load carrying capacity) and a full crack is not seen as the fibers are bridging the crack.
- Displacement went upto 200 μ m after crack initiation.
- Displacement increases as some fibers get pulled straight and when the fibers get aligned, the load starts increasing again.
- The load does not increase substantially, and the fibers elongate. To about 3% of the fiber length.
- The specimen fails at an average of 870 μ m displacement.



Graph 8 -Graph of 4-point bending test for Type 2 samples

$E=0.356$

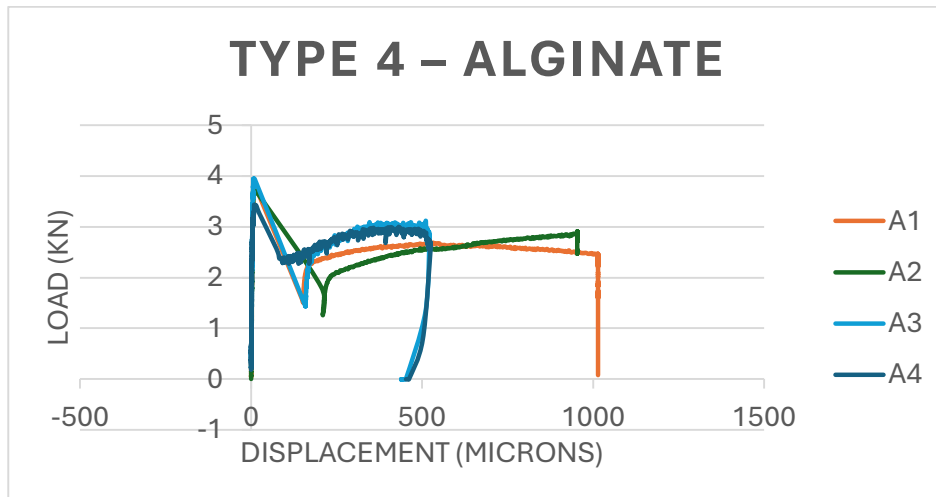
For the PLA samples, the pattern of cracking is similar to the plain samples but the displacement after the crack is on an average upto 300 μm and fails at 1000 μm .



Graph 9 - Graph of 4-point bending test for Type 3 samples

$E=0.096$

- When the load increases, there is almost no displacement.
- Crack initiates and displacement starts which goes on till 60 μm .
- Then the load increases again as the fibers align in the direction of the load.
- The strain-hardening (hump) in the graph has undulations
- The sample fails at around 900 μm .



Graph 10-Graph of 4-point bending test for Type 4 samples

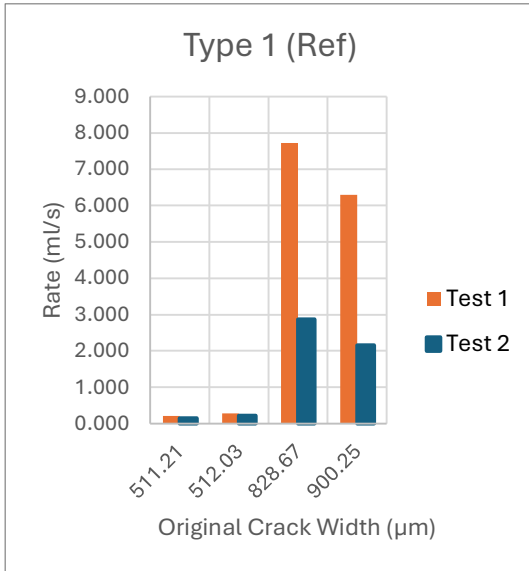
$E=0.364$

For the Alginate samples, the pattern of cracking is similar to the plain samples but the displacement after the crack is on an average 185 μm and fails around 1000 μm .

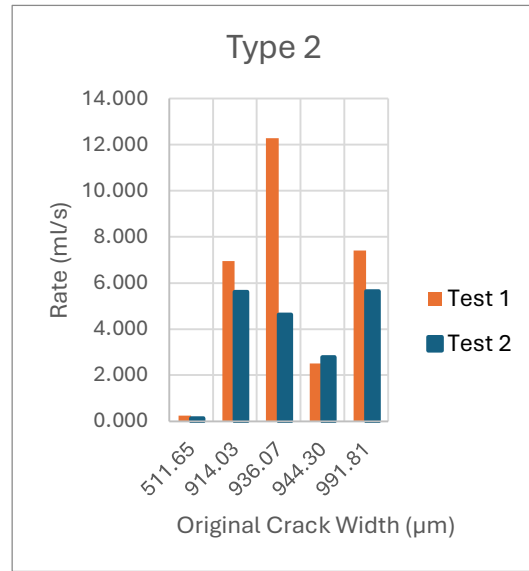
5.3.5 Permeability Test Results –

The graphs below show the permeability of different types of samples at 1 month and 2 months of healing. The results of the permeability test are based on the minimum crack width of the full length of the crack but as the specimens were intact and not break open at the time of the test, the permeability is compared to the crack width at the surface. Furthermore, the rate of flow is not compared to the current crack width in the graphs below as the cracks surface was damaged slightly over time which showed a higher surface crack width but in reality, the crack inside was not as wide as measured on the surface.

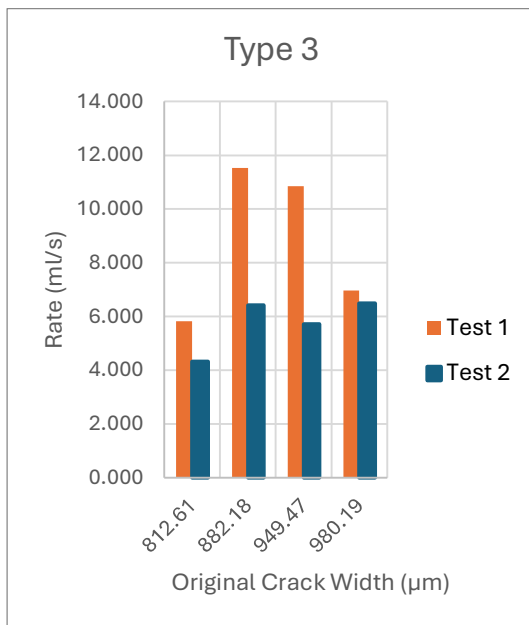
A detailed table is provided in the appendix.



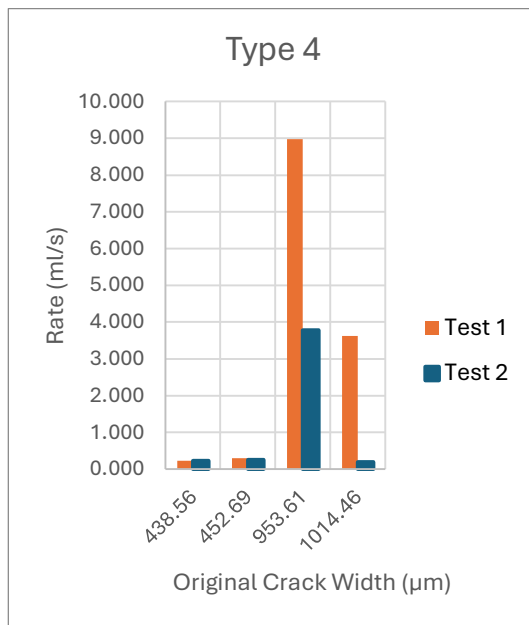
Graph 11 – Permeability of Plain (Reference) Sample



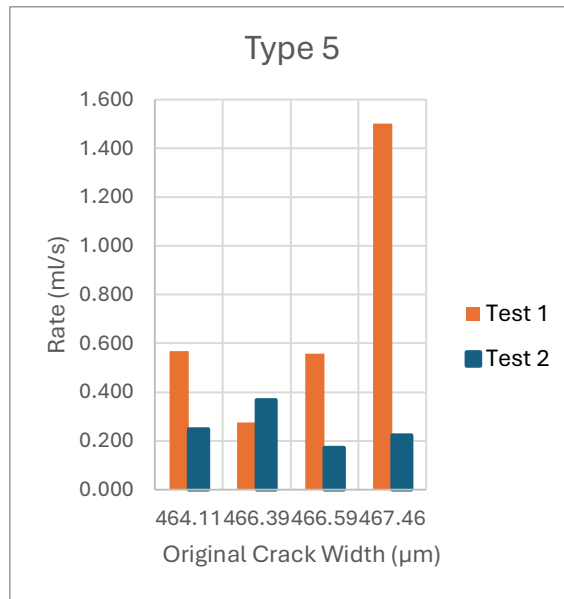
Graph 12 -Permeability of PLA sample



Graph 13 – Permeability of Expanded Clay Sample

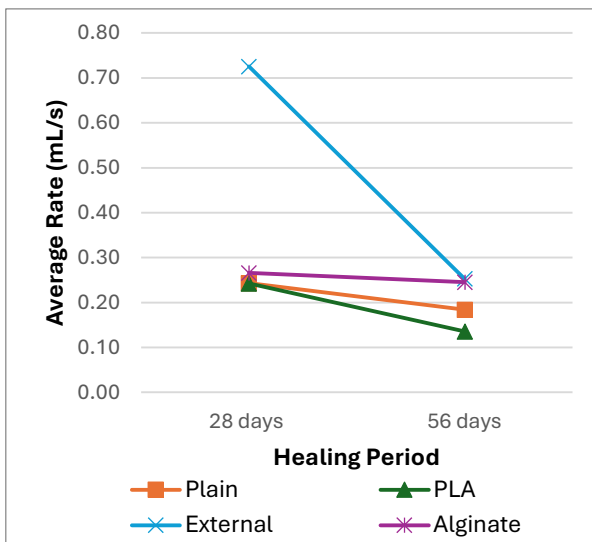


Graph 14 – Permeability of Alginate Sample



Graph 15- Permeability of Externally Heated Sample

The results from the tests show that the permeability of most samples decreased regardless of the initial crack width which means that the cracks narrowed over time. The samples with original maximum crack width under 500μm were chosen to make a comparison.



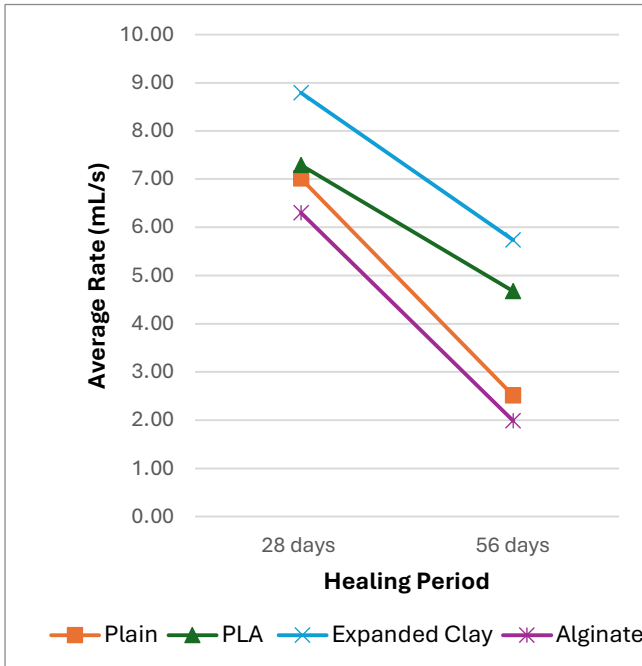
Graph 16 - Graph showing the comparison of permeability of different samples having a crack width of under 500μm

Table 13 - Flow rate corresponding to the crack width and healing period. Crack width 500μm

Series	Healing Period	Average Flow Rate (ml/s)	Average Current Crack width (μm)
Plain	28 days	0.24	240.92
	56 days	0.18	135.92
PLA	28 days	0.24	166.75
	56 days	0.14	143.40
Alginate	28 days	0.27	288.54
	56 days	0.25	319.08
External	28 days	0.73	288.62
	56 days	0.25	280.53

From the comparison above it can be observed that the permeability of all samples decreases with time but for the externally heated samples, the permeability decreases at a higher rate.

For samples with an original maximum crack width above 500 μm another comparison was made. It was observed that the rate of decrease in permeability rate was much higher as compared to samples with original crack widths under 500 μm .



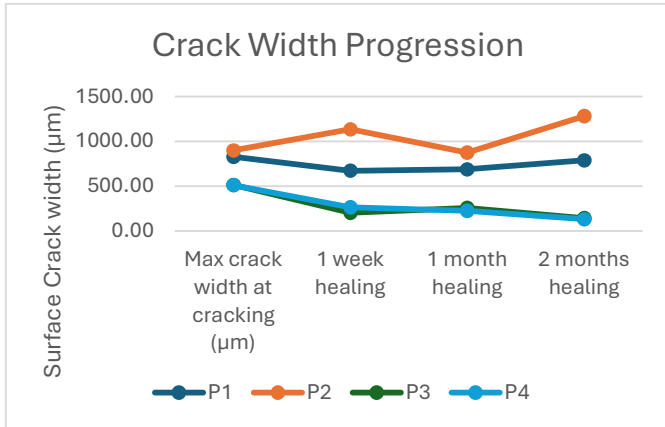
Graph 17-Graph showing the comparison of permeability of different samples having a crack width of higher than 500 μm

Table 14- Flow rate corresponding to the crack width and healing period. Crack width higher than 500 μm

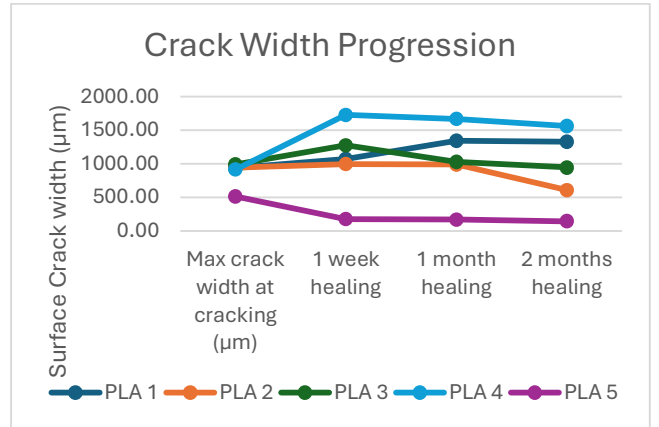
Series	Healing Period	Average Rate (ml/s)	Average Crack Width (μm)
Plain	28 days	7.01	780.86
	56 days	2.51	1034.88
PLA	28 days	7.29	1256.29
	56 days	4.67	1109.95
Expanded Clay	28 days	8.79	862.50
	56 days	5.74	613.34
Alginate	28 days	6.30	566.17
	56 days	1.99	859.68

5.3.6 Surface Crack Width Progression –

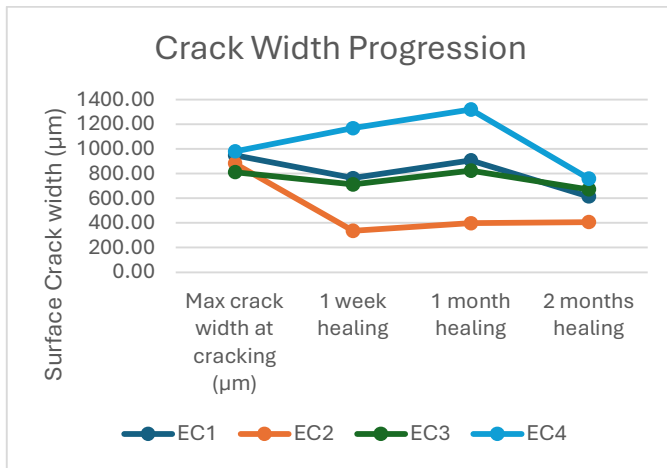
The table below, shows the observed surface crack widths of the specimens. The variation in the crack widths is discussed later.



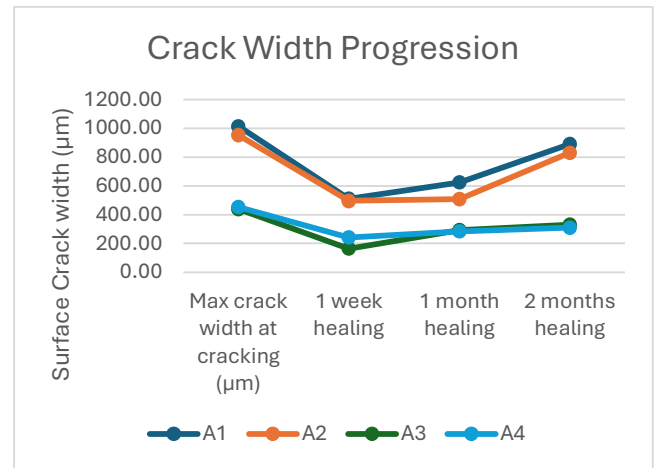
Graph 18 - Surface Crack Width Progression for Type 1 (plain) Samples



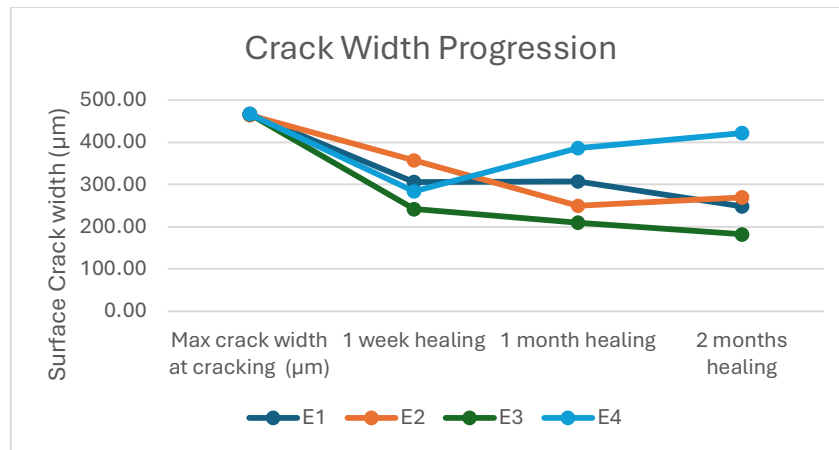
Graph 19- Surface Crack Width Progression for Type 2 (PLA) Samples



Graph 20 - Surface Crack Width Progression for Type 3 (Expanded Clay) Samples



Graph 21 - Surface Crack Width Progression for Type 4 (Alginate) Samples



Graph 22- Surface Crack Width Progression for Type 5 (External Healing) Samples

From the graphs above it can be observed that the surface crack width has a decreasing trend in general but in some cases that trend becomes increasing

Given below are some optical photomicrographs which show the crack closure in samples for time $t=0$, $t=1$ month and $t=2$ months.



Figure 35 -Photomicrographs of sample PLA5 (Type 2) at cracking (left), 1 month healing (middle), 2 months healing (right). Healing can be seen in the crack. Scale: 1000 µm (0.222 pixels/micron)

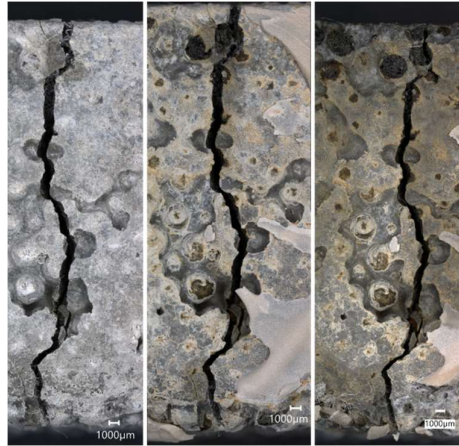


Figure 36- Photomicrographs of sample EC1 (Type 3) at cracking (left), 1 month healing (middle), 2 months healing (right). Healing can be seen in the crack at 1 month. Scale: 1000 µm



Figure 37-Photomicrographs of sample A1(Type 4) at cracking (left), 1 month healing (middle), 2 months healing (right). Healing can be seen in the crack. Scale: 1000 µm



Figure 38-Photomicrographs of sample E1 (Type 5) at cracking (left), 1 month healing (middle), 2 months healing (right). Healing can be seen in the crack. Scale: 1000 µm

From the images above it observed that over time the surface crack width reduces but in some cases the crack widths increase. More insight into this is provided under discussion.

5.3.7 Microscopy –

At 54 days after healing, polished samples were subjected to electron microscopy where the areas around the crack were observed under element mapping to observe the limestone formation inside the crack.

Type 2

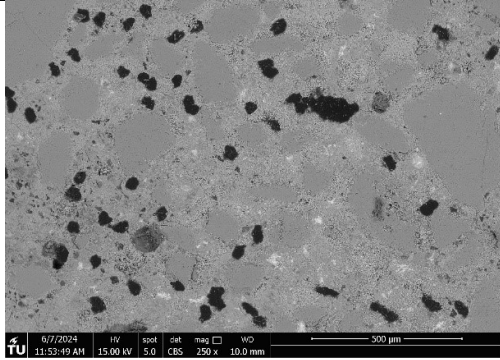


Figure 39 -Electron micrograph of PLA1 polished section showing irregular shaped PLA capsules (black spots). Scale: 500μm

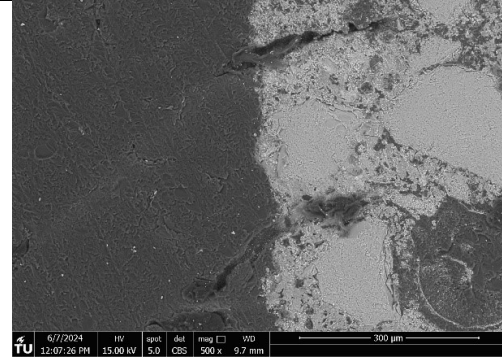


Figure 40 – Electron micrograph of PLA1 polished section showing an imprint of PE fiber near the crack. Scale: 300μm

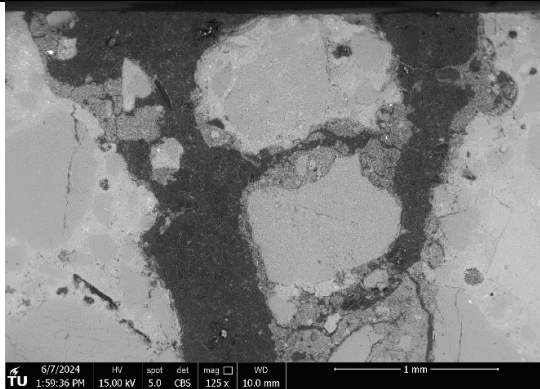
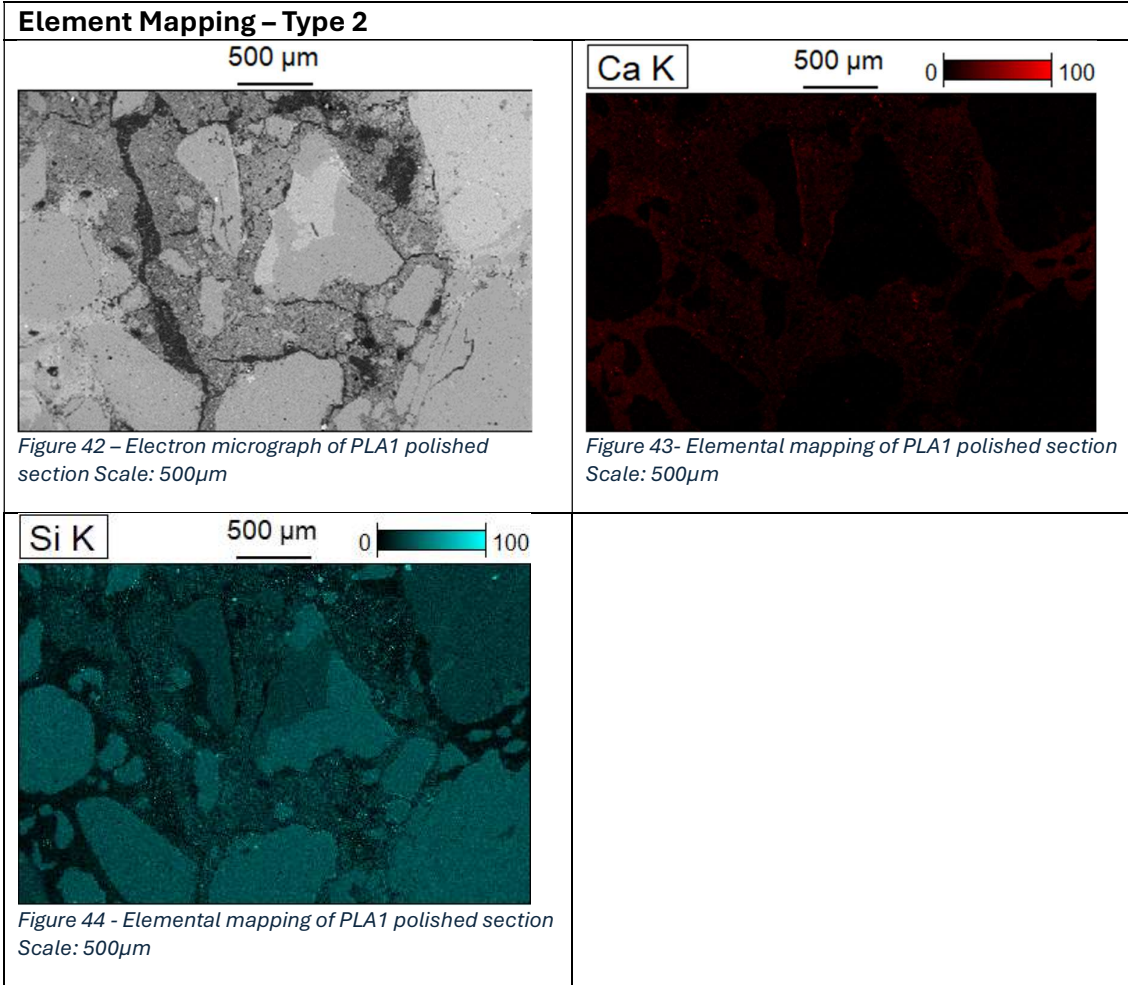


Figure 41 – Electron micrograph of PLA1 polished section showing CaCO₃ precipitate on the crack walls. Scale: 1mm

The polished PLA sections when observed under an electron microscope show PLA capsules in the matrix and some fiber imprints near the crack suggesting fiber bridging of the crack. Limestone precipitation was also observed along the crack walls using element mapping.



Electron microscopy was performed on polished sections of Type 3 (expanded clay) mortar samples and the capsules were investigated closely. It was seen that the capsules where the cracks went through them had healing precipitates along the crack wall.

Type 3

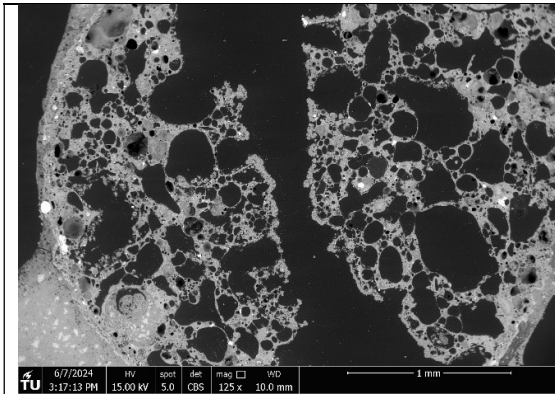


Figure 45- Electron micrograph of EC3 polished section showing an expanded clay capsule. Scale: 1mm

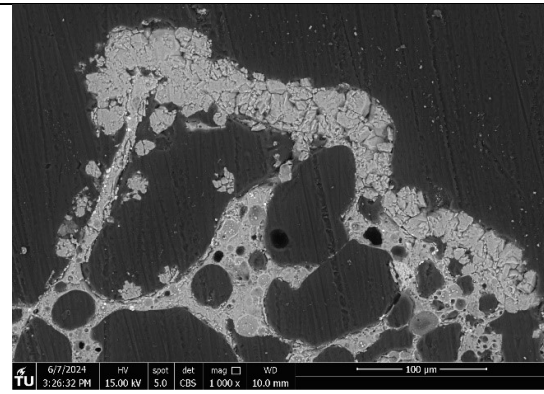


Figure 46 - Electron micrograph of EC3 polished section showing the inside of an expanded clay capsule. The crack walls show healing. Scale: 100μm

Element Mapping

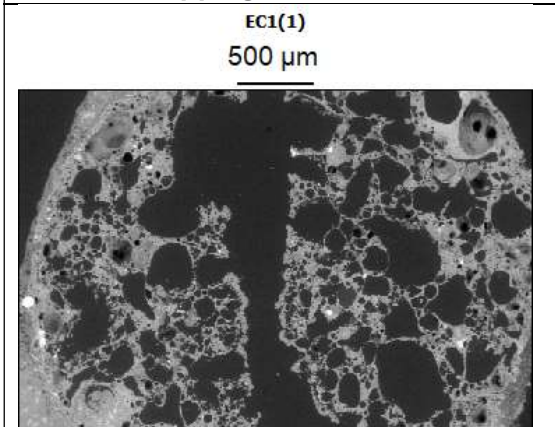


Figure 47 -Electron micrograph of EC3 polished section showing a crack going through a capsule. Scale: 500μm

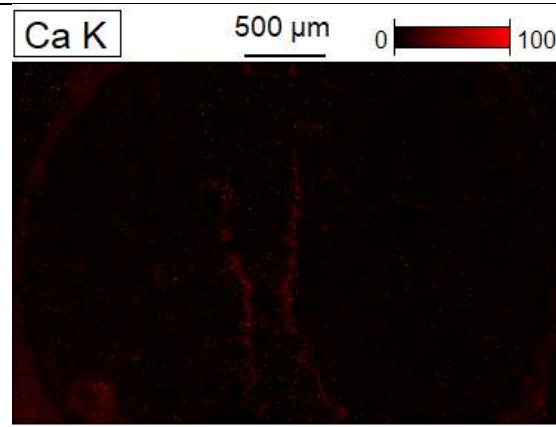


Figure 48 -Elemental mapping of EC3 polished section. Showing CaCO_3 deposition along the crack wall Scale: 500μm

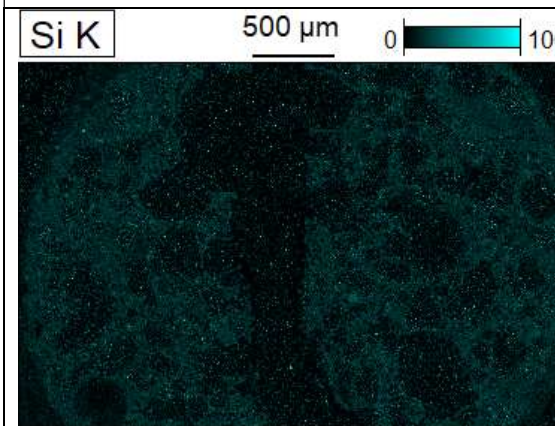


Figure 49 -Elemental mapping of EC3 polished section Scale: 500μm

Unfortunately, not all samples could undergo electron microscopy as the polished sections had a slightly thicker layer of epoxy on them which prevented the electron

microscope from being able to identify components of the sample correctly. So, samples were subjected to optical microscopy (Appendix).



Figure 50 - Photomicrograph of polished sample A1 showing crack. Scale: 1000µm

The figure above shows an embedded alginate capsule. The capsule could not be identified during electron microscopy.

5.3.8 Void Analysis –

The porosity of the healed samples was checked using ImageJ software. The cracks were not included in the analysis. The porosity found for the same w/c i.e. 0.5 was as tabulated –

Table 15 - Porosity of samples

Sample Name	Porosity (%)
P3	9.04
PLA1	7.76
EC3	19.28
A1	8.97
E1	9.72

From the table above, it can be seen that the porosity of the samples are comparable except for EC3 (Type 3) while the PLA (Type 2) sample had a lower porosity.

6

Discussion

In this chapter, the results presented throughout this thesis are critically analysed. The results obtained from tests are interpreted and the relationship between the crack widths and healing are investigated. This section also focuses on calculations of healing efficiency. The reliability of surface crack widths is also assessed.

KEY –

Type 1 – Plain (Reference) specimen

Type 2 – PLA capsule embedded specimen

Type 3 – Expanded Clay embedded specimen

Type 4 – Alginate Based capsule embedded specimen.

6.1 Fresh Properties –

When it comes to the slump properties of the mixtures, no clear distinction was observed between the mixes. The slump for all mixes was observed to be identical but the consistency for all mixes was not identical. Types 1,2 and 4 had a good consistency and did not show any signs of segregation but Type 3 which had expanded clay capsules did not show the same consistency. This mix showed segregation of the binder from the capsules. The fresh properties of most mixtures were quite consistent with each other, indicating that the mixtures were comparable in terms of processability. Finally, no significant effect of the addition of healing agent on the fresh properties was observed.

On further inspection it can be said that for mix of Type 3, good adhesion was not present between the expanded clay particles and the binder, as the binder was flowable. This could be attributed to the lack of fine aggregates in the mix which would have increased the adhesion between the expanded clay and the binder.

Also the mix did not slump because of the compaction that the mix received during the slump test and interlocking action of the expanded clay particles and fibers due to the rough surface of the expanded clay.

6.2 Compaction –

For all mixtures except expanded clay mix, compaction gave a smooth surface on all sides but for Type 3 mixture, the top surface had a rough texture. For this type of mixture it was observed that the expanded clay particles were less dense than water, as they floated during the specific gravity test. This meant that when the mix was mixed and compacted, the lighter particles rose up while the binder settled down causing segregation which can be seen in Figure 51. The expanded clay particles were able to move through the wet cement paste due to the absence of sand particles as smaller particles would have obstructed the downward movement of the cement particles.

Some balling of fibers was observed when a cross section of Type 3 sample was cut. This could have been because of the healing agent which coated the clay particles. When the samples were cast, the healing agent was not completely absorbed by the expanded clay particles and remained on the surface as residue which gave some particles a slimy texture. This would have restricted the interlocking action between the fiber and the particles resulting in balling.



Figure 51- C/S of Type 3 sample.

For all other types of samples, balling of fibers was not observed.

6.3 Flexural Strength –

The flexural strength of uncracked samples was checked at 7,28 and 84 days. The graph comparing the strengths of all types of mixes is given under results. [Graph 4]

The inferences from the graph are listed below –

- The shape of the particles influences the flexural strength of the samples as irregularly shaped particles or particles with a rough surface provides good interlocking with the fibers and binder.
- PLA samples give a higher strength than plain samples as sand of 0-2mm was partially replaced with 0.1-1mm of PLA particles, the particle size distribution

changed in the sample, which means that there were larger number of smaller, irregularly shaped particles than larger ones in the matrix.

- Comparing PLA samples and Expanded Clay with Alginate samples, it is observed that the PLA capsules are very small and are densely distributed in the matrix and the Expanded Clay capsules are large and densely distributed in the matrix while the alginate capsules are medium sized but are sparsely distributed in the samples.

Samples with more and large capsules have more ITZ present which means there is more discontinuity in the sample which makes it easier to break in flexural test.

6.4 Compressive Strength –

The compressive strength of uncracked samples was checked at 7,28 and 84 days after casting while the compressive strength of healed samples was checked at 56 days post healing i.e. sample age: 84 days. [Graph 5]

The inferences made from the data are listed below –

- The strength behaviour of type 2 and 3 is similar to the reference i.e. strength rapidly increases from 7 to 28 days and then slows down while type 4 has a linear strength progression.
- The strength of type 2 is higher than the reference samples because of the change in particle size. Sand of 0-2mm was replaced with 0.1-1mm of PLA particles which gives more packing and makes the mix denser as shown by the porosity of the samples [**Error! Reference source not found.**].
- The higher strength of type 3 samples, than the reference (type 1) sample, could be attributed to the spherical shape of the capsules. These capsules could transfer load to a larger area.
- Type 4 samples had a linearly increasing strength as the alginate capsules were rough on the surface and irregularly shaped with a tail which could have given a better interlock with the sand and the binder particles.

The compressive strength of the healed samples at 2 months was checked and it was found that the compressive strength of the sample depends on the width of the crack in the sample. So, in Graph 6, the compressive strengths have been compared to the crack width of the specimen. It can be observed that in general higher the crack width lesser is the compressive strength of the sample. But in some cases, even with a higher crack width, the sample shows a higher compressive strength. This is because the crack on the surface could be wider due to surface damage from other tests but there could be narrow crack inside which gives this the higher strength value.

Comparing cracked samples at 56 days of healing with uncracked samples both sets of samples are of the same age i.e. 84 days. It was observed that the samples that are

healed have a much lower compressive strength than the uncracked samples. This means that no matter the width of the crack, healed samples do not have the same strength as pristine samples.

6.5 4-Point Bending Test –

At 28 days, a 4-point bending test was performed on the samples in order to induce cracking for healing.

The expected cracking pattern of a fiber reinforced sample is multiple cracks but in this study it was not observed except for type 3 sample which had 2 cracks side by side. All other samples had one crack each. This type of behaviour was unexpected. There are several possible reasons for this type of observation –

- The bond between the fiber and the matrix was not good which led to a bond slip and fibers pulled out. So even if the load was increased, the crack width kept increasing instead of a new crack forming.
- The fibers had a high elongation which could have led to an increase in crack width.
- Another reason could be that the matrix was too strong to break and so the first crack kept increasing instead of forming more cracks. Also, the crack observed was a straight crack which would support this theory.



Figure 52 -Photomicrograph of fiber pullout across the crack. Scale: 1000µm



Figure 53 - Photomicrograph of elongation of fibers across the crack. Scale: 1000µm

The type 3 sample did not have one singular crack but had 2 cracks next to each other. This could have happened because of several reasons –

- There was segregation between the binder and the capsules in the samples and as the particle size of the capsules was larger which caused the boundary between the two particles to act like a crack nucleation point which made it easier for the crack to propagate.
- Also, due to segregation, the top texture of the sample was rough which meant that the expanded clay particles were exposed. These were also easy to crack.

So, it is possible that the second crack could be only on the surface and not throughout the sample.

Expanded Clay samples had a distinct strain hardening behaviour with undulations (small load drops) which could be attributed to several reasons –

- Fiber slippage -The sample takes more load than the load required to form the crack.
- This behaviour could also be due to balling of fibers which implies that the fibers act together to bear the load.
- Another reason could be that the EC aggregates crack/break which could also result in undulations in the graph.

Another notable observation was that for some particles, the cracks went through the binder and not the capsule as was intended. This could have happened due to the binder displacing the healing agent from the aggregate pores while mixing leading to a denser capsule structure.

6.6 Permeability –

The permeability test is based on the minimum crack width of the full length of the crack as the rate of water flow is governed by the minimum crack width, narrower is the crack width lesser is the permeability. As the specimens were intact and not cut open at the time of the test, the permeability was compared to the crack width at the surface. The rate of water flow was not compared to the current crack width in the graphs on Page 71, as the surface of the crack was damaged slightly over time which showed a higher surface crack width but in reality, the crack inside was not as wide as measured on the surface.

Two permeability tests were performed on the specimens. First at 1 month of healing and the second at 2 months of healing.

The results from the tests indicated that permeability of most samples decreased regardless of the initial crack width which means that the cracks narrowed over time. This could have happened because of bacterial healing and autogenous healing. The increase of rate in some samples could have happened because of removal of healing products or due to water leak from the side cracks.

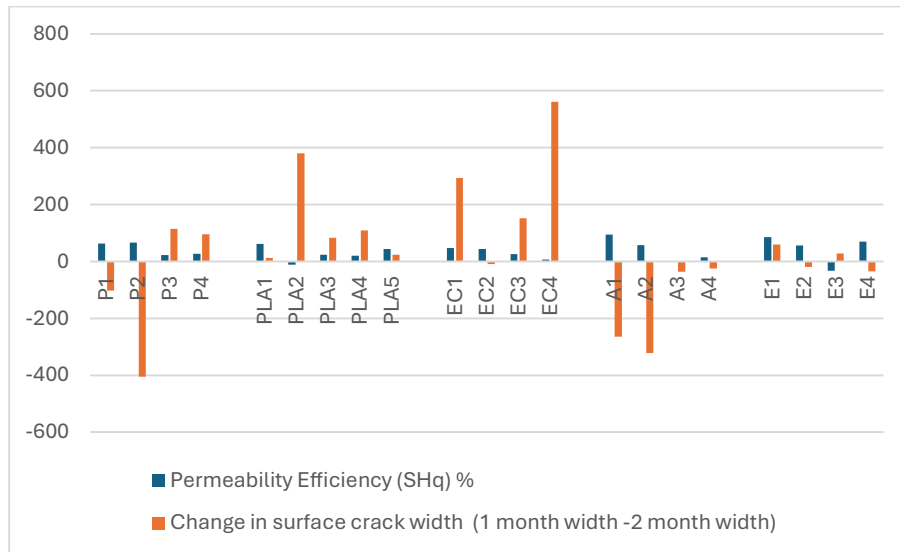
The permeability efficiency was calculated using the formula given below[22] –

Equation 8

$$SH_q = \left[1 - \frac{q(t)}{q_0} \right] * 100(\%)$$

Where, q_0 is the initial flow rate, $q(t)$ is the flow rate at time t and the derived value of SH_q for $q(t)$ can be interpreted as how much of the water tightness is recovered.

The self-healing performance can be evaluated by calculating the healing index, which is expressed as a relative change of the permeability, by using the equation above. This healing index can be interpreted as the reduction rate of water flow attained at a given period. The permeability efficiency shows the water tightness regain of the samples at t=1 month and t=2 months. [Table 38 and Table 39]



Graph 23- Permeability efficiency vs change in surface crack width

P – Type 1 (Ref Mix)
 PLA – Type 2 (PLA Mix)
 EC – Type 3 (Expanded Clay Mix)
 A – Type 4 (Alginate Mix)
 E – Type 5 (Externally Healed)

The graph above compares the calculated permeability efficiency to the change in surface crack width where a negative change indicates a loss of permeability or an increase in surface crack width. From the graph above it can be interpreted that it is difficult to correlate the surface crack width to the permeability as the surface crack width could be wider than the crack inside the specimen. So, a negative change of width (crack widened) can have a decreased permeability and vice versa.

Additionally, from this test, it was observed that when samples with original maximum crack width above 500 µm were compared, the permeability of samples dropped at a much higher rate than the samples with an original maximum crack width under 500 µm. This behaviour could be credited to –

- Oxygen availability for the bacteria is higher due to a higher crack width.
- Water/moisture availability for the bacteria is also higher than that in a narrow crack.
- The surface crack could have been larger than the actual crack on the inside of the sample.

6.7 Healing Efficiency –

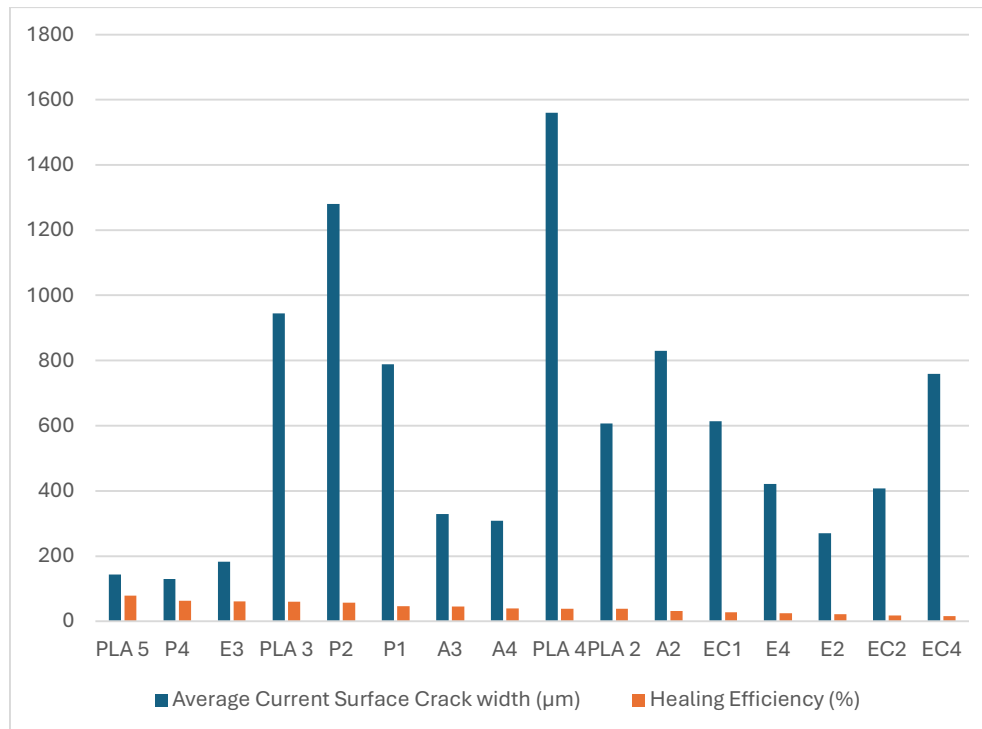
In the case of self-healing cementitious materials, healing efficiency and permeability efficiency are similar concepts. Both efficiencies are used as indicators for regain of mechanical properties of the material. Permeability uses the rate of flow of water as an indicator for water tightness and subsequently strength regain while the healing efficiency is based on the comparison of compressive strengths which quantifies the strength regain of the sample indicating the underlying healing of the sample.

The healing efficiency of samples was found by the following formula –

Equation 9

$$\eta\% = \frac{\sigma_2}{\sigma_1} * 100$$

where, σ_1 is the maximum compressive strength of pristine samples and σ_2 is the maximum compressive strength of healed samples both sets having the same age.[24]



Graph 24 – Healing efficiency vs Average current surface crack width

- P – Type 1 (Ref Mix)
- PLA – Type 2 (PLA Mix)
- EC – Type 3 (Expanded Clay Mix)
- A – Type 4 (Alginate Mix)
- E – Type 5 (Externally Healed)

The graph above compares the calculated healing efficiency of the healed specimens to the average current crack width of the specimen. PLA specimens with the narrowest crack gave the best healing efficiency at 78.9% [Table 42 - Healing Efficiency]. Plain

sample with a narrower crack width than the PLA sample did not recover as much strength as the PLA sample.

The data proves that the surface crack width is not a reliable way to find the actual healing of the sample as cracks with narrower widths have a lower strength regain than samples with a higher surface crack.

6.8 Void Analysis –

Porosity is used as an indicator of strength. Porosity of a material is inversely proportional to its strength. This is because, higher porosity implies a larger volume of voids within the mortar matrix, which weakens the material's structural integrity.

The porosity of the healed samples with $w/c=0.5$ was checked using ImageJ software. The cracks were not included in the analysis.

The results show that the porosity of the samples are comparable except for EC3 (type 3) as the expanded clay had a higher porosity which contributed to the overall porosity and weight of the sample. PLA sample had a lesser porosity than the rest due to the partial replacement of sand particles of 0-2mm with PLA particles of 0.1-1mm.

6.9 Crack Surface Closure –

The surface of the samples was observed using an optical microscope at monthly intervals to observe the progression of the crack closure on the surface.

From the photomicrographs of the samples, some observations and inferences were drawn –

- For Type 1 sample the cracks narrowed due to autogenous healing but from month 1 to 2, the crack seemed to have widened possibly due to handling.
- Type 2 sample saw significant healing when the crack width was under 500 microns but when the crack was wider, then surface healing was not seen.
- Type 3 samples did not show significant healing on the surface but there was some internal healing as suggested by the electron micrograph.
- Not all Type 4 samples showed surface healing but showed internal healing as suggested from the permeability tests. This means that healing of the crack is local.
- For type 4 mix, the alginate capsules in the mix were not sufficient so the capsules did not break. Hence the samples did not show healing in multiple locations in the crack.
- For sample of type 5, samples showed cracked surface healing, but the healing was not uniform and was not as effective as the PLA samples of the same crack width.

6.9.1 The relation between visually observed surface healing and permeability –

Visually observed surface healing cannot be correctly correlated to permeability. This can be seen in some samples. For example, sample E2 (Type 5) did not show any visual healing but the water tightness regain shows that the crack was indeed healed as the permeability efficiency increased by 56.52% in the duration of 1 month i.e. $t=1$ and $t=2$. Similarly, for sample EC2 (Type 3), visually healing cannot be seen on the crack mouth but the permeability efficiency increased by 44.33% in the duration of 1 month i.e. $t=1$ and $t=2$.

These examples suggest that visual observation of the crack does not provide conclusive inference of the water tightness regain and crack being healed.

6.10 Probability of Crack Healing –

The efficacy of a self-healing system depends on the probability of crack hitting a capsule, the filling capacity of the intersected capsules, and the depth at which a capsule is first intersected [48].

In case of internally healed samples, a crack heals when it propagates through an embedded capsule, breaking it, which releases the encapsulated bacteria and nutrients that enable healing.

The probability of a crack healing using capsules depends on a variety of factors.

- Number of capsules embedded in the matrix –
A higher number of capsules increases the chance of the crack hitting (cracking) a capsule
- Location of the capsule –
If the capsule is located close to the surface the probability that the crack will reach the capsule is high. Also, having the capsules close to the surface increases the durability of the mortar by cutting off the ingress of external elements once healing starts.
- Number of spores per capsule and the availability of required nutrient –
A higher number of spores per capsule along with the corresponding amount of nutrient facilitates a faster healing.
- Stiffness of Capsules (Material Property) –
The capsule should be stiffer than the surrounding matrix such that the capsule does not undergo any deformation. This would lead to the rupture of the capsule otherwise there would be no release of bacteria and no healing thereafter.

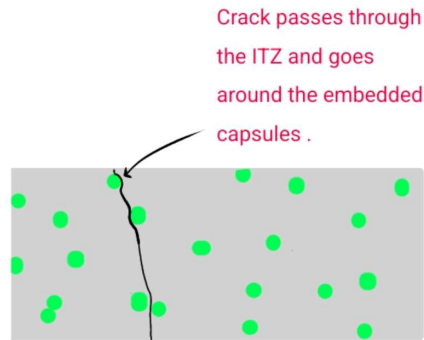


Figure 54 - Sketch of crack pattern in matrix embedded with soft capsules

The sketch above shows the crack pattern of a sample of mortar where the capsule has a lower stiffness than the matrix resulting in the crack passing through the ITZ between the matrix and the capsule. Whereas, when the capsule is made stiffer than the matrix, the crack goes through the capsule as a capsule with a higher stiffness (hard capsule) allows for less deformation than a softer capsule with respect to the matrix.

7

Conclusions and Recommendations

This final chapter summarizes conclusions and recommendations of this research. The conclusions relate the objective of this thesis to the results that were obtained in the process. The conclusions are followed by some recommendations which could help future research. There is also some insight provided into the limitation of the experiment process.

7.1 Conclusions –

An experimental study was carried out to characterize and compare bacteria enabled crack-healing behaviour of mortar. This study used bacteria in both encapsulated and external forms. The materials used for encapsulation were expanded clay aggregates, PLA capsules and alginate capsules.

Healing under short term ideal condition was investigated. This study quantifies healing by relating it to permeability and by studying the formation of healing products at the crack mouth. The mechanical performance of the samples embedded with the capsules was also studied.

The main findings of this study are listed below –

7.1.1 Mechanical Properties -

- Flexural strength of all samples increased with time, but trend of increase was the same for all samples i.e. an increase from 7 to 28 days and then a gradual increase (plateau) except the alginate sample which had a linear increasing trend.
- Alginate shows the highest flexural strength at 84 days while expanded clay shows the lowest flexural strength at 84 days. This behaviour is according to the initial hypothesis.
- From compressive strength tests, it was found that the healed specimens had a much lower strength than the pristine samples of the same age. Healing did not help in complete strength regain which is in line with the initial hypothesis.
- From 4-point bending tests, it was found that the fibers influenced the cracking behaviour of the samples. The PE fibers did not have a good adhesion with

hydration products as they are hydrophobic in nature and fewer hydration products stick to them. [40] Hence, there was bond slip of the fiber which did not permit more than one crack to be formed in the sample. Also, elongation of the fiber contributed to the lack of additional cracks in the sample.

7.1.2 Quantification of Healing –

- The healing products initially precipitated on the bridging fibers near the crack mouth.



Figure 55 -Photomicrograph of precipitate along the fiber across the crack. Scale: 1000µm

- Healing is local so healing does not occur throughout the entire crack depth.
- Healing could occur on the surface i.e. the crack mouth, but the crack could be potentially unhealed inside and conversely, the crack mouth might appear to have no healing, but the crack depth might which is supported by the results of the permeability test.
- PLA capsules could heal surface cracks up to 170 µm in 2 months of healing.
- Alginate capsules formed precipitate inside some samples but not all. This was because the capsules were not sufficiently distributed so the crack did not hit a capsule. There was no surface healing seen. This confirms the original hypothesis.
- Expanded Clay capsules did not show much healing. The healing seen was deep inside the crack. This could be due to the method of preparation of capsules. The healing agent could have been washed off into the binder while mixing so not all capsules had enough healing agent to heal the crack.
- Permeability is a good test for understanding the healing status of the crack. Although there is a problem with correlating the crack width to the permeability as the actual crack width of the sample is unknown until the sample is cut open and the surface crack width could be wider due to external damages. So, it could be misleading and difficult to correlate permeability with the surface crack width.
- Externally healed samples showed a higher rate of healing aka. water tightness regain for crack widths under 500µm.

- The healing for externally applied paste was also not uniform in the crack which suggested that the paste could have been washed off while curing in the mist room.
- For cracks wider than 500 μ m, the alginate and plain samples had the highest rate of water tightness regain.
- PLA and alginate performed well for internal healing with the only drawback being the sparsity of capsules in the matrix for alginate.
- For existing structures that require healing, external healing with paste is recommended but it should be ensured that the paste is not washed off with too much water.

7.2 Experimental Limitations –

There are several experimental limitations of this study namely –

- The type of fiber used was PE so only one crack was formed in the samples a different fiber should have been used to get more cracks in the sample which would have increased the probability of capsules rupturing.
- More number of alginate capsules should have been used in the mix so that the probability of the crack hitting a capsule would have been more. Then the effectiveness of the alginate capsules could have been better measured.
- Expanded clay capsules should have been made differently but as they were made to imitate realistic site conditions, they were dried for a very less amount of time which resulted in poor healing of samples.
- The glue used for 4-point bending and permeability testing damaged the surface of the sample. So, the surface crack measurements were affected as the value was higher.
- During the permeability test it was difficult to prevent the water from leaking out of the side cracks which affected the rate of flow of water.
- External healing was expected to give better results, but the paste could have been washed off during curing in the mist room which would explain the uneven healing in the sample.

7.3 Future Recommendations –

There are several recommendations that can be made based on this study.

- A low-cost method of preparation capsules with less manpower requirement can be devised which would make the use and casting self-healing cementitious materials easier.
- Materials other than bacteria like fungi and other inorganic materials can be used to heal mortar.

- Fillers can be added to the mix to make the mix denser which could compensate for the strength loss due to the addition of capsules.
- Expanded clay capsules can be better prepared by drying them out overnight in an oven. This might help decrease the mixing of the healing agent with the binder during casting.
- A study could be performed comparing self-healing with samples with different w/c ratio having crack widths higher and lower than 500 μ m.
- A permeability test setup should be used for testing this would help ensure that the surface of the crack is as less damaged as possible.
- Samples embedded with capsules can be modelled to simulate the fracture patterns and their healing behaviour.
- There is a need for proper guideline for making self-healing materials as researchers have used different materials with different shapes and different specification and methods for tests. Having a guideline would help reduce the variability in testing and would make results comparable.

References

1. Chang, H., et al., *Mechanical properties, durability and self-healing performance of mortar containing double-layers capsules*. *Materials Today Communications*, 2024. **38**.
2. Standard, B., *Code of practice for Design of concrete structures for retaining aqueous liquids BS 8007*. 1987.
3. He, S., et al., *Effects of bacteria-embedded polylactic acid (PLA) capsules on fracture properties of strain hardening cementitious composite (SHCC)*. *Engineering Fracture Mechanics*, 2022. **268**.
4. Fahimizadeh, M., et al., *Biological Self-Healing of Cement Paste and Mortar by Non-Ureolytic Bacteria Encapsulated in Alginate Hydrogel Capsules*. *Materials (Basel)*, 2020. **13**(17).
5. Feiteira, J., E. Gruyaert, and N. De Belie, *Self-healing of moving cracks in concrete by means of encapsulated polymer precursors*. *Construction and Building Materials*, 2016. **102**: p. 671-678.
6. He, S., et al., *Microstructural characterization of crack-healing enabled by bacteria-embedded polylactic acid (PLA) capsules*. *Cement and Concrete Composites*, 2023. **143**.
7. Wiktor, V. and H.M. Jonkers, *Quantification of crack-healing in novel bacteria-based self-healing concrete*. *Cement and Concrete Composites*, 2011. **33**(7): p. 763-770.
8. Jonkers, H.M., et al., *Application of bacteria as self-healing agent for the development of sustainable concrete*. *Ecological Engineering*, 2010. **36**(2): p. 230-235.
9. Kumari, C., et al., *Effect of Nonureolytic Bacteria on Engineering Properties of Cement Mortar*. 2017.
10. Tziviloglou, E., et al., *Preparation and optimization of bio-based and light weight aggregate-based healing agent for application in Concrete*. 2015.
11. De Muynck, W., et al., *Bacterial carbonate precipitation as an alternative surface treatment for concrete*. *Construction and Building Materials*, 2008. **22**(5): p. 875-885.
12. Bhaskar, S., et al., *Effect of self-healing on strength and durability of zeolite-immobilized bacterial cementitious mortar composites*. *Cement and Concrete Composites*, 2017. **82**: p. 23-33.
13. Achal, V., A. Mukherjee, and M.S. Reddy, *Microbial Concrete: Way to Enhance the Durability of Building Structures*. *Journal of Materials in Civil Engineering*, 2011. **23**(6): p. 730-734.
14. Basit Ehsan Khan, M., D. Dias-da-Costa, and L. Shen, *Factors affecting the self-healing performance of bacteria-based cementitious composites: A review*. *Construction and Building Materials*, 2023. **384**.
15. Nodehi, M., T. Ozbakkaloglu, and A. Gholampour, *A systematic review of bacteria-based self-healing concrete: Biomineralization, mechanical, and durability properties*. *Journal of Building Engineering*, 2022. **49**.
16. Van Wylick, A., et al., *A review on the potential of filamentous fungi for microbial self-healing of concrete*. *Fungal Biol Biotechnol*, 2021. **8**(1): p. 16.

17. Zhang, X., et al., *Study on the behaviors of fungi-concrete surface interactions and theoretical assessment of its potentials for durable concrete with fungal-mediated self-healing*. Journal of Cleaner Production, 2021. **292**.
18. Lv, L., et al., *Light induced self-healing in concrete using novel cementitious capsules containing UV curable adhesive*. Cement and Concrete Composites, 2020. **105**.
19. Salimi, A., N. Kamboozia, and M.R.M. Aliha, *Experimental Investigation of the self-healing capability of Roller-Compacted Concrete (RCC) containing epoxy-filled glass tubes through fracture properties*. Case Studies in Construction Materials, 2024.
20. Wang, J.Y., N.D. Belie, and W. Verstraete, *Diatomaceous earth as a protective vehicle for bacteria applied for self-healing concrete*. J Ind Microbiol Biotechnol, 2012. **39**(4): p. 567-77.
21. Lucas, S.S., et al., *Study of self-healing properties in concrete with bacteria encapsulated in expanded clay*. Science and Technology of Materials, 2018. **30**: p. 93-98.
22. Lee, K.M., et al., *Self-Healing Performance Evaluation of Concrete Incorporating Inorganic Materials Based on a Water Permeability Test*. Materials (Basel), 2021. **14**(12).
23. Tziviloglou, E., et al., *Bacteria-based self-healing concrete to increase liquid tightness of cracks*. Construction and Building Materials, 2016. **122**: p. 118-125.
24. Alghamri, R., A. Kanellopoulos, and A. Al-Tabbaa, *Impregnation and encapsulation of lightweight aggregates for self-healing concrete*. Construction and Building Materials, 2016. **124**: p. 910-921.
25. Feng, J., et al., *Rapid self-sealing of macro cracks of cementitious composites by in-situ alginate crosslinking*. Cement and Concrete Research, 2023. **165**.
26. Bergh, J.M.v.d., et al., *Preliminary approach to bio-based surface healing of structural repair cement mortars*. Construction and Building Materials, 2020. **248**.
27. Bagga, M., et al., *Advancements in bacteria based self-healing concrete and the promise of modelling*. Construction and Building Materials, 2022. **358**.
28. <NEN En 197-1.PDF>.
29. Reinhardt, H.W., *Beton als constructiemateriaal : eigenschappen en duurzaamheid*. 1985, Delft: Delftse Universitaire Pers.
30. Association, P.C., *Ettringite Formation and the Performance of Concrete*.
31. Zhang, X., et al., *Role of a high calcium ion content in extending the properties of alginate dual-crosslinked hydrogels*. Journal of Materials Chemistry A, 2020. **8**(47): p. 25390-25401.
32. Abbasiliasi, S., et al., *Use of sodium alginate in the preparation of gelatin-based hard capsule shells and their evaluation in vitro*. RSC Adv, 2019. **9**(28): p. 16147-16157.
33. Rybak, A.S., *Microencapsulation with the usage of sodium alginate: A promising method for preserving stonewort (Characeae, Charophyta) oospores to support laboratory and field experiments*. Algal Research, 2021. **54**.
34. Mercuri, L., *On the role of soft inclusions on the fracture behaviour of cement paste*, in *Proceedings of the 10th International Conference on Fracture Mechanics of Concrete and Concrete Structures*. 2019.

35. Roiron, C., et al., *A Review of the Mechanical and Physical Properties of Polyethylene Fibers*. Textiles, 2021. **1**(1): p. 86-151.
36. Zhou, S., et al., *Review of Cementitious Composites Containing Polyethylene Fibers as Repairing Materials*. Polymers (Basel), 2020. **12**(11).
37. Said, S.H., H.A. Razak, and I. Othman, *Strength and deformation characteristics of engineered cementitious composite slabs with different polymer fibres*. Journal of Reinforced Plastics and Composites, 2015. **34**(23): p. 1950-1962.
38. Ahmed, S.F.U., M. Maalej, and P. Paramasivam, *Analytical Model for Tensile Strain Hardening and Multiple Cracking Behavior of Hybrid Fiber-Engineered Cementitious Composites*. 2007.
39. Ding, T., et al., *Anisotropic behavior in bending of 3D printed concrete reinforced with fibers*. Composite Structures, 2020. **254**.
40. Xu, Y., et al., *The reinforcement effects of PVA, PE, and steel fibers on AAS material*. Case Studies in Construction Materials, 2022. **17**.
41. Shin, K.J., et al., *Parameters influencing water permeability coefficient of cracked concrete specimens*. Construction and Building Materials, 2017. **151**: p. 907-915.
42. Jiang, L., et al., *Optimization of Sporulation and Germination Conditions of Functional Bacteria for Concrete Crack-Healing and Evaluation of their Repair Capacity*. ACS Appl Mater Interfaces, 2020. **12**(9): p. 10938-10948.
43. *NEN EN 196-1*. 2016.
44. *NEN-EN 933-1 Tests for geometrical properties of aggregates - Part 1: Determination of particle size distribution - Sieving method*. 2021.
45. *NEN-EN 1097-6 Tests for mechanical and physical properties of aggregates - Part 6: Determination of particle density and water absorption*. 2022.
46. *NEN-EN 1015-11 Methods of test for mortar for masonry - Part 11: Determination of flexural and compressive strength of hardened mortar*. 2019.
47. RILEM, *Rilem Method No. II 4- Revised (MEASUREMENT OF WATER ABSORPTION UNDER LOW PRESSURE)*.
48. Guo, S. and S.E. Chidiac, *Probability Characteristics of a Crack Hitting Spherical Healing Agent Particles: Application to a Self-Healing Cementitious System*. Materials (Basel), 2022. **15**(20).

Appendix A –

A.1 Particle Size Distribution –

The particle size distribution results of sand and expanded clay particles are tabulated below.

A.1.1 Sand –

The sand used in the casting of samples is standard sand which has a particle size distribution of 0-2mm according to DIN-EN 196-1/ NEN-EN 196-1.

The particle size distribution was obtained from NEN-EN 196-1 [Table 16] where $1350 \pm 5g$ of sand was tested for particle size distribution.

Table 16- Particle Size distribution of Normsand

SIEVE SIZE (MM)	CUMULATIVE PERCENTAGE PASSING		
	Lower Bound	Mean	Upper Bound
2	100	100	100
1.6	98	93	88
1	72	67	62
0.5	38	33	28
0.16	18	13	8
0.08	2	1	0

A gradation curve was obtained from the data. This curve shows that the sand is densely graded. [Graph 3]

A.1.2 Expanded Clay –

The particle size distribution of expanded clay particles is given below.

Table 17- Particle Size Distribution of Expanded Clay Aggregates

SIEVE SIZE (MM)	WEIGHT OF AGGREGATES RETAINED (G)	PERCENTAGE RETAINED	CUMULATIVE PERCENTAGE RETAINED	CUMULATIVE PERCENTAGE PASSING	WEIGHT OF AGGREGATES PASSING (G)
4	56.2	5.64	5.64	94.36	940.30
2	901.6	90.48	96.12	3.88	38.70
1	35.6	3.57	99.69	0.31	3.10
0.50	0.2	0.02	99.71	0.29	2.90
0.25	0.1	0.01	99.72	0.28	2.80
0.125	0.3	0.03	99.75	0.25	2.50
0.063	0.2	0.02	99.77	0.23	2.30
0.053	0.4	0.04	99.81	0.19	1.90
PAN	1.9	0.19	100	0	0
TOTAL	996.50				

From the table above, a few observations can be made –

- There was some loss of mass during the sieving process as the total was 3.5g less than what was fed into the sieves.
- The expanded clay was in the range of 1-4mm but 5.64% of aggregates were retained on the 4mm sieve which indicated that there were aggregates that were larger than 4mm.
- Most of the aggregates were retained on the 2mm sieve which indicated that most of the aggregates were between 4 and 2mm.
- The particles retained on the 4mm sieve were discarded.

Appendix B –

B.1 Specific Gravity and Water Absorption Test –

The formulas below were used for the water absorption and specific gravity test performed on expanded clay particles.

A – Weight of Vessel Assembly (Pycnometer + Sample +Water)

B – Weight of Pycnometer + Water

C – Weight of Surface Dry Sample

D – Weight of Oven Dried Sample

Specific gravity (ρ), apparent specific gravity (ρ_{app}) and water absorption (WA%) were calculated according to Equations 1, 2 and 3, respectively.

$$\rho = \frac{D}{C - (A - B)} \quad \text{Equation 1}$$

$$\rho_{app} = \frac{D}{D - (A - B)} \quad \text{Equation 2}$$

$$\text{WA\%} = \frac{(C-D)}{D} * 100 \quad \text{Equation 3}$$

Table 18 - Specific Gravity, Apparent Specific Gravity and Water Absorption of Expanded Clay Aggregates

	A (G)	B (G)	C (G)	D (G)	SPECIFIC GRAVITY	APPARENT SPECIFIC GRAVITY	WATER ABSORPTION AS % OF DRY WEIGHT
SAMPLE 1	1980.3	2028.7	279.1	247.2	0.75	0.84	12.90
SAMPLE 2	1980.6	2016.7	291.5	248.2	0.76	0.87	17.44
MEAN						0.76	15.17

Appendix C –

C.1 Detail of Mix Designs –

C.1.1 Type 1 Mix (Plain Reference Mix)–

A standard reference mix was used for making the control/reference specimens.

Once the standard reference was obtained, the quantities for 15 prisms and their volumes were determined.

Table 19 - Reference Mix Design

	Volume (cm ³)	Density (g/cm ³)	Mass (g) for 4.68dm ³	Mass (g) for 1 dm ³
Cement (CEM I 42.5N)	725.81	3.1	2250	480.77
Sand (0-2mm)	2812.5	2.4	6750	1442.31
Water	1125	1	1125	240.38
PE	22.96	0.98	22.50	4.80
Total Volume	4686.27			

This mix was sufficient was making 4.68 L of mortar.

C.1.2 Type 2 (PLA Mix) –

The PLA Mix was designed by keeping the volume of the ingredients same as the plain mix and altering the mass of sand by volumetric sand replacement.

The volume of sand was adjusted due to the addition of the PLA capsules, the quantity of which was determined by the amount of healing agent that was inside the capsules. The amount of healing agent in the PLA capsules was kept as the reference for other capsules as these capsules were readily available.

The ingredients in 1Kg of PLA capsules are listed below.

Table 20 - List of ingredients in 1Kg of PLA capsules

Ingredients	Quantity (g)
Yeast Extract	21
Bacteria Spores	1
PLA	978
Total	1000

In 1000g of capsules there is 15g of nutrient.

Table 21 - Calculation for determining the quantities of the healing agent mix.

1L mortar (dm ³) → 3 prisms	15 Prisms
Yeast Extract	1.21 g
$\frac{15}{1000} * 21 = 0.315 \text{ g}$	

<i>Bacteria Spores</i>	$\frac{15}{1000} * 1 = 0.015 \text{ g}$	0.0576 g
<i>PLA</i>	$\frac{15}{1000} * 978 = 14.67 \text{ g}$	56.33 g
<i>Total</i>	15 g	57.6 g

So, 57.6g of PLA capsules were taken as the mass of PLA capsules that had to be mixed in the mortar for making 15 prisms.

Equation 10

*1g of bacteria contains $5 * 10^8$ spores*

Equation 11

*0.015g of bacteria contains $7.5 * 10^6$ spores*

Hence, the number of spores that went into 1L of mortar were $7.5 * 10^6$. This forms the basis for all mixes i.e. all mixes would have the same number of spores/dm³.

After calculating the mass of the PLA capsules the volume of the capsules was determined. Then the same volume of sand was replaced by the PLA capsules and a new mass for sand was obtained. The volume of all the other ingredients was kept the same as the reference mix as shown above in Table 19.

Table 22 - Mix Design with PLA Capsules

	Volume (cm ³)	Density (g/cm ³)	Mass (g) for 4.68dm ³	Mass (g) for 1dm ³
Cement (CEM I 42.5N)	725.81	3.1	2250	480.15
Sand (0-2mm)	2764.50	2.4	6634.8	1415.88
Water	1125	1	1125	240.08
PE Fibre (6mm)	22.96	0.98	22.50	4.80
PLA Capsules	48.00	1.2	57.60	12.29
Total Volume	4686.27			

C.1.3 Type 3 (Expanded Clay Mix) –

The Expanded Clay Mix was also designed by keeping the volume of the ingredients same as the plain mix and replacing the volume of sand by the same volume of expanded clay capsules.

A mix design was prepared based on the volume of ingredients obtained from the plain mix [Table 19].

Table 23 - Mix design for Expanded Clay Based Mix

	Volume (cm ³) for 4.68dm ³	Density (g/cm ³)	Mass (g) for 4.68dm ³	Mass (g) for 1dm ³
Cement (CEM I 42.5N)	725.81	3.1	2250	480.77
Expanded Clay Capsules with HA (Healing Agent)	2812.50	0.8	2250	480.77
Water	1125.00	1	1125	240.08
PE Fibers (6mm)	22.96	0.98	22.50	4.81
Total Volume	4686.27			

The expanded clay particles were impregnated by the process described in the previous chapter [Page 48].

The quantities of the ingredients in the capsule were determined based on the ingredients present in the PLA capsule [Table 20, Table 21] and the amount of raw expanded clay required was determined from Table 22 and Table 23.

Volume of Expanded Clay Required in 4.68 dm³ = 2812.5 cm³
 Volume of water absorbed in 2812.50cm³ of Expanded Clay = $\frac{15}{100} * 2812.5 = 421.875$ mL
 Volume of Raw Expanded Clay (carrier) = 2812.50cm³ – 421.875mL = 2390.63 cm³
 Volume of Raw Expanded Clay (carrier) 4.68dm³ = 2390.63 cm³
 Mass of Raw Expanded Clay (carrier) for 4.68dm³ = 1912.5g
 Mass of Raw Expanded Clay (carrier) for 1 dm³ = 408.6 g

The ingredients and their quantities are as follows –

Table 24 - Ingredients and their quantities for making Expanded Clay Capsules

	1L mortar (dm ³) → 3 prisms	4.68dm ³ → 15 Prisms
Yeast Extract	$\frac{15}{1000} * 21 = 0.315$ g	1.21 g
Bacteria Spores	$\frac{15}{1000} * 1 = 0.015$ g	0.0576 g
Calcium Lactate	$\frac{15}{1000} * 978 = 14.67$ g	56.33 g
Water	90.14 mL	421.875 mL
Raw Expanded Clay	1912.5 g	408.6 g

C.1.4 Type 4 (Alginate Mix) –

This mix was also prepared in the same way as the other mixes. Although the sand replacement was not 100% unlike the expanded clay mix.

The alginate-based capsules had to be prepared prior to designing the mix as the mass and density of the capsules was unknown. The capsules were prepared with the same amount of healing agent as all the other mixes.

Specification approach was used for preparing the capsules.

Table 25- Ingredient list for making alginate-based capsules.

	QUANTITIES FOR MAKING CAPSULES FOR 4.68DM ³ MORTAR	QUANTITIES FOR MAKING CAPSULES FOR 1 DM ³ MORTAR	CONCENTRATION (%)
HEALING AGENT SOLUTION –			
YEAST EXTRACT	1.2096 g	0.315 g	
BACTERIA SPORES	0.0576 g	0.015 g	
WATER	270 mL	70.3 mL	3.7%
SODIUM ALGINATE	10 g	2.6 g	concentration
BATH –			
CALCIUM LACTATE	56.33 g		20%
WATER	280 g		concentration

A mix design was made based on the mass of the capsules that were prepared.

Table 26 - Mix design for alginate-based capsules

	Volume (cm ³) for 4.68dm ³	Density (g/cm ³)	Mass (g) for 4.68dm ³	Mass (g) for 1dm ³
Cement (CEM I 42.5N)	725.81	3.1	2250.00	480.15
Sand (0-2mm)	2798.77	2.4	6745.33	1433.43
Water	1125.00	1	1125.00	240.08
PE Fibers	22.96	0.98	22.50	4.80
Alginate Capsules	13.73	1.02	14.00	2.99
Total Volume	4686.27			

C.1.5 Type 5 (Externally Applied Paste) –

The specimen used for this type of sample was a plain mortar sample. A paste of the healing agent was made for making type 5 specimens. This proportion for this paste are given below –

Table 27 - Paste for External Healing

Paste Recipe		
Water	50	ml
Yeast Extract	0.32	g
Bacteria	0.02	g
Calcium Lactate	15.02	g

Appendix D –

Table 28 - Photomicrographs of samples 1 week after cracking

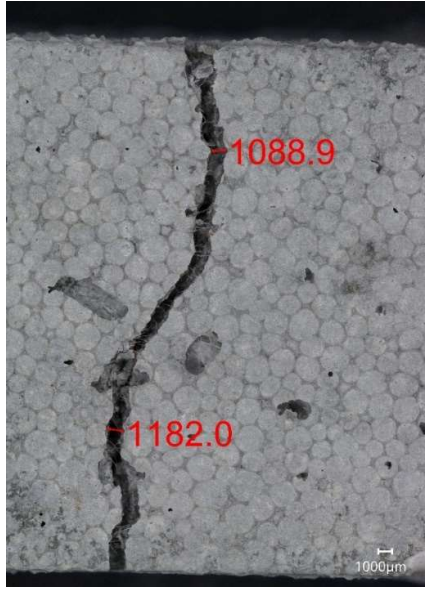
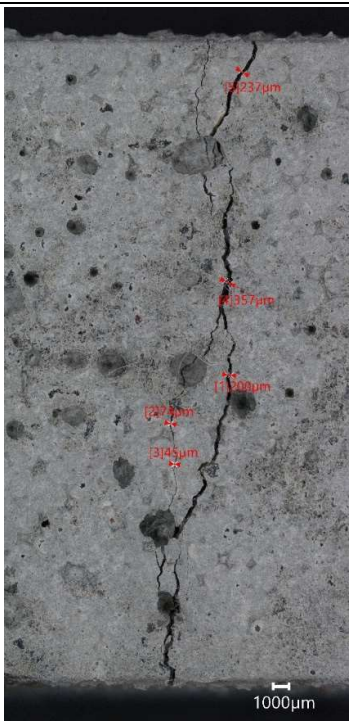
Type 1 Sample –	
	
<p>Figure 56 - Photomicrograph of mortar sample P1 showing crack. Scale: 1000µm</p>	<p>Figure 57 - Photomicrograph of mortar sample P2 showing crack. Scale: 1000µm</p>
	
<p>Figure 58 - Photomicrograph of mortar sample P3 showing crack. Scale: 1000µm</p>	<p>Figure 59 - Photomicrograph of mortar sample P4 showing crack. Scale: 1000µm</p>
Type 2 Sample (PLA)–	



Figure 60 - Photomicrograph of mortar sample PLA1 showing crack. Scale: 1000µm



Figure 61 - Photomicrograph of mortar sample PLA2 showing crack. Scale: 1000µm



Figure 62 - Photomicrograph of mortar sample PLA3 showing crack. Scale: 1000µm



Figure 63 - Photomicrograph of mortar sample PLA4 showing crack. Scale: 1000µm



Figure 64 -Photomicrograph of mortar sample PLA5 showing crack. Scale: 1000µm

Type 3 Sample (Expanded Clay) –

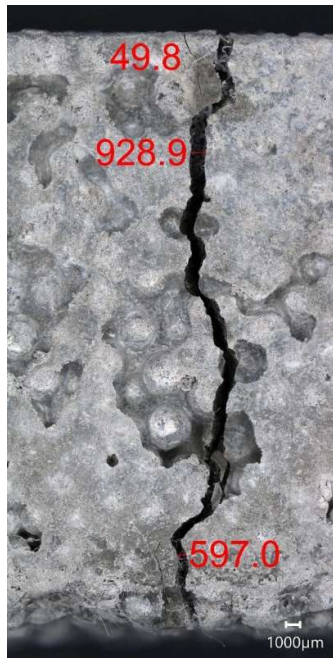


Figure 65 -Photomicrograph of mortar sample EC1 showing crack. Scale: 1000µm

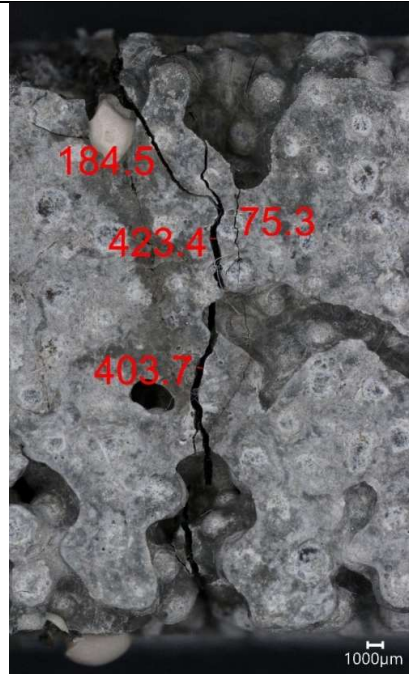


Figure 66 - Photomicrograph of mortar sample EC2 showing crack. Scale: 1000µm

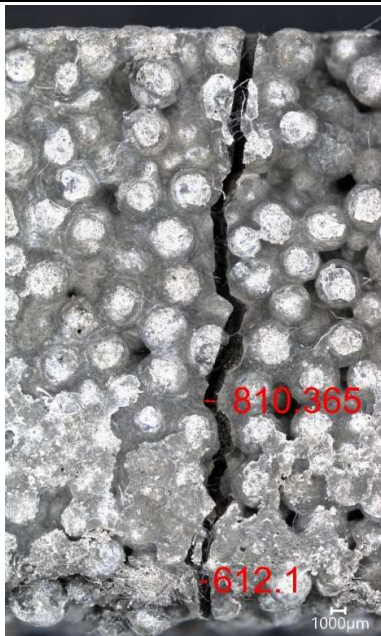


Figure 67- Photomicrograph of mortar sample EC3 showing crack. Scale: 1000µm

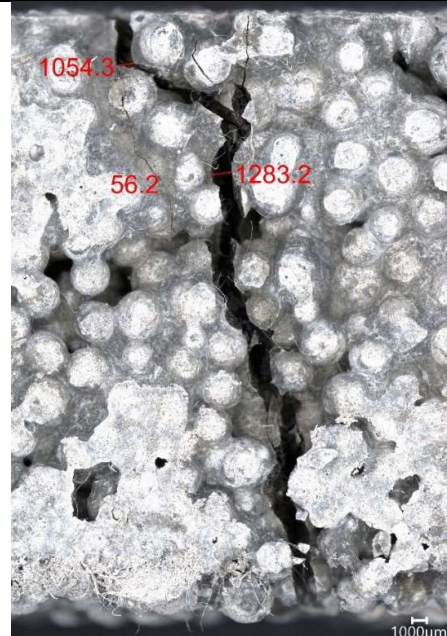


Figure 68 -Photomicrograph of mortar sample EC4 showing crack. Scale: 1000µm

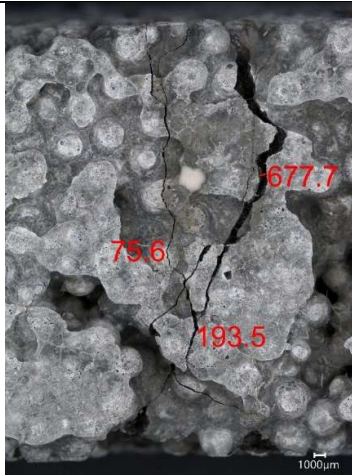


Figure 69- Photomicrograph of left side of mortar sample EC4 showing crack. Scale: 1000µm

Type 4 Sample (Alginate) -

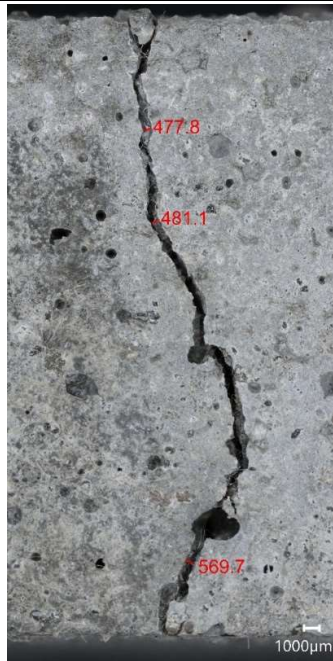


Figure 70 -Photomicrograph of mortar sample A1 showing crack. Scale: 1000µm



Figure 71 -Photomicrograph of mortar sample A2 showing crack. Scale: 1000µm

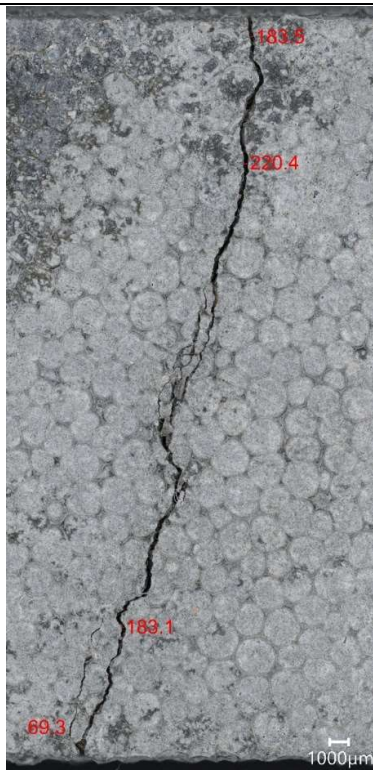


Figure 72-Photomicrograph of mortar sample A3 showing crack. Scale: 1000µm

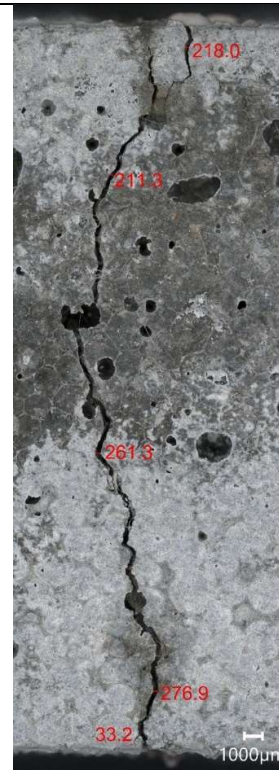


Figure 73-Photomicrograph of mortar sample A4 showing crack. Scale: 1000µm

Type 5 Sample (External Application) –

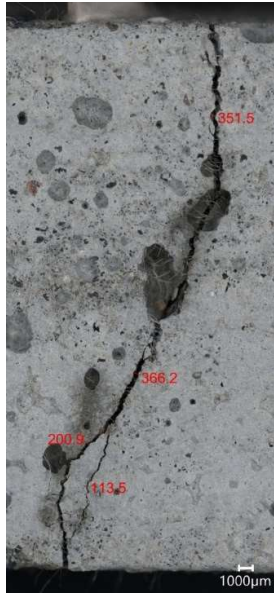


Figure 74 -Photomicrograph of mortar sample E1 showing crack. Scale: 1000µm



Figure 75-Photomicrograph of mortar sample E2 showing crack. Scale: 1000µm

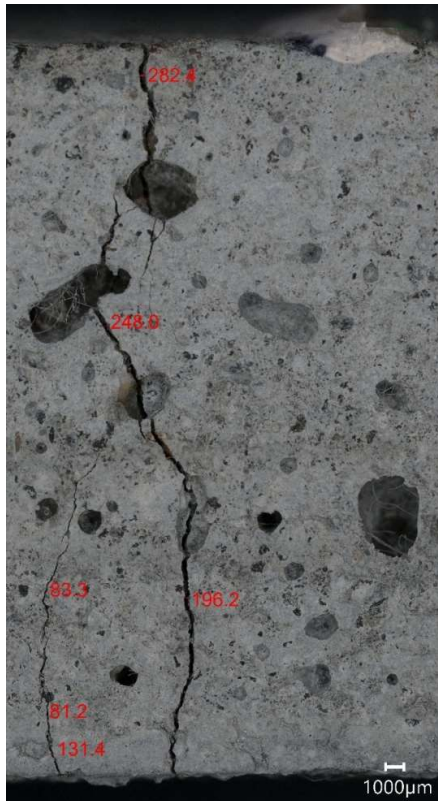


Figure 76-Photomicrograph of mortar sample E3 showing crack. Scale: 1000µm

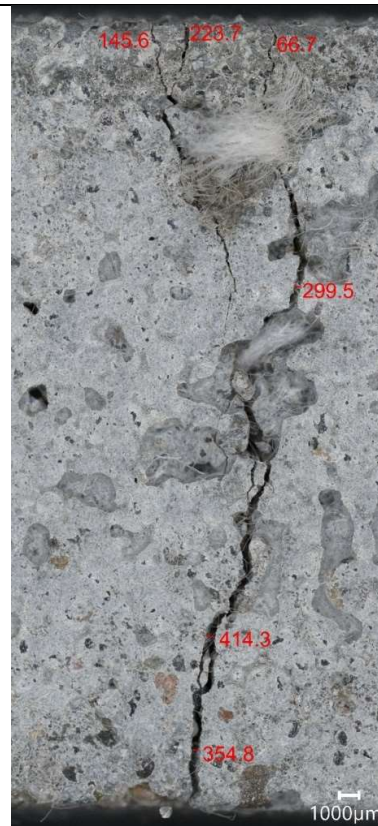


Figure 77 -Photomicrograph of mortar sample E4 showing crack. Scale: 1000µm

Type 1 Sample –



Figure 78 - Photomicrograph of mortar sample P1 showing crack. Scale: 1000µm

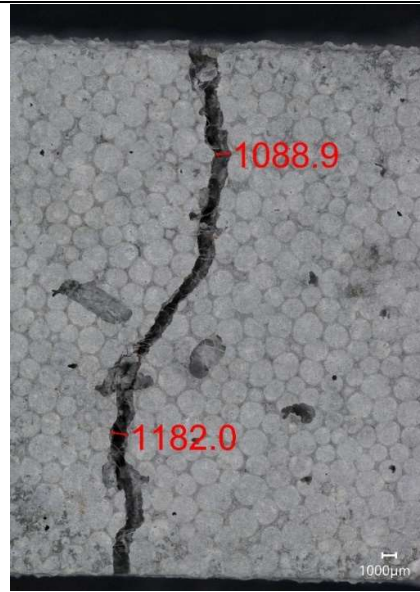


Figure 79 - Photomicrograph of mortar sample P2 showing crack. Scale: 1000µm



Figure 80 - Photomicrograph of mortar sample P3 showing crack. Scale: 1000µm

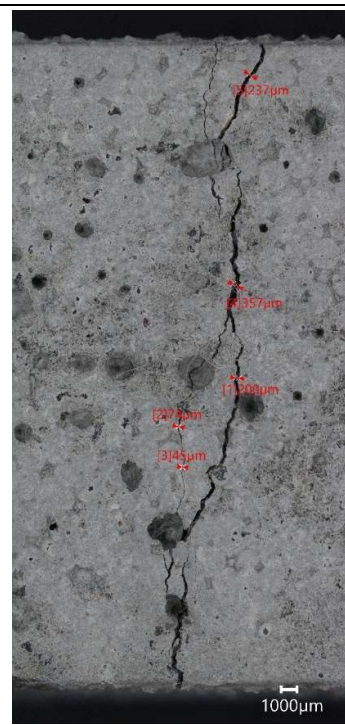


Figure 81 - Photomicrograph of mortar sample P4 showing crack. Scale: 1000µm

Type 2 Sample (PLA)-



Figure 82 - Photomicrograph of mortar sample PLA1 showing crack. Scale: 1000µm



Figure 83 - Photomicrograph of mortar sample PLA2 showing crack. Scale: 1000µm

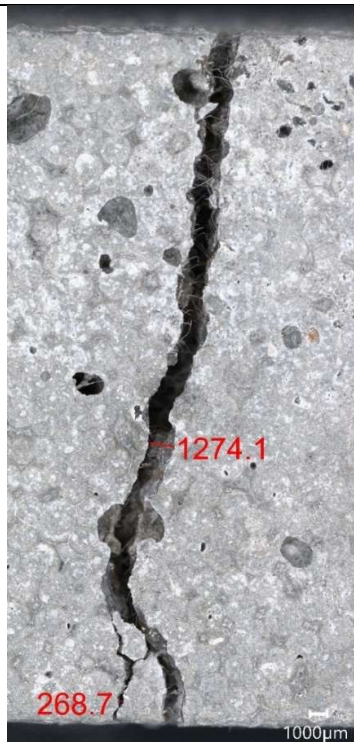


Figure 84 - Photomicrograph of mortar sample PLA3 showing crack. Scale: 1000µm



Figure 85 - Photomicrograph of mortar sample PLA4 showing crack. Scale: 1000µm



Figure 86 -Photomicrograph of mortar sample PLA5 showing crack. Scale: 1000µm

Type 3 Sample (Expanded Clay) –

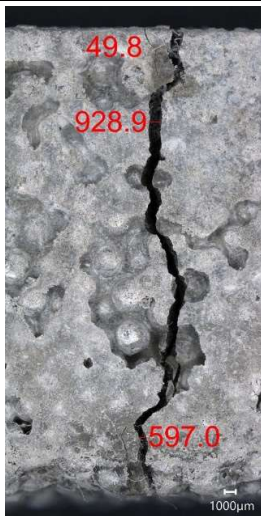


Figure 87 -Photomicrograph of mortar sample EC1 showing crack. Scale: 1000µm

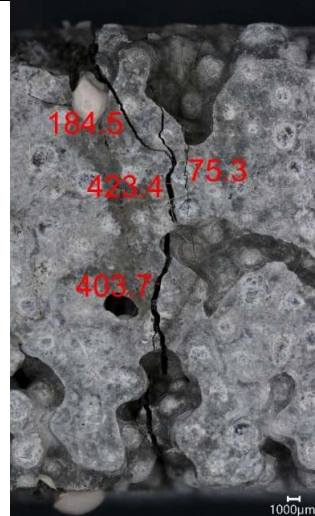


Figure 88 - Photomicrograph of mortar sample EC2 showing crack. Scale: 1000µm

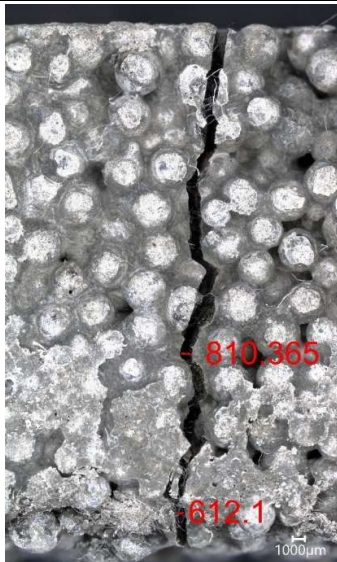


Figure 89- Photomicrograph of mortar sample EC3 showing crack. Scale: 1000µm

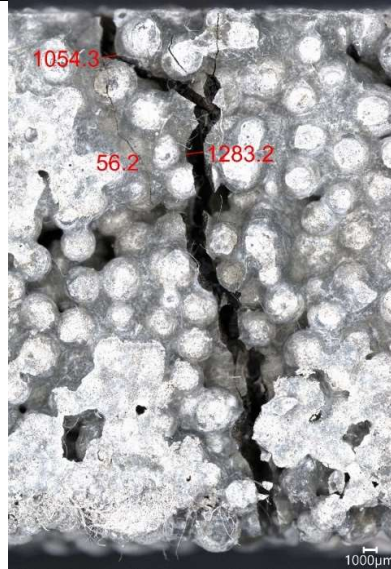


Figure 90 -Photomicrograph of mortar sample EC4 showing crack. Scale: 1000µm

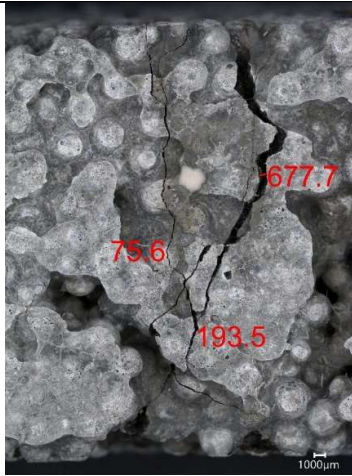


Figure 91- Photomicrograph of left side of mortar sample EC4 showing crack. Scale: 1000µm

Type 4 Sample (Alginate) -

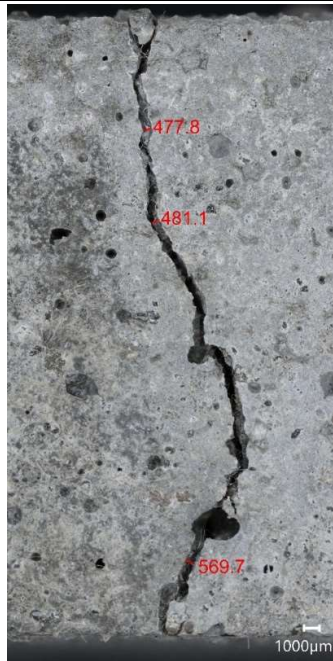


Figure 92 -Photomicrograph of mortar sample A1 showing crack. Scale: 1000µm



Figure 93 -Photomicrograph of mortar sample A2 showing crack. Scale: 1000µm

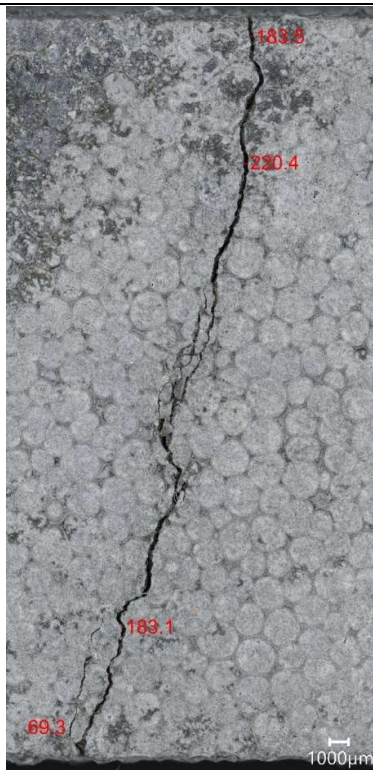


Figure 94-Photomicrograph of mortar sample A3 showing crack. Scale: 1000µm

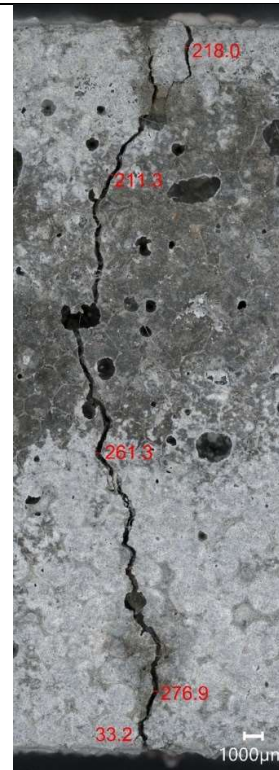


Figure 95-Photomicrograph of mortar sample A4 showing crack. Scale: 1000µm

Type 5 Sample (External Application) –



Figure 96 -Photomicrograph of mortar sample E1 showing crack. Scale: 1000µm



Figure 97-Photomicrograph of mortar sample E2 showing crack. Scale: 1000µm



Figure 98-Photomicrograph of mortar sample E3 showing crack. Scale: 1000µm

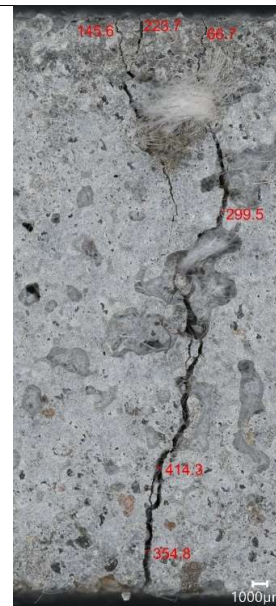


Figure 99 -Photomicrograph of mortar sample E4 showing crack. Scale: 1000µm

Table 29- Photomicrograph of the samples after 1st permeability test (1 month healing duration)

Type 1 Sample –



Figure 100 - Photomicrograph of mortar sample P1 showing crack. Scale: 1000µm

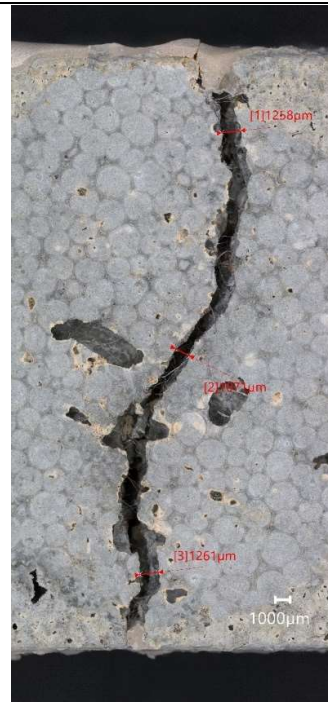


Figure 101 - Photomicrograph of mortar sample P2 showing crack. Scale: 1000µm



Figure 102 - Photomicrograph of mortar sample P3 showing crack. Scale: 1000µm

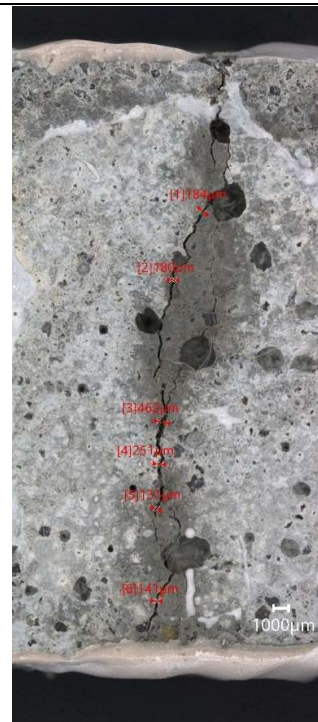


Figure 103 -Photomicrograph of mortar sample P4 showing crack. Scale: 1000µm

Type 2 Sample (PLA)–



Figure 104 - Photomicrograph of mortar sample PLA1 showing crack. Scale: 1000μm



Figure 105 - Photomicrograph of mortar sample PLA2 showing crack. Scale: 1000μm



Figure 106 - Photomicrograph of mortar sample PLA3 showing crack. Scale: 1000μm



Figure 107 - Photomicrograph of mortar sample PLA4 showing crack. Scale: 1000μm



Figure 108 – PLA 4 sample showing precipitate along the crack Scale: 1000µm



Figure 109 -Photomicrograph of mortar sample PLA5 showing crack. Scale: 1000µm

Type 3 Sample (Expanded Clay) –



Figure 110 -Photomicrograph of mortar sample EC1 showing crack. Scale: 1000µm



Figure 111 - Photomicrograph of mortar sample EC2 showing crack. Scale: 1000µm



Figure 112- Photomicrograph of mortar sample EC3 showing crack. Scale: 1000µm



Figure 113 -Photomicrograph of mortar sample EC4 showing crack. Scale: 1000µm



Figure 114- Photomicrograph of left side of mortar sample EC4 showing crack. Scale: 1000μm

Type 4 Sample (Alginate) -



Figure 115 -Photomicrograph of mortar sample A1 showing crack. Scale: 1000µm



Figure 116 -Photomicrograph of mortar sample A2 showing crack. Scale: 1000µm



Figure 117-Photomicrograph of mortar sample A3 showing crack. Scale: 1000µm



Figure 118-Photomicrograph of mortar sample A4 showing crack. Scale: 1000µm

Type 5 Sample (External Application) –



Figure 119 -Photomicrograph of mortar sample E1 showing crack. Scale: 1000µm

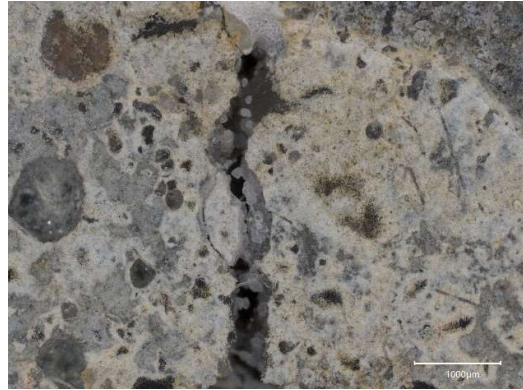


Figure 120 - Photomicrograph of mortar sample E1 precipitate along the crack wall. Scale: 1000µm



Figure 121- Photomicrograph of mortar sample E2 showing crack. Scale: 1000µm



Figure 122-Photomicrograph of mortar sample E3 showing crack. Scale: 1000µm



Figure 123-Photomicrograph of mortar sample E4 showing crack. Scale: 1000µm

Table 30 - Photomicrograph of the samples after 2nd permeability test (2 month healing duration)

Type 1 Sample –



Figure 124 - Photomicrograph of mortar sample P1 showing crack. Scale: 1000µm



Figure 125 - Photomicrograph of mortar sample P2 showing crack. Scale: 1000µm



Figure 126 - Photomicrograph of mortar sample P3 showing crack. Scale: 1000µm

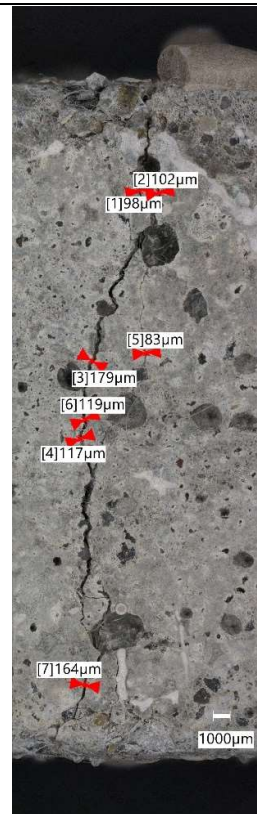


Figure 127 - Photomicrograph of mortar sample P4 showing crack. Scale: 1000µm

Type 2 Sample (PLA)-



Figure 128 - Photomicrograph of mortar sample PLA1 showing crack. Scale: 1000µm

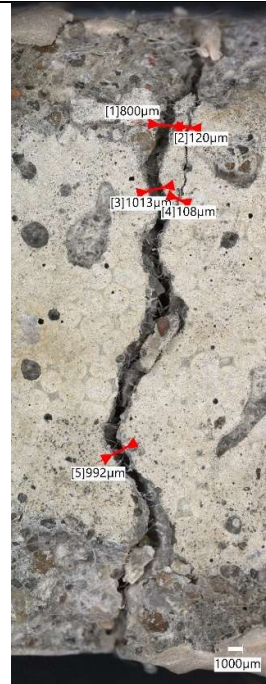


Figure 129 - Photomicrograph of mortar sample PLA2 showing crack. Scale: 1000µm



Figure 130 - Photomicrograph of mortar sample PLA3 showing crack. Scale: 1000µm



Figure 131 - Photomicrograph of mortar sample PLA4 showing crack. Scale: 1000µm



Figure 132 -Photomicrograph of mortar sample PLA5 showing crack. Scale: 1000µm

Type 3 Sample (Expanded Clay) –



Figure 133 -Photomicrograph of mortar sample EC1 showing crack. Scale: 1000µm



Figure 134 - Photomicrograph of mortar sample EC2 showing crack. Scale: 1000µm



Figure 135 - Photomicrograph of mortar sample EC3 showing crack. Scale: 1000µm

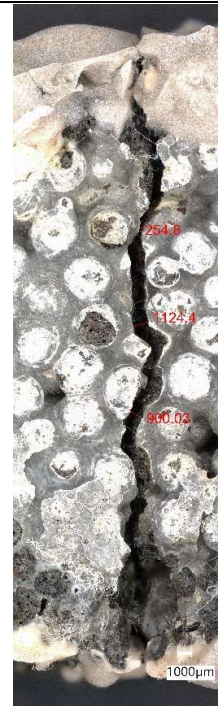


Figure 136 -Photomicrograph of mortar sample EC4 showing crack. Scale: 1000µm

Type 4 Sample (Alginate) -

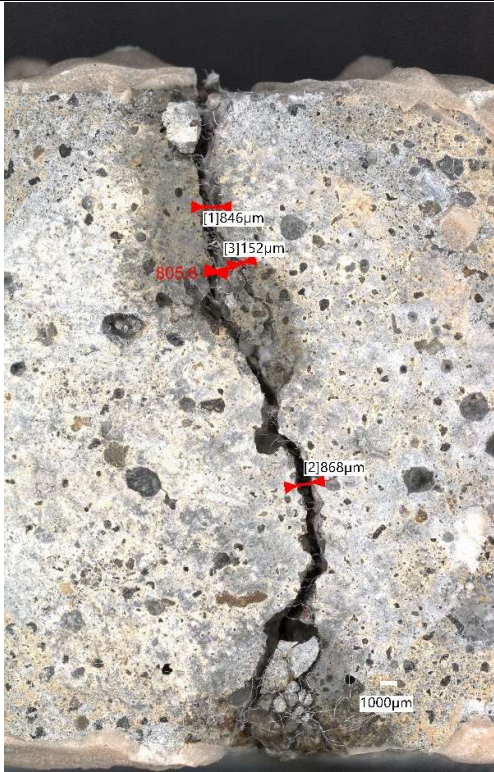


Figure 137 -Photomicrograph of mortar sample A1 showing crack. Scale: 1000µm

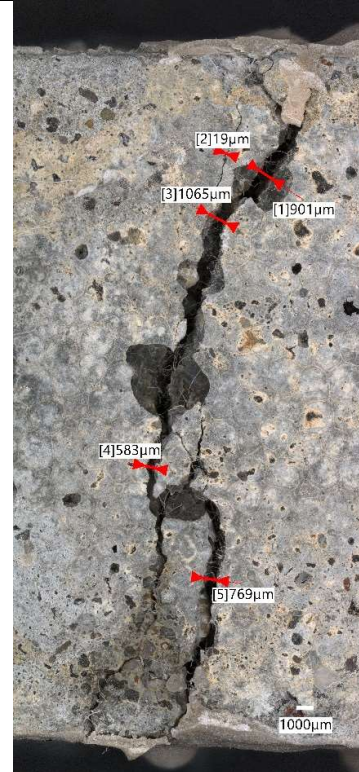


Figure 138 -Photomicrograph of mortar sample A2 showing crack. Scale: 1000µm



Figure 139-Photomicrograph of mortar sample A3 showing crack. Scale: 1000µm

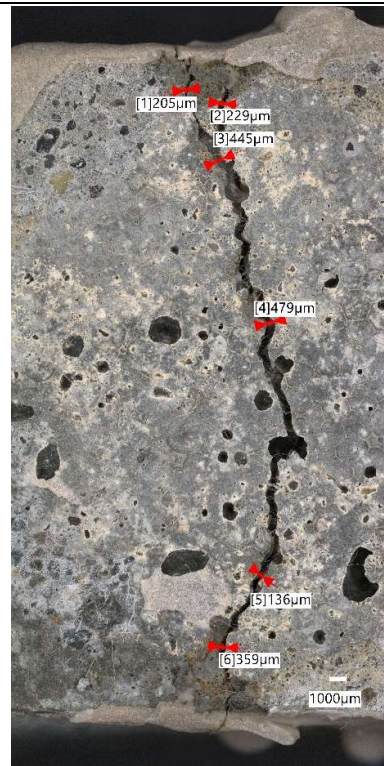


Figure 140-Photomicrograph of mortar sample A4 showing crack. Scale: 1000µm

Type 5 Sample (External Application) –



Figure 141 -Photomicrograph of mortar sample E1 showing crack. Scale: 1000µm

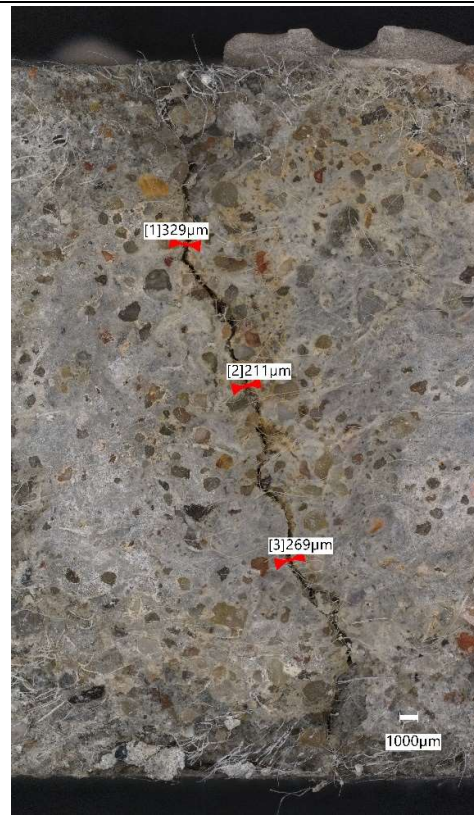


Figure 142 - Photomicrograph of mortar sample E2 precipitate along the crack wall. Scale: 1000µm

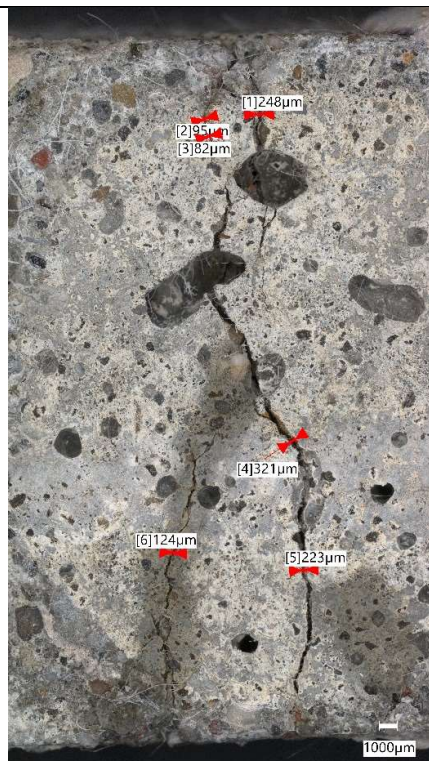


Figure 143- Photomicrograph of mortar sample E3 showing crack. Scale: 1000µm

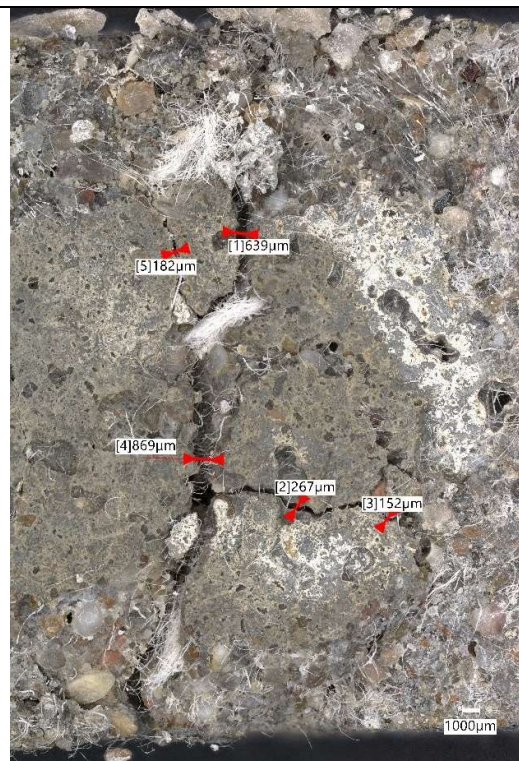


Figure 144-Photomicrograph of mortar sample E4 showing crack. Scale: 1000µm

Appendix E –

E.1 Flexural Strength –

The tables below show the flexural strength of specimens at 7,28 and 84 days.

Table 31-Flexural Strengths of 7 days specimens

	Type 1 (MPa)	Type 2 (MPa)	Type 3 (MPa)	Type 4 (MPa)
Sample 1	4.70	5.46	6.62	7.43
Sample 2	2.61	4.70	6.76	5.88
Sample 3	5.83	2.78	5.99	5.41
Average Flexural Strength	4.38	4.31	6.45	6.24
Std. Deviation	1.63	1.38	0.41	1.05

Table 32 -Flexural Strengths of 28 days specimens

	Type 1 (MPa)	Type 2 (MPa)	Type 3 (MPa)	Type 4 (MPa)
Sample 1	7.35	7.66	7.91	8.33
Sample 2	8.33	8.23	7.53	9.17
Sample 3	7.42	8.31	7.15	6.97
Average Flexural Strength	7.70	8.07	7.53	8.15
Std. Deviation	0.55	0.35	0.38	1.11

Table 33 - Flexural Strength of 84 days uncracked samples

	Type 1 (MPa)	Type 2 (MPa)	Type 3 (MPa)	Type 4 (MPa)
Sample 1	7.87	7.66	7.63	10.05
Sample 2	7.55	7.75	8.26	9.50
Sample 3	8.26	8.24	7.52	9.01
Average Flexural Strength	7.89	7.90	7.80	9.52
Std. Deviation	0.36	0.31	0.40	0.52

E.2 Compressive Strength–

The tables below show the compressive strength of specimens at 7,28 and 84 days. The last table shows the compressive strength of cracked specimens at 56 days post cracking.

Table 34 – 7 days compressive strengths of specimens

	Type 1 (MPa)	Type 2 (MPa)	Type 3 (MPa)	Type 4 (MPa)
Sample 1	11.12	9.78	12.73	9.25
Sample 2	9.21	11.05	12.18	9.45
Sample 3	10.01	7.31	14.62	9.25
Sample 4	9.10	10.10	14.40	8.86
Sample 5	11.82	11.42	15.10	9.29
Sample 6	12.24	12.52	13.24	6.79
Average Compressive Strength	10.58	10.36	13.71	8.81
Std. Deviation	1.34	1.79	1.16	1.01

Table 35- 28 days compressive strengths of specimens

	Type 1 (MPa)	Type 2 (MPa)	Type 3 (MPa)	Type 4 (MPa)
Sample 1	33.3	39.27	36.25	31.11
Sample 2	32.19	29.73	36.12	28.36
Sample 3	35.19	38.42	34.36	29.72
Sample 4	36.31	39.51	35.76	28.74
Sample 5	35.42	38.10	37.26	28.00
Sample 6	36.28	38.04	36.95	24.12
Average Compressive Strength	34.80	37.18	36.12	28.34
Std. Deviation	0.55	0.35	0.38	1.11

Table 36 - 84 days compressive strengths of specimens

	Type 1 (MPa)	Type 2 (MPa)	Type 3 (MPa)	Type 4 (MPa)
Sample 1	30.85	34.39	33.25	44.48
Sample 2	30.75	37.39	34.07	44.74
Sample 3	35.62	41.30	36.98	39.24
Sample 4	27.77	41.71	36.56	42.13
Sample 5	31.13	42.11	36.03	39.01
Sample 6	37.73	43.57	35.54	35.07
Average Compressive Strength	32.97	40.08	35.40	40.78
Std. Deviation	3.70	3.47	1.46	3.72

The samples after healing were tested for compressive strength on the crack.

Table 37 -Compressive Strength of 56 days healed samples (Sample age :84 days)

Sample Name	Compressive Strength (MPa)	Average Surface Crack Width (µm)
Type 1		
P1	15.34	788.75

P2	18.81	1281.00
P4	20.93	129.33
Type 2		
PLA 2	15.21	606.60
PLA 3	23.74	945.00
PLA 4	15.37	1560.50
PLA 5	31.62	143.40
Type 3		
EC1	9.78	613.75
EC2	6.26	407.66
EC4	5.63	759.74
Type 4		
A2	12.86	829.50
A3	18.52	329.33
A4	15.88	308.83
Type 5		
E2	7.11	269.67
E3	20.28	182.17
E4	7.96	421.80

E.3 Permeability Test –

The tables below show the details of the permeability test of samples for 1 month and 2 months of healing.

Table 38 - 1st permeability test

TEST 1						
Sample Name	Time			Volume of water (ml)	Rate (q(t)) (ml/s)	Current Crack Width (µm)
	Minutes	Seconds	Total seconds			
P1	1	4.69	64.69	500	7.729	686.39
P2	1	19.46	79.46	500	6.292	875.33
P3	26	0.9	1560.9	434	0.278	257.00
P4	29	0.61	1740.61	362.6	0.208	224.83
PLA1	0	40.71	40.71	500	12.282	1340.30
PLA2	3	18.69	198.69	500	2.516	986.75
PLA3	1	7.57	67.57	500	7.400	1028.45
PLA4	1	11.97	71.97	500	6.947	1669.67
PLA5	34	21.9	2061.9	500	0.242	166.75
EC1	0	46.1	46.1	500	10.846	907.00

EC2	0	43.38	43.38	500	11.526	398.33
EC3	1	25.96	85.96	500	5.817	824.00
EC4	1	11.77	71.77	500	6.967	1320.67
A1	2	17.83	137.83	500	3.628	625.00
A2	0	55.71	55.71	500	8.975	507.33
A3	25	0.43	1500.43	348.8	0.232	293.33
A4	23	0.28	1380.28	413.5	0.300	283.75
E1	5	33.09	333.09	500	1.501	307.80
E2	14	38.99	878.99	500	0.569	250.00
E3	26	30	1590	438	0.275	210.00
E4	14	57.12	897.12	500	0.557	386.67

Table 39 - 2nd Permeability Test

TEST 2						
Sample Name	Time			Volume of water (ml)	Rate (q(t)) (ml/s)	Current Crack Width (µm)
	Minutes	Seconds	Total seconds			
P1	2	53.96	173.96	500	2.874	788.75
P2	1	26.15	86.15	185.2	2.150	1281.00
P3	38	40.74	2320.74	500	0.215	142.50
P4	54	37.18	3277.18	500	0.153	129.33
PLA1	1	47.67	107.67	500	4.644	1327.70
PLA2	2	52.08	172.08	480	2.789	606.60
PLA3	1	28.61	88.61	500	5.643	945.00
PLA4	1	25.43	85.43	480	5.619	1560.50
PLA5	40	0.39	2400.39	326	0.136	143.40
EC1	1	27.54	87.54	500	5.712	613.75
EC2	1	17.92	77.92	500	6.417	407.66
EC3	1	55.52	115.52	500	4.328	672.20
EC4	1	16.99	76.99	500	6.494	759.74
A1	43	52.94	2632.94	500	0.190	889.86
A2	2	12.23	132.23	500	3.781	829.50
A3	35	48.03	2148.03	500	0.233	329.33
A4	32	21.63	1941.63	500	0.258	308.83
E1	37	20.86	2240.86	500	0.223	248.50
E2	33	41.67	2021.67	500	0.247	269.67
E3	22	41.45	1361.45	500	0.367	182.17
E4	31	23.72	1883.72	324	0.172	421.80

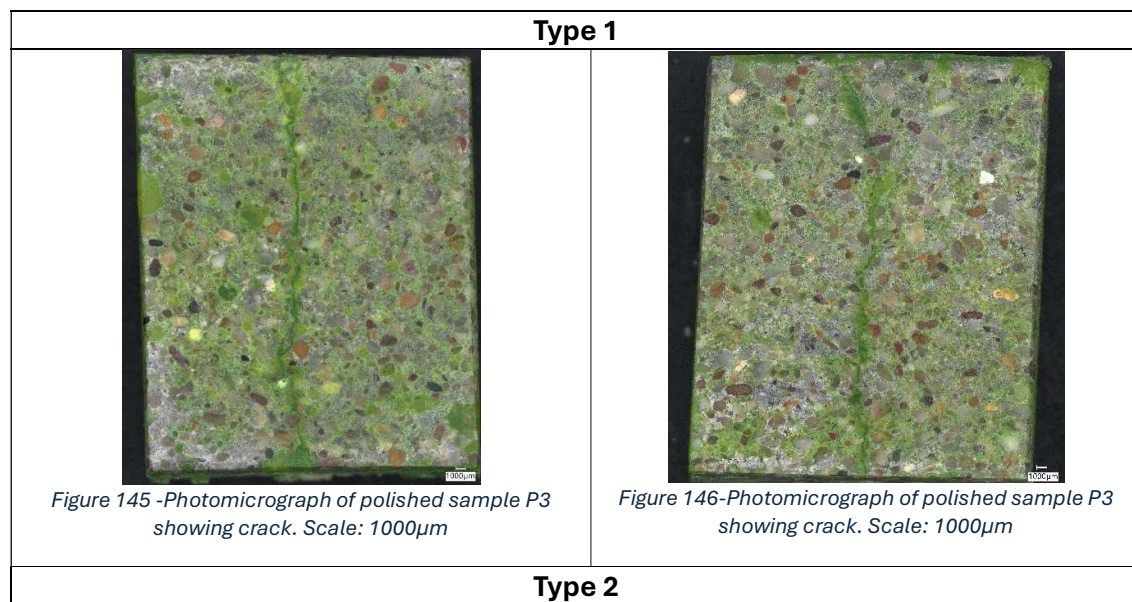
E.4 Surface Crack Width Progression –

The table below shows the progression of surface crack width as measured using an Optical Microscope at different time intervals.

Table 40 – Surface Crack width progression

Sample type	Max crack width at cracking (μm)	Average Surface Crack Width (μm)		
		1 week healing	1 month healing	2 months healing
P1	828.67	672.53	686.39	788.75
P2	900.25	1135.45	875.33	1281.00
P3	512.03	202.00	257.00	142.50
P4	511.21	264.67	224.83	129.33
PLA 1	936.07	1070.75	1340.30	1327.70
PLA 2	944.30	995.95	986.75	606.60
PLA 3	991.81	1274.10	1028.45	945.00
PLA 4	914.03	1728.85	1669.67	1560.50
PLA 5	511.65	176.00	166.75	143.40
EC1	949.47	762.95	907.00	613.75
EC2	882.18	337.20	398.33	407.66
EC3	812.61	711.23	824.00	672.20
EC4	980.19	1168.75	1320.67	759.74
A1	1014.46	509.53	625.00	889.86
A2	953.61	496.14	507.33	829.50
A3	438.56	164.08	293.33	329.33
A4	452.69	241.87	283.75	308.83
E1	467.46	306.20	307.80	248.50
E2	464.11	357.00	250.00	269.67
E3	466.39	242.20	210.00	182.17
E4	466.59	283.83	386.67	421.80

E.5 Optical Microscopy –



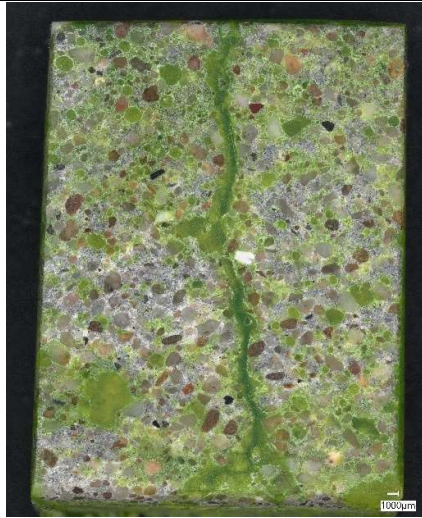


Figure 147 -Photomicrograph of polished sample PLA1 showing crack. Scale: 1000µm



Figure 148- Photomicrograph of polished sample PLA1 showing crack. Scale: 1000µm

Type 3

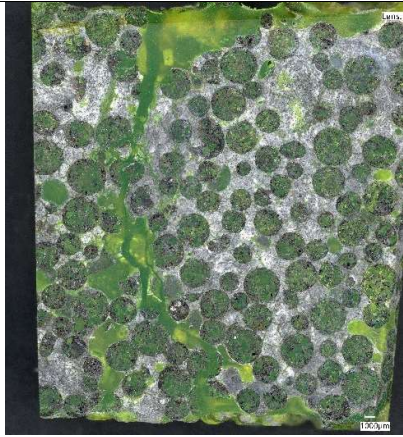


Figure 149 - Photomicrograph of polished sample EC3 showing crack. Scale: 1000µm



Figure 150 -Photomicrograph of polished sample EC3 showing crack. Scale: 1000µm

Type 4

Alginate
Capsule

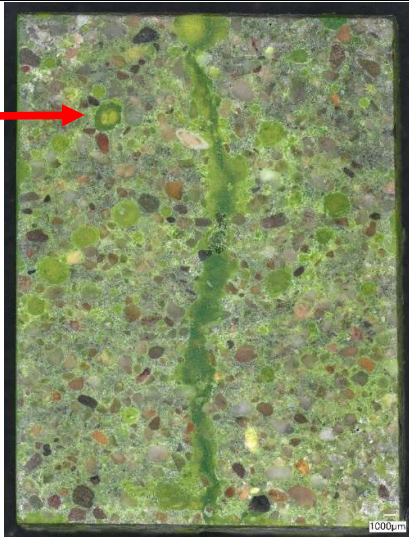


Figure 151 - Photomicrograph of polished sample A1 showing crack. Scale: 1000µm



Figure 152 - Photomicrograph of polished sample A1 showing crack. Scale: 1000µm

Type 5



Figure 153 - Photomicrograph of polished sample E1 showing crack. Scale: 1000µm



Figure 154 - Photomicrograph of polished sample E1 showing crack. Scale: 1000µm

E.6 Porosity –

Raw Images	Processed Images
------------	------------------

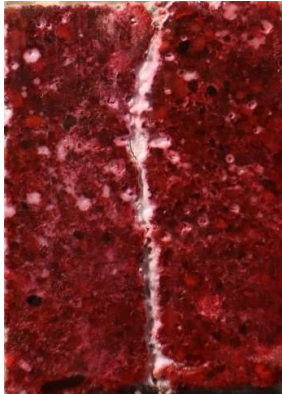


Figure 155 - Prepared surface of sample P3

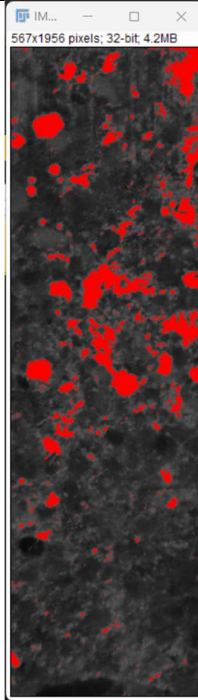


Figure 156 – Processed image of left side of the sample

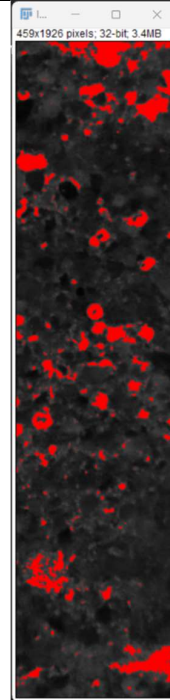


Figure 157 - Processed image of right side of the sample

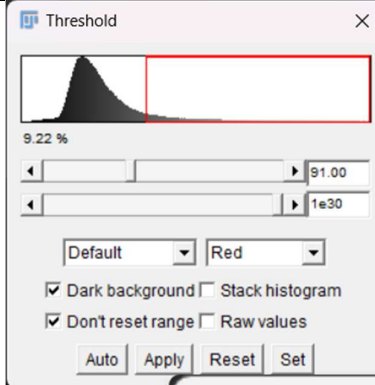


Figure 158- Threshold value

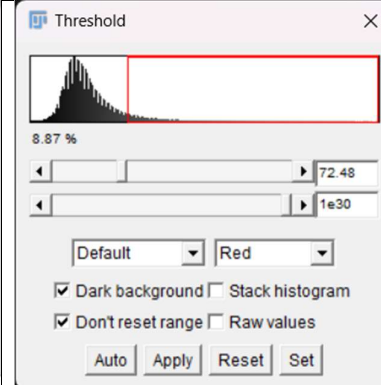


Figure 159-Threshold value

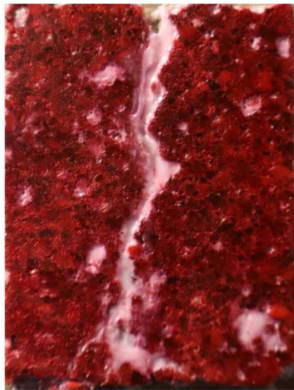


Figure 160 - Prepared surface of sample PLA1

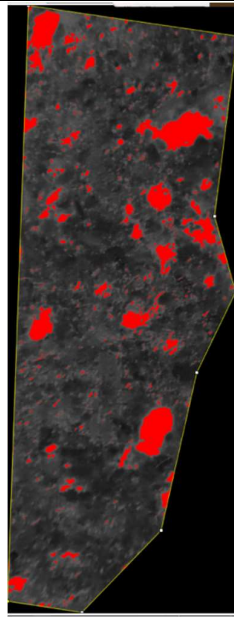


Figure 161- Processed image of left side of the sample

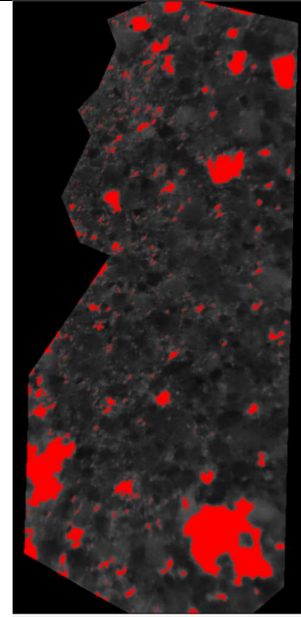


Figure 162- Processed image of right side of the sample

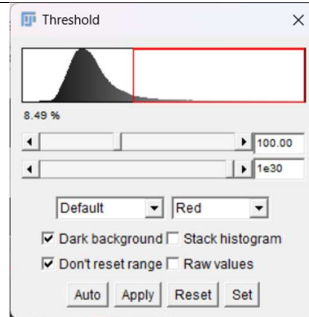


Figure 163 -Threshold value

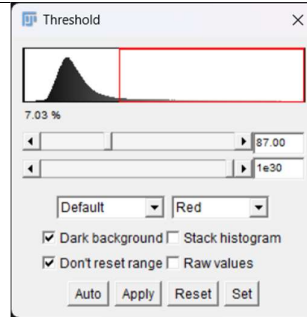


Figure 164- Threshold value



Figure 165 - Prepared surface of sample A1

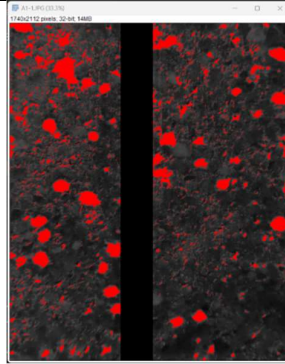


Figure 166 - Processed image of full sample minus crack

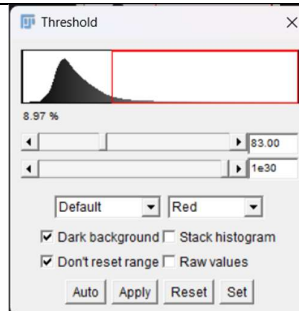


Figure 167 - Threshold value of the full sample without crack

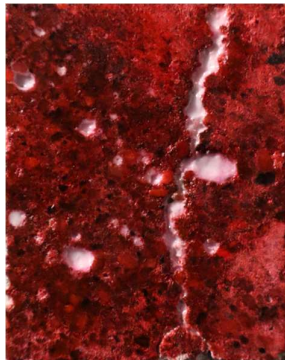


Figure 168 - Prepared surface of sample E1

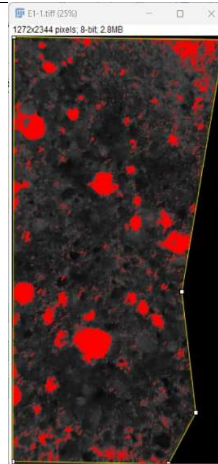


Figure 169 - Processed image of left side of the sample

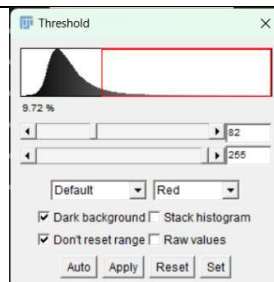


Figure 170 - Threshold value

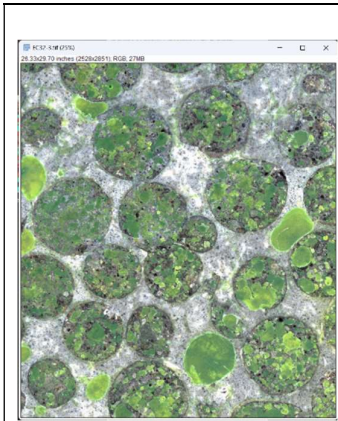


Figure 171 - Part of polished section of sample EC3

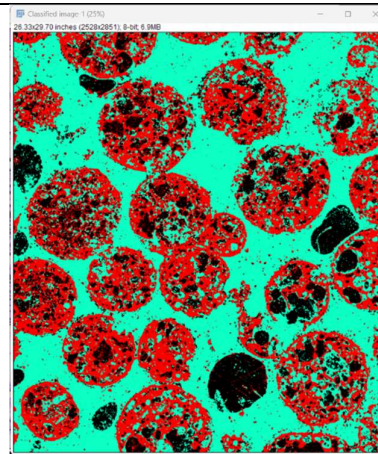


Figure 172 - WEKA segmentation result
[Green: Binder, Red: Clay particles, Black: Voids]

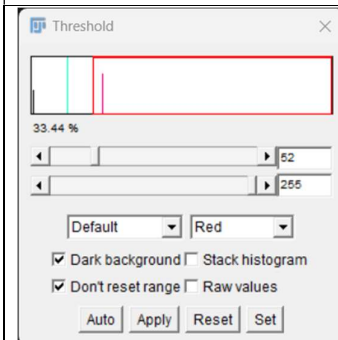


Figure 173 - Threshold value of Expanded Clay

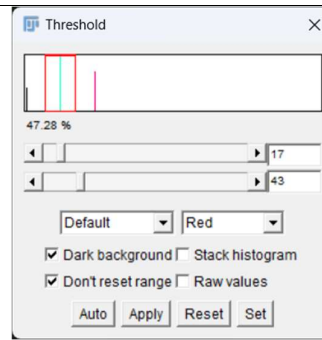


Figure 174 -Threshold value of Binder

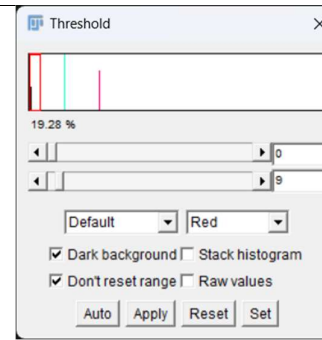


Figure 175 -Threshold value of voids

E.6 Healing Efficiency –

Table 41 -Permeability Efficiency

Sample Name	Permeability Efficiency (SH _q) %	Change in surface crack width (1 month width -2 month width)
P1	62.81	-102.36
P2	65.84	-405.67
P3	22.51	114.50
P4	26.76	95.50
PLA1	62.19	12.60
PLA2	-10.85	380.15
PLA3	23.74	83.45
PLA4	19.13	109.17
PLA5	43.99	23.35
EC1	47.34	293.25
EC2	44.33	-9.33

EC3	25.59	151.80
EC4	6.78	560.93
A1	94.77	-264.86
A2	57.87	-322.17
A3	-0.13	-36.00
A4	14.04	-25.08
E1	85.14	59.30
E2	56.52	-19.67
E3	-33.32	27.83
E4	69.14	-35.13

E.7 Healing Efficiency –

Table 42 - Healing Efficiency

Name of healed sample	Compressive strength of healed samples (MPa)	Average current Surface Crack width (μm)	Average compressive strength of pristine samples (MPa)	Healing Efficiency (%)
PLA 5	31.62	143.40	40.08	78.91
P4	20.93	129.33	32.97	63.47
E3	20.28	182.17	32.97	61.49
PLA 3	23.74	945.00	40.08	59.23
P2	18.81	1281.00	32.97	57.04
P1	15.34	788.75	32.97	46.51
A3	18.52	329.33	40.78	45.41
A4	15.88	308.83	40.78	38.95
PLA 4	15.37	1560.50	40.08	38.34
PLA 2	15.21	606.60	40.08	37.95
A2	12.86	829.50	40.78	31.54
EC1	9.78	613.75	35.40	27.63
E4	7.96	421.80	32.97	24.12
E2	7.11	269.67	32.97	21.56
EC2	6.26	407.66	35.40	17.69
EC4	5.63	759.74	35.40	15.90

Appendix F –

Preparation of Polished Samples –

After all the permeability tests were completed, 5 samples that had an average amount of healing, as observed from the surface were chosen to prepare polished samples. The prisms were cut using a power saw. The size of the cut specimen was - H: 40mm, W:30mm, T:15mm. Each prism was cut into 2 pieces, keeping the crack in the middle of the cut sample.

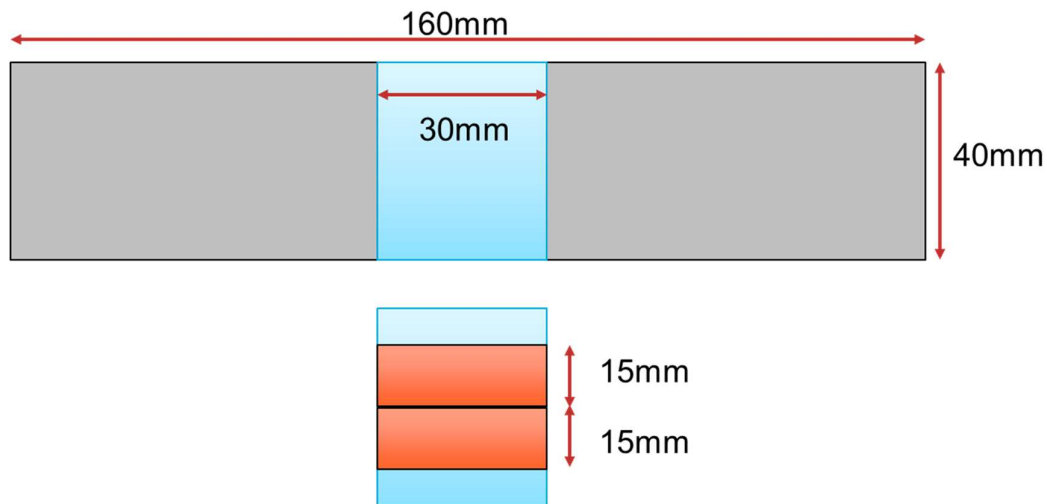


Figure 176 -Sketch for cutting the prism. Not to scale.

The samples were oven dried at 40°C for 24 hours before epoxy impregnation. This was done to remove all moisture from the sample which allows the epoxy to impregnate the voids of the samples.

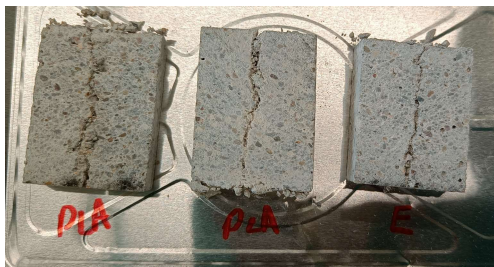


Figure 177 - Oven dried sawed samples

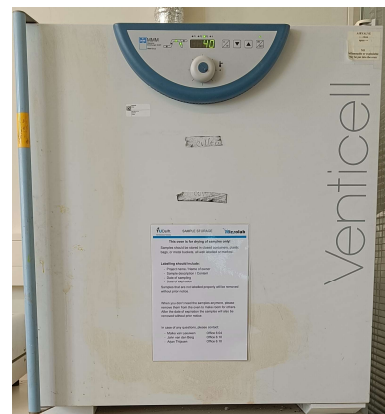


Figure 178- Oven for drying samples



Figure 182- Ultrasonic Cleaner

- The sample is then ready to be polished.
- For Polishing, the disk speed is set at 150 rpm.
- Polishing disks of different grit sizes are used ranging from 9mm to 1mm. All polishing cloths use ethanol as a lubricant and diamond suspension as the abrasive fluid and after each disk the samples are cleaned using the ultrasonic cleaner.
- The samples are first polished by a 9mm disk (Largo) using a 9 μ m diamond suspension for about 4 minutes.
- The second disk used was a 6mm grit disk with a 6 μ m diamond suspension for about 3 minutes.
- Then a 3mm grit disk (DAC) with a 3 μ m diamond suspension was used for about 3 minutes.
- At the end a 1mm disk with a 1 μ m diamond suspension was used for about 1 minute.